Høgskulen på Vestlandet

ING5002 - Master Thesis

ING5002

Predefinert informasjon

Startdato:	17-08-2021 09:00	**Termin:**	2021 VÅR1
Sluttdato:	31-08-2021 14:00	**Vurderingsform:**	Norsk 6-trinns skala (A-F)
Eksamensform:	Masteroppgave		
Flowkode:	203 ING5002 1 MOPPG 2021 VÅR1		
Intern sensor:	Xiaoqin Hu		

Deltaker

Navn:	Sigurd Bjørvig Henriksen
Kandidatnr.:	202
HVL-id:	583716@hvl.no

Informasjon fra deltaker

Tittel *:	Scenario Based Fire Risk Assessment; The Effects of Longitudinal Ventilation in Case of Fire in an Existing Road Tunnel
Antall ord *:	23312
Engelsk tittel *:	Scenario Based Fire Risk Assessment; The Effects of Longitudinal Ventilation in Case of Fire in an Existing Road Tunnel

Sett hake dersom besvarelsen kan brukes som eksempel i undervisning?:	Ja	**Egenerklæring *:**	Ja
		Inneholder besvarelsen konfidensielt materiale?:	Nei
Jeg bekrefter at jeg har registrert oppgavetittelen på norsk og engelsk i StudentWeb og vet at denne vil stå på vitnemålet mitt *:	Ja		

Jeg godkjenner avtalen om publisering av masteroppgaven min *
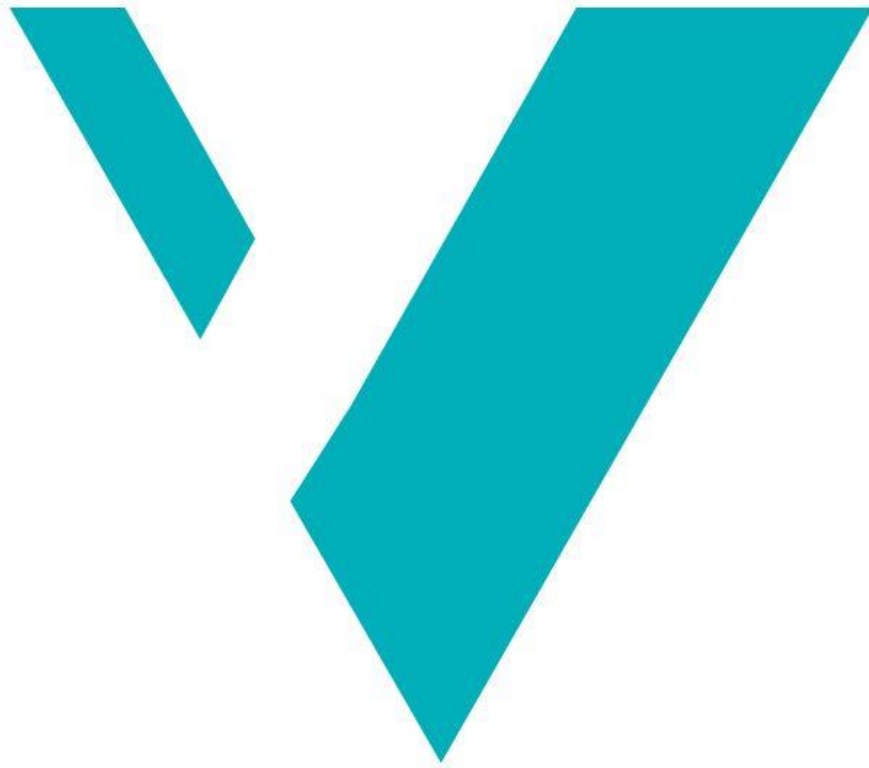
Ja

Er masteroppgaven skrevet som del av et større forskningsprosjekt ved HVL? *

Nei

Er masteroppgaven skrevet ved bedrift/virksomhet i næringsliv eller offentlig sektor? *

Ja, Troms og Finnmark Fylkeskommune

Scenario Based Fire Risk Assessment; The effects of longitudinal ventilation in case of fire in an existing road tunnel

Sigurd Bjørvig Henriksen

WESTERN NORWAY UNIVERSITY OF APPLIED SCIENCES
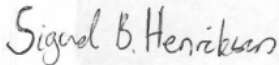
Master Thesis in Fire Safety Engineering

Haugesund

[August 2021]

Western Norway
University of
Applied Sciences

Scenario Based Fire Risk Assessment; The Effects of Longitudinal Ventilation in Case of Fire in an Existing Road Tunnel

Master thesis in Fire Safety Engineering

Author: Sigurd Bjørvig Henriksen	Author sign. *Sigurd B. Henriksen*
Thesis submitted: Spring 2021	Open thesis

Tutor: Sanjay K. Khattri External tutor: Andreas Albrigtsen	
Keywords: Tunnel Fire Dynamics; Fire safety; Longitudinal Ventilation; FDS; Pathfinder; Evacuation; Tenable Conditions; Backlayering; Air Velocity	Number of pages: 73 + Appendix: 18 Haugesund, 31. Aug, 2021 Place/Date/year

Abstract

This study examines the effect of longitudinal ventilation in case of fire in an existing road tunnel. The purpose of fire ventilation in road tunnels is to control heat and smoke transfer. Large tunnel fires can be a major challenge for safe evacuation and emergency efforts, emphasizing the importance of fire safety measures in road tunnels. Hence, the study aimed to evaluate the effect of the longitudinal ventilation related to smoke control and tenable conditions. Fire simulations were conducted in *FDS*, which consisted of fire scenarios with rapid developing HGV-fires at 50 MW, 100 MW and 200 MW. Evacuation simulations was performed in *Pathfinder*.

The work of the study indicates that the existing ventilation configuration could not prevent smoke from moving upstream. Furthermore, the results show that evacuees with reaction times $\leq$ 5 minutes did avoid exposure to toxicity levels above the acceptance criteria. However, acceptable visibility levels proved to be a challenge to maintain for all the fire scenarios. The author believes the findings of the study might provide valuable knowledge regarding the effect of longitudinal ventilation in the existing road tunnel in case of fire. Nonetheless, further research is recommended in order to validate the results in this study.

Acknowledgements

Summary

The purpose of fire ventilation in tunnels is to keep one side of the fire clear of smoke to extinguish the fire at an early stage. The supply of air from the longitudinal ventilation will increase airflow velocity in the tunnel and control the direction of the fire- and smoke gases. To achieve the desired effect of the ventilation strategy, airflow velocity must exceed the opposing forces produced by the fire. A successful ventilation strategy will prevent fire- and smoke gases upstream.

The thesis examines the effects the longitudinal ventilation during a fire the middle of the Langnes Tunnel in Tromso, Norway. The tunnel is 1700 m long and is in an urban environment with an average daily traffic of 16 000 vehicles. A fast-developing HGV-fire will be examined with heat release rate (HRR) 50 -, 100- and 200 MW. The input data is based on a full-scale HGV-fire experiment consisting of plastic- and wood materials. The goals of the thesis are to examine the ventilation systems ability (1) to prevent smoke upstream (backlayering) and to (2) evaluate the tenable conditions downstream of the fire. The CFD-program *FDS 6.7.5* is used to analyse available safe evacuation time (ASET), while required safe evacuation time (RSET) is determine by the evacuation program *Pathfinder*.

Observations in the fire scenarios 50-, 100- and 200 MW with the existing jet fan configuration show backlayering lengths between 46 to 67.3 m. The fire scenario with increased jet fan capacity were able to prevent backlayering. Furthermore, the results show that evacuees with reaction times ≤ 5 minutes did avoid exposure to toxicity levels above the acceptance criteria. However, acceptable visibility levels proved to be a challenge to maintain for all the fire scenarios. Based on the results, ASET were determined to be in the region of 9 min 50 sec and 11 min for the fire scenarios with existing jet fan configurations. The evacuation results revealed that the RSET were between 13 min and 20 min 30 sec.

The backlayering in all the fire scenarios, except one, indicates that the longitudinal ventilation was unable to prevent backlayering for fast-developing HGV-fires ≥ 50 MW. Furthermore, the RSET exceeded the ASET for the fire scenarios performed in the study. This suggests that the longitudinal ventilation fails to facilitate safe evacuation and emergency efforts. However, the author recommends further research to confirm if the results are valid regarding the existing road tunnel.

Sammendrag

Formålet med brannventilasjon i tunneler er å holde den ene siden av brannen røykfri for å muliggjøre tidlig slukkeinnsats. Tilførsel av luft ved langsgående ventilasjon vil øke lufthastigheten i tunnelen, og dermed kontrollere hvilken retning brann- og røykgasser beveger seg. For å oppnå ønsket effekt av ventilasjonsstrategien må lufthastigheten blant annet overgå brannens oppdriftskrefter. Det er for å unngå at brann- og røykgasser beveger seg mot luftstrømmen.

Oppgaven undersøker hvilken effekt den langsgående ventilasjonen har på brann i midten av Langnestunnelen i Tromsø, Norge. Tunnelen har en lengde på 1700 meter og befinner seg i et urbant miljø med en dagsgjennomsnitt (AADT) på mer enn 16 000 kjøretøy. I oppgaven undersøkes det en hurtigutviklende brann i vogntog med varmeutslippshastighet (HRR) på henholdsvis 50-, 100- og 200 MW. Brannen er basert på inngangsdata fra et tidligere full-skala brannforsøk i en tunnel med vogntog bestående av plast- og trematerialer. Oppgaven undersøker ventilasjonsanleggets evne til å forhindre at røykgasser i å bevege seg oppstrøms i tunnelen (backlayering). I tillegg kartlegges rømningsforholdene nedstrøms i tunnelen. CFD-programmet *FDS* 6.7.5 benyttes for å undersøke tilgjengelig tid til rømning (ASET), mens nødvendig tid til rømning (RSET) er beregnet ved hjelp av rømningsprogrammet *Pathfinder*.

Observasjoner i brannscenarioer på 50-, 100- og 200 MW med den eksisterende vifte konfigurasjonen viser røyk oppstrøms mellom 46 m til 67.3 m. Brannscenarioet med økt vifte kapasitet var i stand til å forhindre røyk oppstrøm. Videre viser resultatene at evakuerende med reaksjonstid ≤ 5 minutter unngikk å bli eksponert for giftige nivåer over aksept kriteriet. Derimot indikerer resultatene at akseptable nivåer på sikt var utfordrende å opprettholde under brannscenarioene. Basert på resultatene ble ASET avgjort til å være på mellom 9 min 50 sek og 11 min for brannscenarioene med eksisterende vifte konfigurasjon. For evakuerings-resultatene var RSET mellom 13 min og 20 min 30 sek.

Da røyk beveget seg oppstrøms i alle brannscenarioene, bortsett fra et, antydes det at den langsgående ventilasjonen ikke hindrer røyk oppstrøms for hurtigutviklende brann i vogntog ≥ 50 MW. Videre viser RSET høyere verdier enn ASET for brannscenarioene i denne studien. Dette antyder at den langsgående ventilasjonen ikke er i stand til å tilrettelegge for sikker evakuering og beredskapsinnsats. Det understrekes at videre undersøkelser anbefales for å validere resultatene opp mot den eksisterende vegtunnelen.

Table of Contents

List of figures

List of tables

Definitions

ASET	Available Safe Evacuation Time
RSET	Required Safe Evacuation Time
CFD	Computational Fluid Dynamic
Risk (R)	The relationship between potential (P) and consequence (C) described with the following equation, $P \times C = R$
Acceptance criteria	Criteria based on regulations, standards, experience and/or theoretical knowledge which are used as a basis for deciding acceptable risk.
FDS	Fire Dynamics Simulator
Pathfinder	A tool for simulating human behaviour in emergency evacuation scenarios.
Heat Release Rate (HRR)	The rate at which fire releases energy.
Fire growth	The increase of the burning rate of a fire.
Evacuee	A person evacuating from a place of danger.
Travel distance	The distance that an evacuee would travel from any point within the tunnel
Road tunnels	An underground passageway for vehicles.
Annual Average Daily Traffic (AADT)	The total volume of vehicle traffic on a road for a year divided by 365 days.
Visibility	The distance a person can see determined by physical conditions.
Fractional Effective dose (FED)	A measure of the airborne toxicity absorbed by a person

1 Introduction

Chapter 1 presents an introduction to give the reader an understanding of fire safety in road tunnels. The background and challenges related to the thesis are presented in the chapter. Furthermore, the thesis statement and research questions are formulated, as well as the purpose and limitations of the thesis.

1.1   Background

Road tunnels have proven to be essential for infrastructure in Norway. Road tunnels provide geographical accessibility, city- and area development with limited impact on the environment. There are many advantages of road tunnels, which Europe and the rest of the world have realised. Tunnels enables crossing of mountainous areas, as well as shortening traffic connection to other areas. In addition, road tunnels have proven to be the safest part of the Norwegian road network in terms of accidents. According to [1], there are more than 1 200 tunnels in Norway. The number of road tunnels will likely increase with the increasing traffic density in the years to come. Hence, road tunnels are important for the Norwegian infrastructure.

The EU Directive 2004/54/EC [2] gives the minimum safety measures related to tunnels with lengths of more than 500 meters in the Trans-European Road Network (TERN). Existing tunnels in operation shall also be subject to the safety requirements which entered into force on 1 December 2006 [3]. The safety measures and equipment for road tunnels depend on the annual average daily traffic (AADT) and tunnel length. A large amount of road tunnels was constructed before the 2000, e.g. more than 400 road tunnels were constructed between 1980-2000 in Norway. As a result, several existing road tunnels need safety upgrades to comply with the minimum safety requirements. In addition, many road tunnels with increasing traffic will be subject to a higher safety classification and hence, higher minimum safety requirements.

Tunnel fires have proven to be a major safety challenge in road tunnels. Statistics show that car accidents are less likely to occur inside road tunnels compared to open roads. However, there are conditions in road tunnels which differs from open roads related to fire and evacuation. The consequences of a tunnel fire can be severe and is highly undesirable. There are on average 30 vehicle fires in Norwegian tunnels every year [4]. Yet, there has not been any catastrophic fires in

Norway as previously seen in Mont Blanc and St. Gotthard. These tunnel fires caused a high number of fatalities. In enclosures, like tunnels, vehicles that are involved in a fire tend to burn more fiercely compared to vehicles in an open fire. [5] The challenges are especially related to high heat release rates, smoke spread and evacuation. Typical bi-directional road tunnels provide two paths for smoke- and heat transfer, which further can limit the evacuation process. Therefore, safety measures in tunnel fire safety are important to reduce consequences of a tunnel fire.

1.2   Road Tunnels in Norway

Many road tunnels in Norway are bi-directional with one tube, while uni-directional tunnels with two separate tubes are becoming more common. An important safety measure in road tunnels are ventilation systems. Most common for Norwegian road tunnels are longitudinal ventilation systems. Longitudinal ventilation can be effective in controlling smoke movement to facilitate firefighting efforts from one side of the fire. Longitudinal ventilation in uni-directional tunnels enables vehicles downstream of the fire to drive safely out of the tunnel, while vehicles upstream of the fire turn around without being affected by smoke. This makes the strategy of preventing smoke to move upstream of the fire – backlayering - beneficial in uni-directional tunnels. However, most road tunnels in Norway are bi-directional tunnels. For these tunnels, the approaching traffic might be exposed to smoke moving downstream which is likely to worsen evacuation conditions.

1.3   Thesis statement

The thesis will involve an assessment of the longitudinal ventilation related to fire safety in an existing bi-directional road tunnel in the City of Tromso, Norway called *Langnestunnelen* (hereby called *The Langnes tunnel*). The longitudinal ventilation ability to facilitate emergency efforts and evacuation in case of fire are being investigated. Based on the results, the thesis will attempt to address whether further safety measures are needed. The thesis statement is as follows:

"The longitudinal ventilation are able to control fires in order to facilitate safe evacuation and emergency efforts."

1.4   Research questions

The following research questions will be the basis for the content of the thesis:

➢ Will the longitudinal ventilation be able to prevent backlayering?

➢ Will the longitudinal ventilation facilitate evacuation downstream of a fire?

1.5   Purpose

The aim of this study is to investigate and examine the effect of longitudinal ventilation in an existing road tunnel in case of fire. As mentioned, fire events in tunnels might be challenging and can have a catastrophic outcome. Hence, the topic are believed to be relevant and important. The thesis will perform a scenario-based risk analysis consisting of fire- and evacuation simulations to quantify the fire safety performance of the longitudinal ventilation in the road tunnel. Furthermore, the results related to backlayering and tenable conditions downstream of the fire will be quantitatively assessed.

1.6   Limitations

The study focuses on the effect of longitudinal ventilation in case of fire in an existing road tunnel with the use of pre-defined performance criteria for the analysis. The road tunnel is included in an underground road tunnel system, which means that the results are limited to the Langnes tunnel. Since the road tunnels in the tunnel system is connected, further studies will be required to identify how the longitudinal ventilation behaves throughout the whole tunnel system. Conditions in other parts of the tunnel system might affect the fire safety in the Langnes tunnel and vice-a-versa. Due to the complexness of the tunnel system and time perspective, the Langnes tunnel were chosen as the main focus of the work. Hence, the findings of this study will only be applicable to the longitudinal ventilation in the Langnes tunnel in case of fire.

The fire- and evacuation simulations were performed using, respectively, FDS and Pathfinder. Furthermore, the author was responsible for deciding the fire scenarios for this study. The design of fire scenarios was mainly motivated by the means to evaluate the conditions on both side of an HGV-fire in the road tunnel. Therefore, the author decided to place the fire in the middle of the tunnel in the fire simulations. There could have been selected numerous fire scenarios for other areas of the road tunnel in this study. However, this proved to be a challenge due to limited time and computational resources during this work.

2 Methodology

This chapter describes the process of solving the thesis statement. The report is divided into 3 sections. A theoretical study, a model case study, and an analysis of the results.

Figure 1 - A flow chart showing the methodology of the report

2.1 Theoretical study

The theoretical study is performed to acquire the necessary background on relevant topics. To find literature, the library database at the Western Norway University of Applied Sciences were used as well as the Scopus database. Scopus is a large database with comprehensive contents from about 25.000 academic journals and other academic materials. The content comes from over 7.000 publishers, that are reviewed and selected by an independent board to be indexed in Scopus [6].

A literature review was conducted for the thesis to find relevant research literature. The intention of the work was to find relevant topics about; tunnel fire dynamics, fire- and smoke control, longitudinal ventilation, fire and evacuation modelling of road tunnels and fire experiments. In the search field in Scopus, one has the option of searching for "article title, abstract and keyword". For the literature review different keywords related to the topics were combined in order identify relevant publications.

In addition to Scopus and the HvL libraries, some publications were found using Ingason's book *Tunnel Fire Dynamics* from 2015 [7]. Of special interest, reports from previous full-scale fire experiments in road tunnels were found in the book's references.

2.1.1 Large-Scale Tunnel Experiments

Full-scale tests of tunnels are and have been of great importance for the development of tunnel fire dynamics. The aim of fire testing in tunnels is usually to investigate specific problems. There could be such as the effects ventilation systems might have on the tunnel fire dynamics. Such as, smoke and temperature distribution along the tunnel, fire development in different vehicles and how integrity and strength of the tunnel is influenced by heat from a fire [7]. The data provides an valuable knowledge for developing standards and guidelines that are used for tunnel design. Also, the data can be used to compare and identify limitations with fire models and calculations [8].

The first large-scale fire tests were performed in Europe in the 1960s, and today the number of tests is increasing. These tests have varied in fire source, HRR, instrumentations, technical documentation, tunnel geometry and ventilation conditions [7]. The tests performed in 1960-1980 usually lacked quality. Important parameters such as HRR was usually not adequately recorded. The focus of the first tests were to establish a basic understanding about how ventilation systems influenced tunnel fires, rather than gathering data for validation of CFD models.

A selection of large-scale experiments performed after 1990 are briefly explained and summarized in this section.

Eureka EU 499 1990-1992

Eureka EU499 was a test program which were performed in an abandoned tunnel near Hammerfest, Troms and Finnmark County in Norway between 1990-1992. The tunnel has a length of 2.3 km and cross-section of approximately between 30-40 m^2. Measurements were recorded from fires in passenger cars, busses, HVGs and railway coaches [9]

Type of vehicle	Max. temperature [°C]	Heat release rate [MW]
Passenger car	400-500	3-5
Bus	700-800	15-20
Heavy goods vehicle (HGV) with burning goods	1000-1200	50-100
Railway coaches	800-900	15-20

Table 1- Maximum temperatures and maximum momentary rates of heat release (Eureka project EU 499, 1995) [9]

For the tests, it was used Oxygen consumption calorimetry (OCC), which made it possible to measure HRR for different vehicles with relatively good accuracy. The tests resulted in new valuable data and information for engineers [7].

Memorial Tunnel Tests 1993-1995

The Memorial Fire Ventilation Test Program was performed in an 850 m long, 8.8 m wide, two-laned abandon tunnel. 98 tests were conducted in the tunnel where type of ventilation, fuel size and FFFSs varied. Full- and partial transverse- and longitudinal ventilations with jet fans was some of the ventilation systems that were tested. For the tests with longitudinal ventilation the original height of 4.3 m, rectangular shaped cross-section of 36,2 m2 was changed to a shape like a "horseshoe" with a cross-section of 60,4 m^2 with a 7,8 m height to the ceiling.

While the EUREKA test series had the largest scope of any other tests, the Memorial test series is the largest in terms of actual tunnel scale. Although, the 98 fire tests only involved pool fires with HRR ranging between 10 MW and 100 MW [10]. The aim of the tests was to compare known fire sources to the performance of different ventilation systems [7].

2nd Benelux Tests 2002

In the Second Benelux Tunnel in the Netherlands, it was performed 14 tests in 2002. The tunnel has a rectangular cross section with a height and width at 5.1 meter and 9.8 m. The tests were design to assess tenability conditions, as well as assessing the efficiency of fire detection system, ventilation system and fixed firefighting systems (FFFS) for different types of fire sources. Temperature, radiation, and visibility was measured during these tests [7].

Runehamar 2003

Runehamar 2003 consisted of fire tests of HGV-trailer cargo in the abandoned Runehamar tunnel in Norway. The tunnel is 1600 m long, 6 m high and 9 m wide, 0,5-1% slope. The cross section of the tunnel varies between 47 – 50 m^2 [7]. There were performed 4 tests in an HGV-trailer mock-up, with both mixtures of cellulosic and plastic materials as fuel. Also, it was conducted one pool fire test [11]. For all the tests, the fire development occurred very fast, even though the ignition source were relatively small.

Singapore 2012

7 tests were conducted in a test tunnel facility in Spain. The fire load consisted of full loaded HGV-mock ups with plastic- and wooden pallets, which were believed to be a credible and realistic representation of a typical cargo truck configuration. The tunnel is 600 m, 7.3 m wide and 5.2 m high. Jet fans generated an air velocity of 3 m/s for all the tests. Tests with and without FFFS was conducted where HRR, temperature and toxicity were measured. In the test without FFFS, the fire growth occurred very fast and reached a peak HRR of 150 MW [12].

2.1.2   Summary of full-scale tunnel fire tests

Table 2 show a summary of relevant full-scale tunnel fire tests after 1990.

Test tunnel/ test series	Length [m]	Height [m]	Width [m]	Cross section [m²]	Fuel type	HRR [MW]	Ventilation [m/s]	Peak gas temperature [℃]
EUREKA, 1990-1992 [9]	2300	4,8 – 5,5		25-35	Heptane, Wood cribs, cars, metro, car, rails, HGV	6 - 128	0 - 8	400 - 1300
Memorial Tunnel, 1993-1995 [13] [14]	853	4,4 & 7,9		30 & 60	Fuel pool (4,5 – 45 m²)	20 - 100	0 - 3	400 - 1360
2nd Benelux Tunnel, 2002 [15]	872	5,1	9,8	50	Heptane, Toluene, car, van, wood pallets	4,5 - 26	1 - 6	110 - 600
Runehamar Tunnel, 2003 [16]	1600	5 - 6		32 - 47	Cellulose, plastic, furniture	6, 66 - 202	2 - 3	267, 1250-1365
Singapore tests, 2012 [12]	600	5,2	7,3	39	Plastic + wood	27 - 150	2,8 – 3	-

Table 2 – Summary of large-scale scale tunnel fire tests performed after 1990.

2.2 Tunnel model – Case study

The intent of this section was to establish a basis for the scenario-based risk analysis. The objective was to develop design scenarios to measure the effect of the longitudinal ventilation during a fire in the middle of the Langnes tunnel. Information about the road tunnel and technical installations, previous reports and risk analysis were acquired from Troms and Finnmark County, which is the owner of the tunnel. This information was important to develop the fire model.

2.2.1 The tunnel system

The Tromso tunnel system contains three connected road tunnels beneath the City of Tromso in Norway. The first tunnel, the Langnes Tunnel and an underground parking lot was developed between 1984-1988 by private companies. The Langnes tunnel connects the Langnes area with the city centre of Tromso.
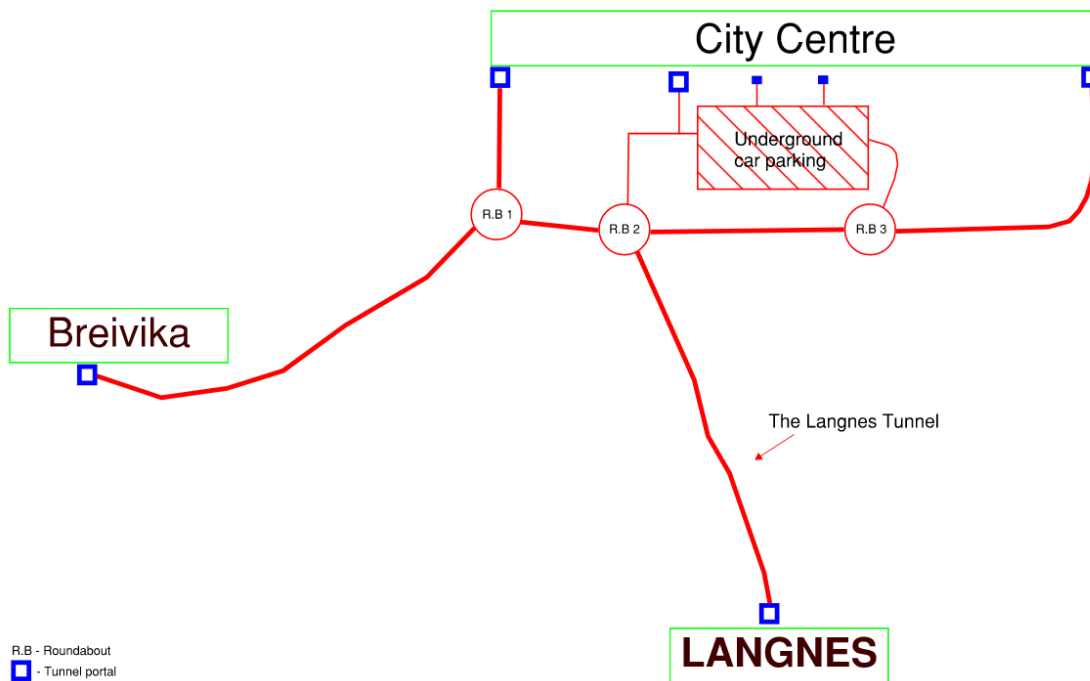
Figure 2 - A sketch of the Tromso tunnel system

Breivikatunnelen were the second tunnel, which was constructed between 1989-1992 by the Norwegian Public Road Administration (NPRA). The tunnel connects Breivika to the north city centre of Tromso. During construction period, a tunnel tube (*mellomtunnelen*) was built, connecting the new tunnel with the Langnes tunnel via a roundabout. The Breivika tunnel was

one of the first tunnels in Northern-Norway which was designed with modern tunnel guidelines, given in the tunnel handbook 021 (replaced by handbook N500 [17])

The third tunnel, *Sentrumstangenten*, opened in 1999. The tunnel connects the South City Centre of Tromso with the Langnes- and Breivikatunnel, and the underground parking lot via two roundabouts. Since the opening of the tunnels, upgrades have been performed. The tunnel system was upgraded between 2006-2007.

2.3 Analysis of the results

2.3.1   Scenario-based risk analysis

A scenario-based risk analysis involves a certain amount of fire and evacuation scenarios. The fire and evacuation scenarios are identified, analysed, and assessed by performing calculations. Typically, the work includes an analysis of people's ability to evacuate from the infrastructure without being exposed to untenable conditions. This is commonly done by comparing the available safe egress time (ASET) to the required safe egress time (RSET) [18].

2.3.2   ASET vs. RSET

The concept of ASET and RSET are typically used in performance-based design. ASET is a function of fire growth and development, which will be the period between the ignition of a fire until the conditions become untenable for humans [10].

$$ASET > RSET + safety\ margin \qquad (2.1)$$

RSET is a function of the occupants, which is the period from detection to safe evacuation. RSET is itself is determined based on relevant time components, such as detection, alarm, pre-movement and movement [19].

$$RSET = \max\left(t_{detection,i} + t_{alarm,i} + t_{pre-movement,i} + t_{movement,i}\right) \qquad (2.2)$$

The following figure summarizes the two concepts
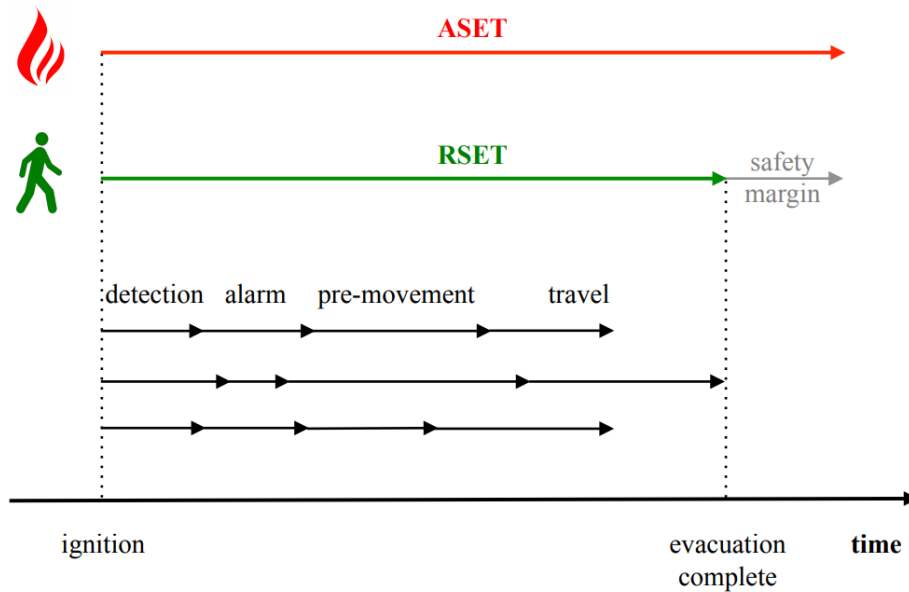
Figure 3 - Summary of the ASET-RSET concept. [19]

2.3.3 Acceptance Criteria

Many of the techniques used in scenario-based analysis offers the option to consider the effect of smoke and toxic gases on humans. That can be achieved by calculating and considering the concentration of the toxic gases produced by a fire and humans exposure time. To perform the scenario-based analysis, the FSE commonly use pre-define, absolute acceptance criteria for the different types of exposures [18].

The standards for tenability acceptance criteria vary from country to country. Furthermore, the article [18] compares absolute values for acceptance criteria for Sweden (BBRAD 3) and New Zealand (C/VM2), which are defined in their regulations. The comparison is presented in Table 3.

Criteria	BBRAD 3 (1)	C/VM2 (1)
Smoke layer above floor level	$Smoke\ layer > 1{,}6 + (ceiling\ height) \cdot 0{,}1\ [m]$	-
Visibility $> 100\ m^2$ $< 100\ m^2$	$Visibility > 10\ m$ $(for\ spaces > 100\ m^2)$	$Visibility_{(2)} > 10\ m$ $(for\ spaces > 100\ m^2)$
	$Visibility > 5\ m$ $(for\ spaces < 100\ m^2)$	$Visibility_{(2)} > 5\ m$ $(for\ spaces < 100\ m^2)$
Thermal radiation	$Radiation < 2{,}5\ \frac{kW}{m^2}$ or a short-term radiation of $< 10\ \frac{kW}{m^2}$ combined with a maximum energy dose of $< 60\ \frac{kJ}{m^2}$ in excess of the energy from a radiation level of $1\ \frac{kW}{m^2}$	Requirements for radiation exposure along egress routes
Temperature	Gas temperature $< 80\ ℃$	$FED_{thermal}$ criteria specified

10

Carbon monoxide toxicity	CO < 2000 ppm	FED_{CO} criteria specified
Carbon Dioxide	$CO_2 < 5\%$	-
Oxygen availability	$O_2 > 15\%$	-
FED	-	$FED_{CO} < 0,3$ $FED_{thermal} < 0,3$ (2)
(1) 2.0 meters above the walking surface *(2)* Does not apply to buildings with sprinklers with fewer people than 1000.		

Table 3 - Comparison of acceptance criteria in the Swedish and New Zealand building regulations [18].

As seen in the table above, the acceptance criteria vary. The acceptance criteria defined in New Zealand building regulations will be used to in the scenario-based risk analysis for toxicity and visibility criteria, while the temperature criteria in BBRAD is used heat exposures. These criteria will be used to examine when untenable conditions will be reached for the different fire scenarios and determine ASET.

2.4   Discussion and conclusion

The discussion and conclusion are based on the results and findings of the fire and evacuation scenarios. A goal of the discussion will be to emphasize the results and findings through this work without excluding uncertainties and possible sources of error. The research questions in Chapter 1.4 and will be attempted answered to reach a conclusion on the thesis statement.

3 Theory

This chapter provides theory for the thesis. The objective of this chapter is to present the reader with relevant theory on tunnel fire dynamics, human behavior, and road tunnel regulations in Norway.

3.1. Tunnel fire dynamics

Significant theoretical- and experimental work was carried out in the 1950s and 1960s in order to gain basic knowledge about fire physics in tunnels. In 1980s and 1990s this work was followed up by numerical applications [7].

3.1.1 Fuel- and ventilation- controlled fires

The fire development in buildings and tunnels will have different characteristics. Compartment fires are commonly defined as either fuel-controlled or ventilation-controlled. In a fire growth stage, the fire will usually be dependent on the access of fuel due to the available oxygen in air. As the fire grows, the fire will need more oxygen to maintain its combustion. During the growth period, the fire will at some point transition to rapid *flashover* period or start to decay. Therefore, in the early phase of a compartment fire, the fire is characterized as *fuel-controlled*. As available oxygen in the compartment is being used, the inflow of oxygen through openings into the compartment will dictate the fire growth. At this point we characterize the fire as *ventilation-controlled*. [7]

There is usually sufficient access to air in tunnels, which means that tunnel fires generally are fuel-controlled. This is because tunnels usually have two or more portals which transports air through the tunnel. Pressure differences between the fire gases and the atmosphere, and possibly the pressure difference between the portals supplies the fire with air. However, tunnel fires might become ventilation-controlled when the air supply becomes insufficient to sustain a complete combustion. In order for that, a large fire needs to occur. The fires in Mont Blanc-, Tauern- and the St- Gotthard tunnels are examples of severe fires which became ventilation-controlled. [7]

3.1.2 Heat Release Rate (HRR) and Fire Growth

The HRR tend to develop very fast in tunnels, as seen in previous full-scale experiments of vehicle fires [9], [11], [16]. In the Runehamar fire tests in 2003 [16], the peak HRR was reached between 8 – 18,5 minutes after ignition. The same fire tests showed that peak HRR from HGV-

mock up fire tests were in the range of 71 to 203 MW. Furthermore, the road and rail vehicles in the EUREKA tests [10] had a fast fire development the first 10-15 minutes, and the Singapore 2012 fire test [12] reached a peak HRR of 150 MW after 13,5 minutes. The full-scale tunnel fire tests indicates that the HRR develop rapidly and can reach high HRR.

An important reason for the high HRR of tunnel fires are the geometry of the tunnel. While smoke in open fires tend to be transported vertically, the smoke in tunnel fires will be transported horisontally. As a result, a hot smokelayer will accumulate in the vicinity of the fire source and transmit thermal radiation back to the fire. The additional heat feedback from the smokelayer will cause the HRR to increase. The following Figure 4 llustrates the heat feedback (a) and the transport of air (b).
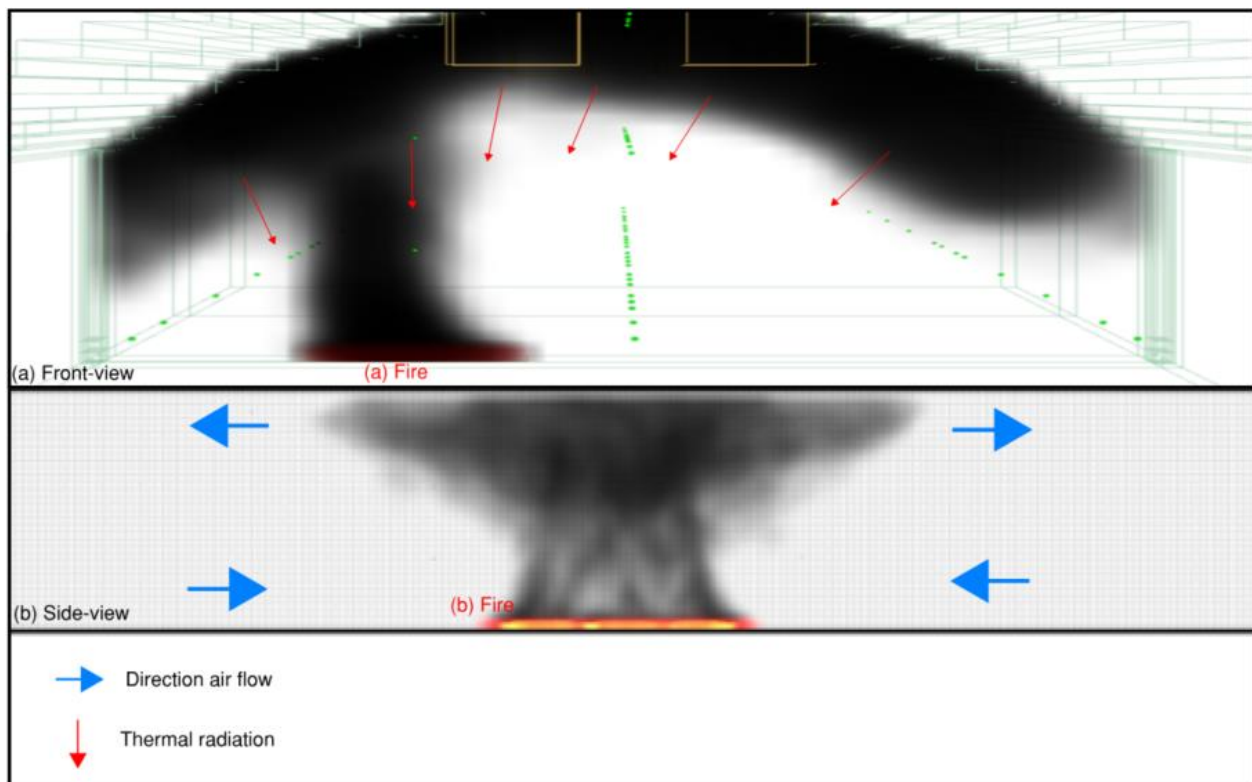
Figure 4 - Simplified illustration of the initial stages a tunnel fire showing thermal radiation and air flow directions.

Furthermore, the ignition source is significant for potential fire growth in road tunnels. The period in which ignition turns into a visible fire growth and start creating smoke is called the incipient period. [7] This incipient period can last for seconds or minutes and are usually not for full-scale tunnel fire tests because of the challenges to control it. After a potential ignition, the geometry of the fuel and height of the flames will play the most important role. Another

13

important parameter for fire growth is the mechanical air flow. In the book of tunnel fire dynamics [7] the following equation have presented to express the fire growth rate as a function of ventilation velocity,

$$\frac{dQ}{dt} = 1{,}2 \times 10^{-3} u_o \sum_{i=1}^{N} C_{f,i} w_{p,i} \tag{3.1}$$

where u_0 $[\frac{m}{s}]$ is the air velocity in the vicinity of the HGV, $C_{f,i}$ is the material property and the wet perimeter, $w_{p,i}$. [m]

3.1.3 Smoke, smoke spread and stratification in tunnels

Smoke is a mixture of gaseous, particulate matter as well as air, which is a result of fire combustion and air entrainment into the fire. [20] Hot smoke creates a pressure difference between the hot smoke and ambient air, which results in a buoyancy force. The smoke flows upwards and hit the tunnel ceiling. Moreover, the hot smoke will travel along the ceiling of the tunnel.

Ventilation velocity and the buoyancy forces created by fire will decide how the stratification of smoke will behave [7]. The spread of smoke during tunnel fires can be divided into two phases. In the beginning of a fire, a smoke front will develop. This smoke front will continue to move along the tunnel until the it reaches an exit. In the developing stage, the smoke continuously moves at a certain velocity. When the smoke reaches an exit portal to the outside, the smoke stratification in becomes stable [21].

Fire source   Smoke front   Fire source

a) The development stage   b) The stable stage
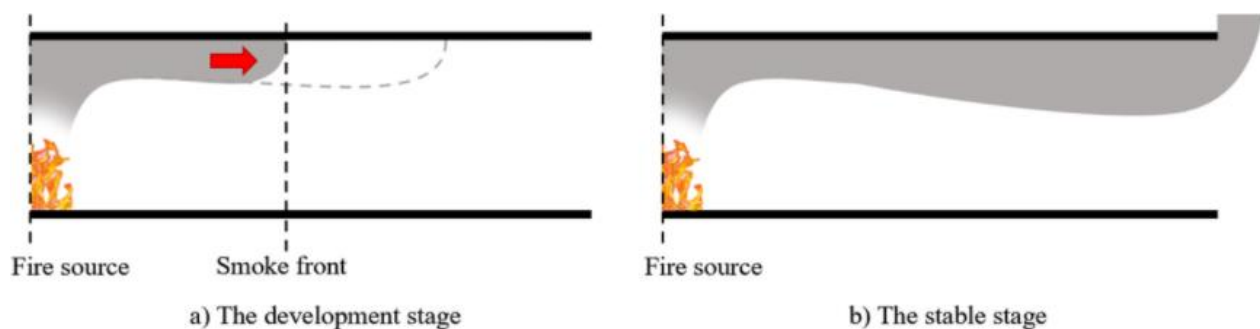
Figure 5 - The two phases of smoke spread [21].

During a fire, smoke- movement, -descent behavior, -temperature, and temperature distribution in the tunnel are important factors. [22] The smoke has a direct influence on safety in road tunnels

and are important to control, which will be discussed in later chapters. The HRR of the vehicles are the most important factor in a tunnel fire to describe its development and likely consequence. Factors such as geometry and ventilation in the tunnel, as well as ignition source, vehicle type, carried load and technical conditions are also important to consider [7] [23]. Therefore, it might difficult to predict precisely how fast a vehicle fire will develop.

3.1.4   Ventilation

Mechanical ventilation is an important safety measure in road tunnels. There are different types of ventilation systems in tunnels. The two main systems are longitudinal- and transverse ventilation. Transverse ventilation can be furthered divided into fully transverse, supply semi-transverse and exhaust semi-transverse systems [24]. The Langnes tunnel have a typical longitudinal ventilation system, which are common in Norway.

Longitudinal ventilations are typically sufficient when the ventilation thrust is equal or exceeds the pressure losses created by air flow from a fire source [25]. This is achieved when air velocity from jet fans exceeds the opposing air flow from the fire, commonly called "critical velocity". The term critical velocity is characterized by the minimum steady state air velocity in the tunnel to prevent back-layering. According to [10], the air flow is dependent on the number of active jet fans and thrust and does not depend on the configuration of the jet fans. Several models can be used to determine critical velocity [25]. E.g, the following equation can be used to determine critical velocity, V_c, given in NFPA 502 Annex D [26]:

$$V_c = K_1 K_g \left(\frac{gHQ}{\rho C_p A T_f} \right)^{\frac{1}{3}}, \tag{3.1}$$

where K_1 is 0.606 (Froude number factor, $Fr^{-\frac{1}{3}}$. K_g is the grade factor, g is the acceleration cause by gravity $[\frac{m}{s^2}]$, H is the height of the tunnel [m], Q is the HRR, ρ is the average density of the approaching air, C_p is the specific heat of air $\left[\frac{kJ}{kgK}\right]$, T_f is the average temperature of the gases from the fire [K], and T is the temperature of the approaching air [K]. Figure 6 illustrate a longitudinal ventilation system which does not provide sufficient air flow to prevent backlayering.
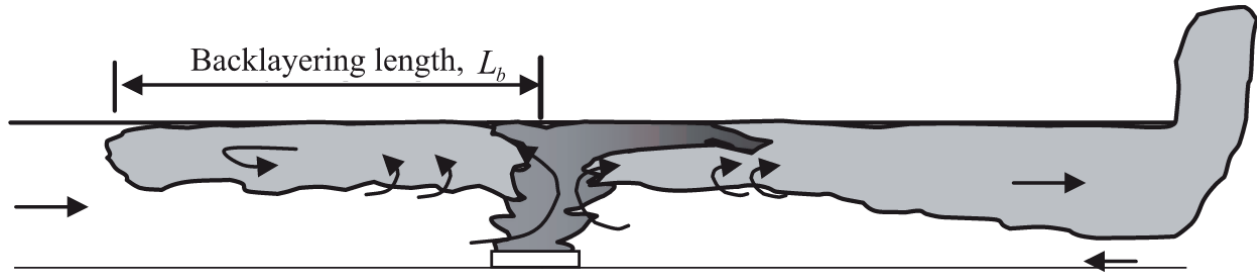
Figure 6 - A sketch showing flow velocity < V_c from [7].

Figure 7 illustrate a longitudinal ventilation system that provide sufficient air flow to prevent backlayering.
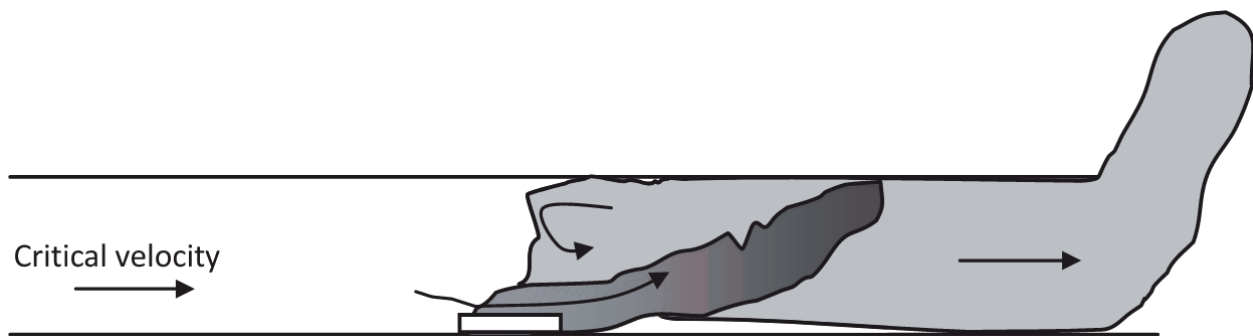
Figure 7 - A sketch showing flow velocity > V_c from [7].

The prevention of backlayering is one of the most researched topics in tunnel fire safety. Keeping on side of the fire clear of smoke are important for firefighters to reach the fire and extinguish it at an early stage. An experiment was carried out in [27] to investigate the optimal extinguishing distances. The results show that the nozzle types; Akron and Fogfighter, were able to fully cover the target at a distance between 9 m and 12 m. In the experiment, the flow rate for the nozzle types were between 115 – 360 L/min and the fire engine provided a discharge pressure of 7 bar.

3.2.   Human behaviour

Human behaviour is complex, and there is currently no comprehensive theory of human fire response. Therefore, human response to fires is often briefly categorized into two main periods; (1) pre-evacuation period and (2) movement period [28].
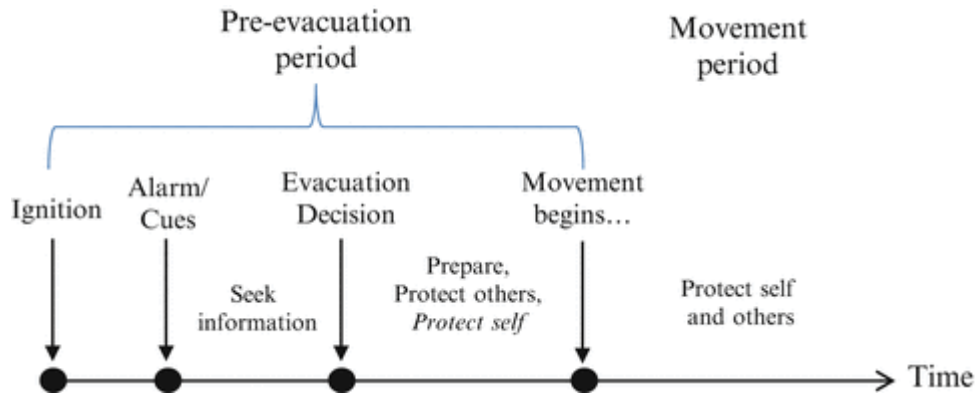
Figure 8 - Timeline of a human response to a building fire emergency [28]

The pre-evacuation period can further be divided into several sub-phases: pre-alarm phase, evacuation decision-making phase and protective action phase. These phases are important to understand because the pre-evacuation period might be significantly longer than the movement period itself [28].

- The pre-alarm phase is the time from ignition until the alarm initiates. In this phase, the occupants will be exposed to cues about a fire event ether by seeing smoke, hearing the alarm, or talking to other people. For a tunnel fire, the pre-alarm phase is typically the time occupants use to stop and step out of the vehicle [29].

- The evacuation decision-making phase us the phase where occupants are exposed to cues or seek out information about the (fire) event. Based on the information the occupants get, they will decide whether it is necessary to evacuate.

- In the protective action phase, occupants typically prepare themselves for evacuation e.g., by gathering belongings or assisting others to prepare for evacuation.

According to Byggforsk [30] there are three main factors that affect the evacuation conditions in buildings. The three main factors are building conditions, occupants, and organisational conditions. For buildings there are usually more options when it comes to adapting the building design for safe evacuation. Fire sections, placement and width of evacuation routes etc. are measures that can increase RSET and decrease RSET, which can be difficult and impractical to develop in bi-directional road tunnels. Therefore, active measures to improve the RSET such as fire alarm systems and guidance- and light systems are especially important for road tunnels. The purpose of active safety measures is early detection, and good information about evacuation out of the building/enclosure [30].

17

Most literature of human behaviour during fires are related to building fires, and literature on tunnel evacuation behaviour is relatively scarce and new [10]. To understand egress behaviour in road tunnels it requires an understanding of factors that shape human behaviour. The author emphasizes importance of active measures to give tunnel users the preconditions for making as effective egress decisions. More knowledge of human behaviour in tunnel can improve both evacuation- and rescue plans. In the research report [27], the following three key characteristics for occupants during tunnel fires are mentioned:

➢ Typically, the occupants sit and wait in the car for more information about the incident or for the queue to start moving.
➢ Occupants moving along the tunnel prefers to exit through the main portal instead of using emergency exits.
➢ Occupants could survive for long periods of time, depending on the concentration of toxic gases and other variables.

The walking speed in road tunnels varies depending on the people. According to the research article from NordFoU [29], the walking speed will be in the interval between 1 m/s to 2 m/s on surfaces with slope < 3 %. The average walking speed for people without physical disabilities are 1,5 m/s [29]. Furthermore, there are research with similar results. In the urban tunnel evacuation experiment performed by Y. Zhang et. al [31], involving safety measures for lightning, alarms and information signs, the average speed was around 1.5 m/s. However, the speed fluctuated in periods where participants would run, stop, look and continue to move. A few of the participants explained this by being anxious about missing guide- and/or exit signs while evacuating [31].

Stress might increase the likelihood of choosing the wrong actions during evacuation [32]. The experiment in [31] indicates that the evacuation without alarm sound caused less anxiety to the participants compared to participants exposed to alarm sound. Furthermore, some participants in the experiment without signs experienced high level of anxiety.

3.3. Rules and regulations: Road tunnels

The regulation on minimum safety requirements for certain road tunnels [33] are valid for new and existing road tunnels in Norway. The purpose of the regulation is to provide a minimum acceptable level of safety for tunnel users. This is achieved by requirements to prevent critical events, which can pose threats to human lives, the environment, and the tunnel structures, and to ensure protection in case of accidents. For existing road tunnels which does not fulfil the requirements, the tunnel manager should propose a plan for improving safety levels. The Norwegian Public Roads Administration (NRPA) are responsible to ensure that the measures provide acceptable safety levels for the existing tunnel [33].

The NRPA have published the Handbook N500 [17] which provides standards for road tunnels in Norway.

3.3.1   Tunnel classification

In Norway, the required safety measures and -equipments for a tunnel is decided by its tunnel classification. The tunnel classification depends the annual average daily traffic (AADT) and the tunnel length [17]. There are some differences to the Norwegian and the EU tunnel classifications. In the EU directive 2004/54EC [2], the AADT are replaced by the term vehicles per lane, which is AADT/number of lanes.

Norwegian classification/risk degree	Description	EU classification	Description
A	ÅDT < 300	Vehicles per lane < 2 000	500 – 1 000 m
B	ÅDT < 4 000		> 1 000 m
C	AADT < 8 000	Vehicles per lane > 2 000	500 – 1 000 m
D	AADT < 12 000 Length < 2 500 m		1 000 – 3 000 m
E	AADT > 12 000		> 3 000 m
F	AADT > 50 000		

Table 4 -Comparison of tunnel classification in Norway and the EU

3.3.2   Ventilation in Road Tunnels

Tunnel ventilation is an important issue when designing tunnels [24]. According to the N500 Standard, all tunnels with AADT > 1 000 or tunnels longer than 1 000 m and with AADT > 1 000 must have a ventilation system. The ventilation system should also be dimensioned to handle

fires and heat exposures between 200 - 400 ℃. The requirements for fire ventilations in low inclined (<2%) road tunnels are as follows [17]:

Tunnel classification	Tunnel length [m]	Dimensioned HRR [MW]	Exposure curve	Time [min]	Minimum air velocity [m/s]
A	> 1 000	50	HC	60	3,0
B	> 1 000	50	HC	60	3,0
C	> 1 000	50	HC	60	3,0
D	< 2 000	50	HC	60	3,0
	> 2 000	100	HC	60	4,5
E	> 1 000	50	HC	60	3,0
F	< 2 000	50	HC	60	3,0
	> 2 000	100	HC	60	4,5

Table 5 - The requirements for fire ventilation in low inclined (<2%) road tunnels in Norway [17]

The N500 handbook [17] have less guidelines related to longitudinal ventilation in bi-directional road tunnels compared with the EU Directive 2004/54/EC [2]. According to [2], longitudinal ventilation should not be allowed in bi-directional tunnels unless the risks are found acceptable and/or by implementation of specific measures. Appropriate traffic management, shorter emergency exit distances, smoke exhaust system are examples of acceptable measures.

3.3.3   Safety Measures in Road Tunnels

Minimum requirements		N500 Handbook	EU Directive 2004/54/EC
Lighting	Evacuation lightning	Mandatory for all tunnels. Lights every 25 m for tunnels < 5 000 m. Continuous lights for tunnels > 5 000 m.	Mandatory for all tunnels. Maximum height 1,5 m.
Ventilation	Mechanical ventilation	Mandatory for tunnels more than 1 000 m when AADT > 1 000.	Mandatory for tunnels more than 1 000 m when traffic volume > 2 000 vehicles per lane. Transverse ventilation in bi-directional tunnels with a control centre.
Emergency stations	Stations with emergency telephone and extinguishers.	Mandatory. Each 125 m for new tunnels Each 250 m for existing tunnels	Mandatory with exceptions. Each 125 m for new tunnels Each 250 m for existing tunnels
Water supply	To ensure sufficient water for the fire services	Mandatory. At least every 250 m.	Mandatory. At least every 250 m.
Control centre		Mandatory in tunnels with video surveillance	Mandatory for tunnels more than 3 000 m when traffic volume > 2 000 vehicles per lane.

Monitoring systems	Video	Mandatory for tunnels > 3 000 m with AADT > 4 000. Mandatory for tunnels > 5 000 m with AADT > 300.	Mandatory for tunnels with control centre.
	Automatic incident detection and/ or fire detection	Mandatory for tunnels with automatic incident detection.	Mandatory for all tunnels
Equipment to close the tunnel	Means to stop approaching vehicles	Mandatory in all tunnels	Mandatory in tunnels > 1 000 m
Communication systems	Radio broadcast for tunnel users	Mandatory in all tunnels	Mandatory in all tunnels
	Loudspeaker system	Mandatory for tunnels > 3 000 m with AADT > 4 000, and tunnels > 5 000 with AADT > 300.	Mandatory in all tunnels
Emergency power supply		Mandatory in all tunnels	Mandatory in all tunnels
Fire resistance of equipment		Mandatory in all tunnels	Mandatory in all tunnels

Table 6 - Comparison of minimum requirements in Norwegian and the EU regulations.

4   Case Study

This chapter describes the case study of the Langnes tunnel in Norway. The existing road tunnel in the city of Tromso was constructed in 1988. The tunnel is included in a complex system of several road tunnels, the Tromso tunnel system, connected by underground roundabouts.

4.1   The Tunnel

The Langnes tunnel is a bi-directional road tunnel with a length of 1700 m. The tunnel connects the urban areas west of Tromsø to the city centre in the east. According to information, the tunnel has the tunnel classification D. This is an important tunnel for commuters as the tunnel provide effective transportation links between different parts in the city. Car queues in the tunnel is quite common during rush hours, both outside and inside the tunnel. According to traffic data [1] from the Norwegian Public Roads Administration (NPRA), the tunnel had an annual average daily vehicle (AADT) of 16 000 in 2019. Based on information given by the county, the AADT is expected to increase to 16 500 in 2031
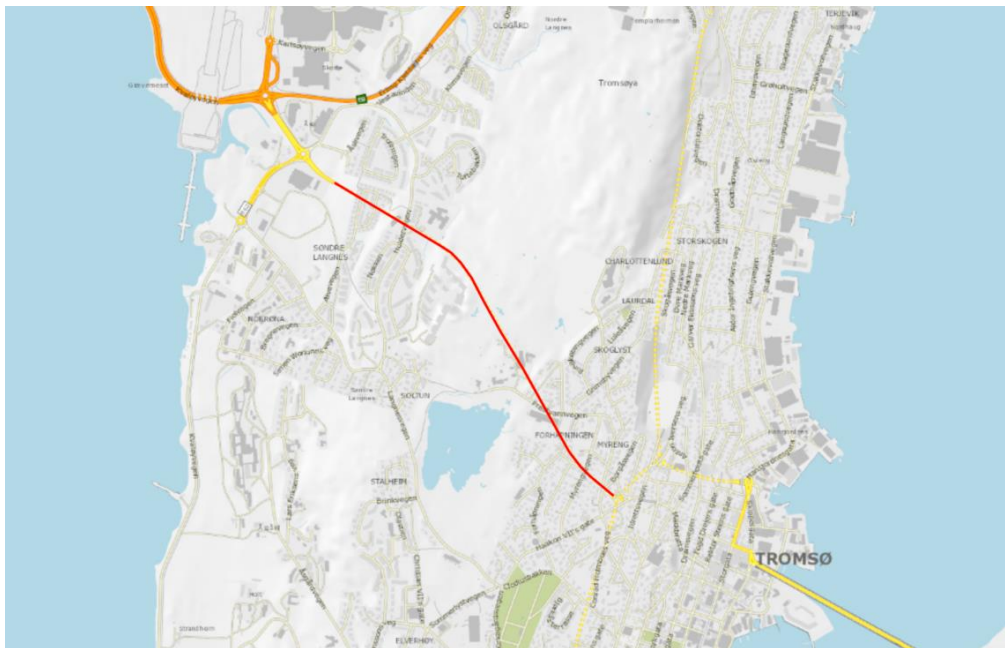
Figure 9 - Situational map of the tunnel (in red) [1]

There are 7 *emergency lay-bys* in the tunnel approximately every 250-meter, and 22 emergency stations with phones and hand-held fire extinguishers every 500-meter. Fire extinguishers are located every 250-meter and the electrical guidance system consists of evacuation lights every

62,5-meter. The fire department is located less than 2 km from the tunnel. Hence, effort times are expected to be between 5-10 minutes in the Langnes tunnel.

4.2   Tunnel Geometry

The tunnel is design with a conventional "horse-shoe" shape, equivalent to a T9,5 profile. As the tunnel is from the 1980s, variation in width and height were excepted. A profile measurement system for roads were used to get accurate measurements. The point-cloud system fulfills the requirements for road measurements in the international standards; ASTM E-1448-92 and European Standard EN 13036-8 [34]. Hence, the data is believed to provide accurate data of the tunnel. Furthermore, the point-cloud data was rendered and inspected in Autodesk ReCap [35], which made it possible to measure distances between optional points. The following figure shows the 3D model of the tunnel.

Figure 10 - An 3D model of the tunnel using point-cloud

The measurements identified variations in the height and width along the tunnel. To take the variations into account, the average height and width will be used for the case study. The following table describes the main characteristics of the tunnel.

Length	Height	Width	Cross-section
1700 m	Ca. 6,4 m	Ca. 10,4 m	Ca. 54-58 m^2

Table 7 - Main characteristics of the road tunnel
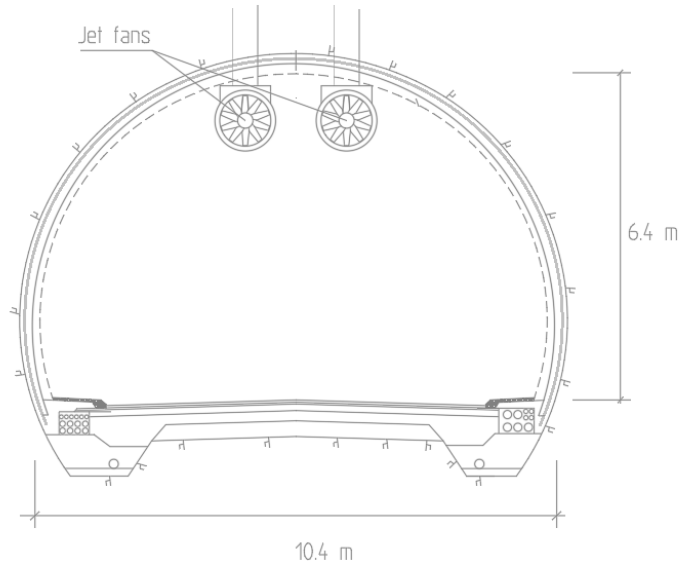
Figure 11 - Illustration of the tunnel cross-section

4.3   Longitudinal Ventilation

The tunnel is designed with longitudinal fire ventilation towards the west portal - Langnes. Each of the 16 jet fans has an effect of 15 kW and maximum air flow rate of 14.4 m^3/s. The configuration of the fans is three-by-two in the start and end of the tunnel, and two-by-two in the middle. Figure 12 illustrates the existing jet fan configuration.
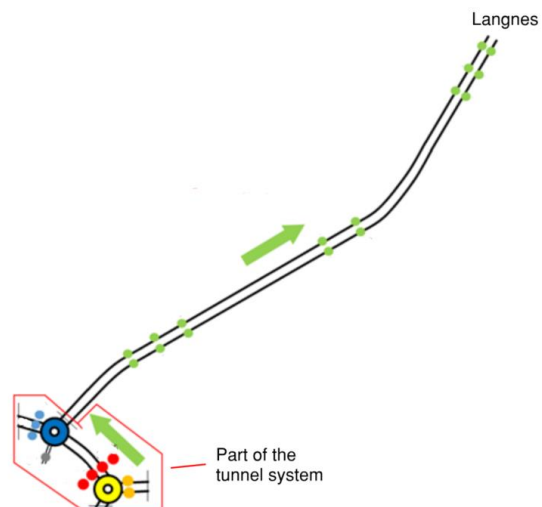
Figure 12 - The location of jet fans (green points) and ventilation direction (green arrow). The tunnel system (red) is not included in the fire simulations.

In normal operation, the effect jet fans are automatically set based on measurements from CO- and NO_2-sensors. The effect will be set to 100% capacity in case of fire. According to previous measurements, the fire ventilation is design to provide an air velocity of 3,5 m/s in the tunnel.

4.4   Technical summary of the tunnel

#	The Langnes tunnel
Tubes	1
Cross-section	Ca. T9,5 [17]
Tunnel classification	D [17]
Emergency exits	0
ADV	16 000, in 2019 [1]
Speed limit (km/hr)	50 & 70
Emergency stations	22
Fire extinguishers	44
Automatic road barriers	2
ITV / AID	No

Table 8 - Summary of technical measures and equipment in the road tunnel.

5   Simulation Set-Up

This chapter describes the simulation set-up used for the fire and evacuation simulations.

5.1   Fire Dynamics Simulator

The Fire Dynamics simulator (FDS) is a computational fluid dynamic (CFD) -solver that perform numerical calculations based on Navier-Stokes equations. The equations are appropriate for heat conduction and low-speed flows with emphasise on heat- and smoke transfer from fires. This study used FDS version 6.7.5. Turbulence is treated by Large Eddy Simulation (LES). The combustion model in FDS uses a single step, mixing-controlled reaction with air, fuel, and products. Fuel and products from the fire are computed. Furthermore, the equation for radiative heat transfer is solved through a similar technique to finite volume methods for convective transport. Given the complexity of radiation heat transfer, the finite volume solver requires about 20 % of the CPU time to perform the calculations [36].

5.2   Tunnel geometry and basic settings

The geometry in FDS is made of rectangular solids [36], which makes the tunnel model less complex than the realistic tunnel. Computational time and limitations in geometry made it necessary to perform some simplifications in the tunnel model design. Therefore, the study attempt to create a model that contain the main characteristics of the Langnes tunnel, related to height, width, cross-section and longitudinal ventilation. Furthermore, the 1% longitudinal gradient and a curve in the tunnel were neglected. The height and width were, respectively 10.4 m and 6.4 m, which resulted in a cross-section of 57.6 m². Figure 13 & 14 illustrates the cross-section and the length of the model.
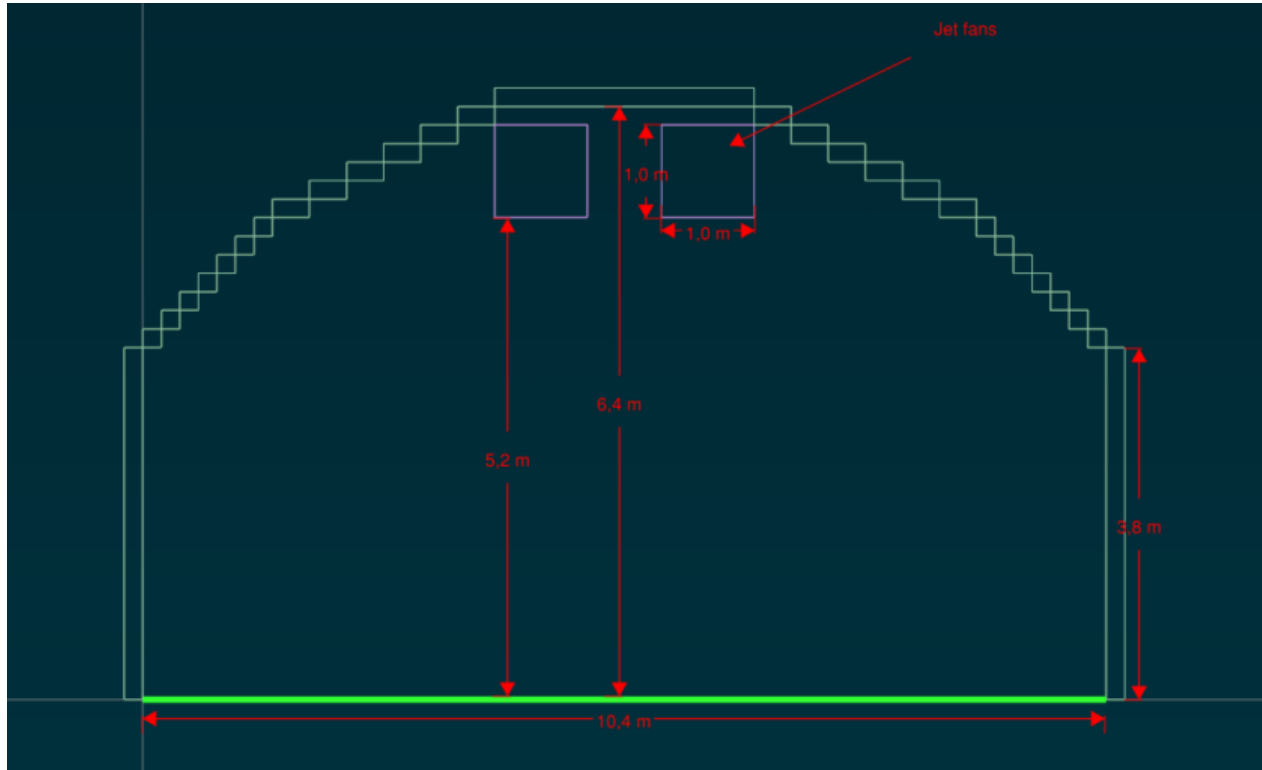
Figure 13 - Cross-section for the tunnel model

The walls and ceilings in the tunnel are defined as concrete with a constant density of 2280 kg/m³, specific heat of 1.04 kJ/kgK and conductivity of 1.8 W/mK. For all fire scenarios the 16 jet fans were set to provide an air flow of 14.4 m³/s (except for fire scenario 5, which were set to 30 m³/s) Ambient temperature is 5 ℃ for all the simulations.
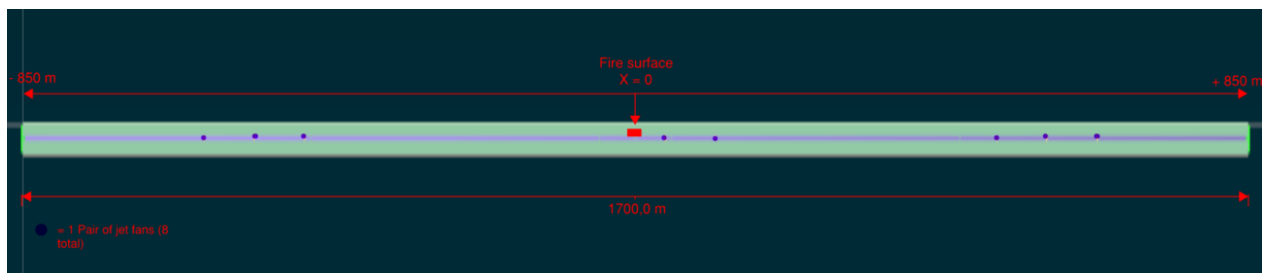
Figure 14 - Top-view illustration of the tunnel model

5.3   The Design Fire

Three different design fires were used for the simulations. The fire is designed to represent three unshielded HGV-fires with HRR of 50 MW, 100 MW and 200 MW. The fire surface was placed on the ground (Z=0) with an area of 16,7 m² and the dimensions 7.6 m (L) x 2.2 m (W).

27
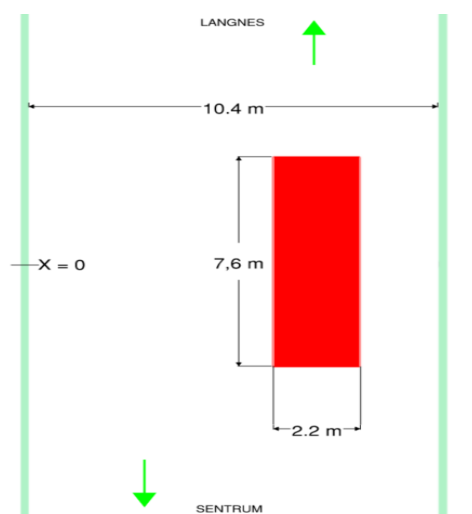
Figure 15 – Illustration of the fire surface

"Simple chemistry" approach in FDS [36] is used for the combustion reaction. The fire load of the HGV-fire was based on data from a full-scale test performed in a tunnel in Spain [37] [12]. In the tests, 48 plastic pallets and 180 wooden pallets were used for the HGV-mock up fire. A plastic and wood density of respectively, 1376 kg/m³ and 566 kg/m³ gives a mass fraction of 38% plastic $(CH_2)_n$ and 62% wood (CH_2O).The mass fraction combined gives the chemical formula $CH_2O_{0,62}$ [37] which is used in the FDS model.

5.4　Fire Scenarios

Six different fire scenarios are analysed in the middle of the tunnel. Fire scenario 1 - 3 are the main scenarios and include the existing longitudinal ventilation for the road tunnel.

Fire scenario # - Category	Description	Fire growth	Egress scenario # Reaction time
01 – 50 MW Fire	- 50 MW HGV-fire. - Fire ventilation starts after 2 minutes - 16 jet fans with existing configuration and air capacity of 14,4 m³/s each (3,4 m/s)	0 min – 6 min: Ultra-fast fire growth 6 min →: 7 MW/min	A01 – 1 min
			B01 – 3 min
			C01 – 5 min
			D01 – 7 min
			E01 – 9 min
02 – 100 MW Fire	- 100 MW HGV-fire. - Fire ventilation starts after 2 minutes - 16 jet fans with existing configuration and air	0 min – 6 min: Ultra-fast fire growth 6 min →: 7 MW/min	A02 – 1 min
			B02 – 3 min
			C02 – 5 min

	capacity of 14,4 m³/s each. (3,4 m/s)		D02 – 7 min
			E02 – 9 min
03 – 200 MW Fire	- 200 MW HGV-fire. - Fire ventilation starts after 2 minutes - 16 jet fans with existing configuration and air capacity of 14,4 m³/s each. (3,4 m/s)	0 min – 6 min: Ultra-fast fire growth 6 min →: 7 MW/min	A03 – 1 min
			B03 – 3 min
			C03 – 5 min
			D03 – 7 min
			E03 – 9 min

Table 9 - The fire scenarios which. 01-03 represent the existing tunnel configuration.

Fire scenario 4-6 contains changes to the existing fire model to investigate how differences might influence the results.

04 – Jet fans with even distribution	- 100 MW HGV-fire. - 16 jet fans in pairs with even distribution along the tunnel length and with air capacity of 14.4 m³/s each.	0 min – 6 min: Ultra-fast fire growth 6 min →: 7 MW/min	A04 – 1 min
			B04 – 3 min
			C04 – 5 min
			D04 – 7 min
			E04 – 9 min
05 – 4,5 m/s air velocity	100 MW HGV-fire. 16 jet fans in pairs with even distribution along the tunnel length and with air capacity of 30 m³/s each.	0 min – 6 min: Ultra-fast fire growth 6 min →: 9 MW/min	A05 – 1 min
			B05 – 3 min
			C05 – 5 min
			D05 – 7 min
			E05 – 9 min
06 – Robustness scenario	- 100 MW HGV-fire - 16 jet fans with existing configuration and air capacity of 14,4 m³/s each. (3,4 m/s) - After 8 minutes. Jet fans in the middle of the tunnel stops due to heat exposure and/or lack of reliability.	0 min – 6 min: Ultra-fast fire growth 6 min →: 7 MW/min	A06 – 1 min
			A06 – 3 min
			C06 – 5 min
			D06 – 7 min
			E06 – 9 min

Figure 16 - The fire scenarios 4-6 represents alternative tunnel configurations.

The report assumes the fire ventilation to start after 2 minutes (t = 120 seconds) upon detection. Additionally, the fire ventilation will take 2 minutes, t = [120,240], to reach maximum air

velocities. The average air velocity in the vicinity of the fire were measured to 3,4 m/s for the existing jet fan capacity.

The following parameters were used in the FDS model.

Parameter	Value	Description	Reference
Reaction material	Unshielded HGV mock-up	The fuel source consists of 180 wooden (566 kg/m³)- and 48 plastic pallets (1376 kg/m³). Mass fraction for the woods and plastics are 62% and 38%.	[37]
Chemical formula	$CH_2O_{0.62}$	Combines values for 62% wood $(CH_2O)_n$ and 38% plastic $(CH_2)_n$	[37]
Heat of combustion	25.5 MJ/kg	The combined heat of combustion based on wood (16,7 MJ/kg) and 38% plastic (40 MJ/kg) pallets.	Table 5.1 in [7]
Fire growth	116 kW/s 7 MW/min	Fire growth is calculated by considering the effect of air flow. The value corresponds to an average air velocity of 3,4 m/s and a wetted perimeter of 15,6 meter. 116 kW/s = 6.96 mW/min 9 MW/min for fire scenario 5.	[7]
Soot yield	0,032	Combines the soot yield of 0,06 g/g for PE and 0,015 g/g for wood. Table A.39 in the SFPE Handbook [38] provides information about yields for different materials.	Table A.39 in [38]
CO production	0,059	Combines the CO yield of 0,060 for PE-plastic and 0,058 g/g for wood.	Table 5 in [39]

Table 10 - Parameters in FDS model

5.5   Tenability criteria

The thesis will use the acceptance criteria mentioned in Table 3 in Chapter 3.5.2. The following table summarizes the criteria which will be assessed in the Chapter 7.

Parameter	Critical value
Toxicity	FED > 0.3
Visibility	Visibility < 5 m
Temperature	T > 80 ℃

Table 11- Summary of tenability criteria used in the thesis.

5.6   Grid and mesh sensitivity

The FDS model are divided into 5 meshes with specific cell sizes. For default simulations, each mesh is assigned to a specific processor, which are performing the fire calculations for each mesh. By having multiple meshes, each processor focuses on a single mesh which can significantly reduce simulation time. In general, the smaller cell sizes used, the more accurate results one can achieve. However, this will increase the simulation times further. Therefore, a goal when performing simulations in FDS will be to create a fire model with sufficient cell sizes so that simulations can be performed within a reasonable timeframe and with accurate results.

The fire mesh ("*Mesh03*") had the smallest grid size with all sides at 20 cm. The fire mesh was in the middle (x = [800,900]) of the tunnel. The grid size of other meshes were 40 cm. A fire mesh of 20 cm resulted in $\frac{D^*}{dx} > 20$ for all the fire scenarios, which is a measure of how the flow field is resolved. D* is the characteristic fire diameter [36].

$$D^* = \left(\frac{Q}{\rho_\infty c_p T_\infty \sqrt{g}}\right)^{\frac{2}{5}} \tag{5.5}$$

Equation 5.5 are explained in the FDS User Guide [36]. The mesh resolution results are presented in the following table.

Fire scenario	D*	$\dfrac{D^*}{dx}$
50 MW fire	4.7	23.5
100 MW fire	6.2	31
200 MW fire	8.2	40.6

Table 12 - Overview of mesh resolution results

$\frac{D^*}{dx}$ is recommended to be in the area of 4 and 16 to resolve the fire accurately, which is stated in [40] and several publications. It is worth mentioning that there is no clear rule on the D*/dx-ratio value. This is because the values will depend on what one is trying to accomplish with the fire simulations [36]. As seen in Table 12, the decided mesh resolution is more detailed than the recommended. Hence, the mesh resolution results indicate that the size of the fire mesh will provide accurate results.

Furthermore, the other meshes should be considered to assure the accurate transfer of data from the fire mesh to the other meshes. A 40 cm grid size were chosen for all meshes in the FDS

31

model, except the fire mesh with 20 cm grid size, as mentioned previously. To reach this decision, two fire simulations were conducted using 20 cm and 40 cm grid size meshes downstream of the fire with a simulation time of 15 minutes. The first sensitivity test was performed related to FED values for a 100 MW fire, while the second test were investigating the difference in visibility. The differences in FED values at 300 m downstream and 2 m above the floor are presented in Figure 17.
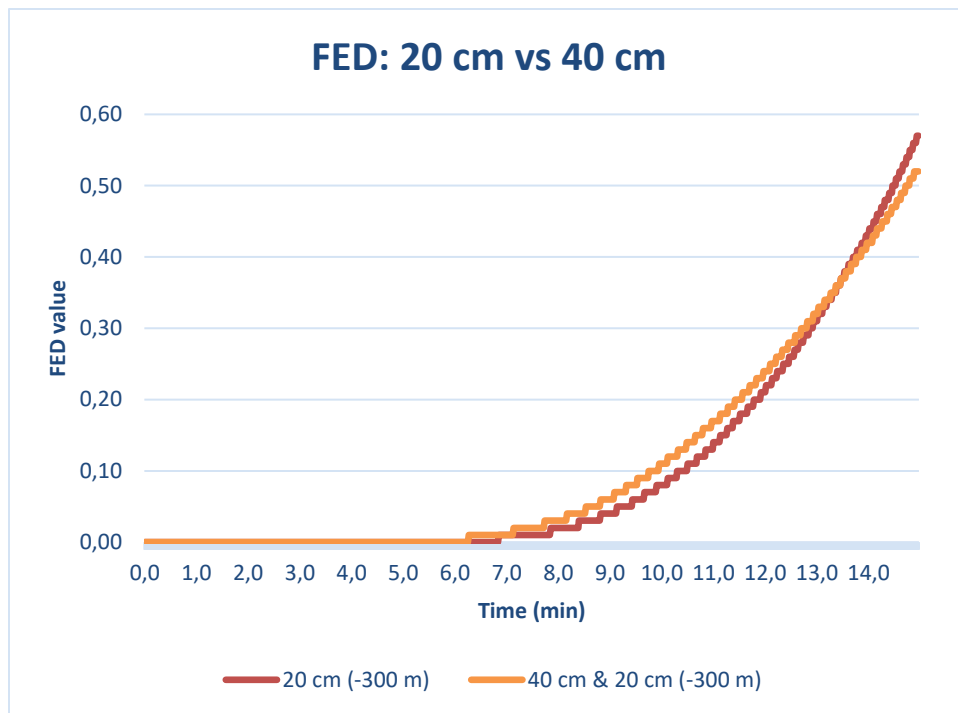
Figure 17 - FED output at 300 meters downstream and of the 100 MW HGV-fire using grid size of 20 cm and 40 cm between x = [0,800].

The results in Figure 17 show minor differences regarding FED values. For the 40 cm grid size the FED increases slightly faster for 10 minutes, while the fire simulation with 20 cm grid size has the highest FED increase afterwards. However, the differences are not significant the first 15 minutes. The visibility in the two simulations show some variations. Visibility begins decreasing earlier in the 40 cm grid simulation, which indicates that larger cells might affect the simulation results slightly. However, the visibility criteria are reached within a time difference of 30 seconds and begin stabilizing after 10 minutes. Figure 18 show the results in visibility at 300 m downstream and 2 m above the floor.
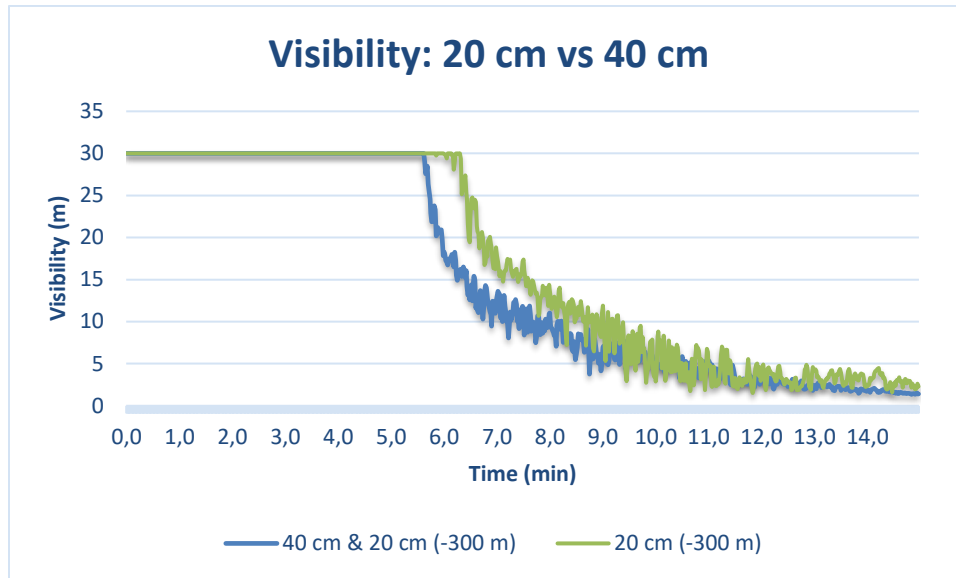
Figure 18 – Visibility output at 300 meters downstream of the 100 MW HGV-fire using grid size of 20 cm and 40 cm between x = [0,800].

Based on the analysis, a 40 cm mesh resolution downstream are concluded to provide accurate results. This is given by the similarities in results and equivalent time to reach performance criteria the two fire simulations results. Furthermore, the author emphasizes the duration of the fire scenarios presented in chapter 6. All the fire scenarios were performed for simulation times of between 25-30 minutes. For longer fire simulations, further considerations regarding grid size might be necessary. However, the mesh resolution used in this study are believed to resolve the fire accurately within a reasonable timeframe.

5.7   Evacuation precondition

The evacuation conditions will depend on the traffic flow at the time of the fire. There has not been performed extensive analysis of traffic. Therefore, assumptions were made based on the AADT = 16 500 (expected traffic in 2031). The report assumes that 60% of the total AADT passes through the tunnel during rush hours between 06:00 – 09:00 and 15:00 – 18:00. This 6-hour period will represent the period in which the most people might be present in the tunnel and exposed to a fire event. The following assumptions were made to quantify the amount of people in the tunnel during the rush hour period:

➢ 1,5 people in each vehicle
➢ Traffic flow of 30 vehicles per minute.

- At the time of ignition, t = 0, there are 30 vehicles on each side of the fire. The vehicles past the fire location drives safely out.

- The tunnel closes in each direction upon fire detection, t = 2 min. Between t = [0 min, 2 min], 30 vehicles drives into the tunnel in each direction.

- 20 vehicles are able to turn around and drive safely out of the tunnel

- A total of 100 vehicles will be present in the tunnel, i.e. in total 150 people.

- An even distribution of occupants on each side of the tunnel.

5.7.1 Reaction time

Evacuation is not a common practice for most people. In general, there are high uncertainties related to how humans will behave during an event which require evasive actions. According to [32], human's reaction to a fire situation is characterized by uncertainties, misunderstandings and ineffectiveness, which can result in slow reaction times. Therefore, the evacuation simulations are performed with reaction times of (A) 1-min, (B) 3-min and (C) – 5-min, (D) – 7-min and (E) – 9-min. Evacuation time will increase as a result of larger reaction times. Hence, the study attempts, if needed, to identify a maximum reaction time. A disability factor of 0.8 is chosen to account for elderly and people with disabilities during evacuation simulations. The relationship between the factor and the average walking speed of 1.5 m/s, presented in Chapter 3, results in a walking speed of 1.2 m/s for the evacuees in the evacuation simulations.

The evacuation model is divided into 4 evacuation groups, respectively, A1, A2, B1 and B2. Group A1 and A2 evacuate downstream of the fire, while group B1 and B2 evacuate upstream of the fire. The occupants in group A1 and B1 are located less than 200 m from the fire source. Group A2 and B2 are located between 200 and 600 m from the fire source. These groups are not able to get information about the fire at first-hand. Furthermore, the reaction time for group A2 and B2 are set to 4 minutes.
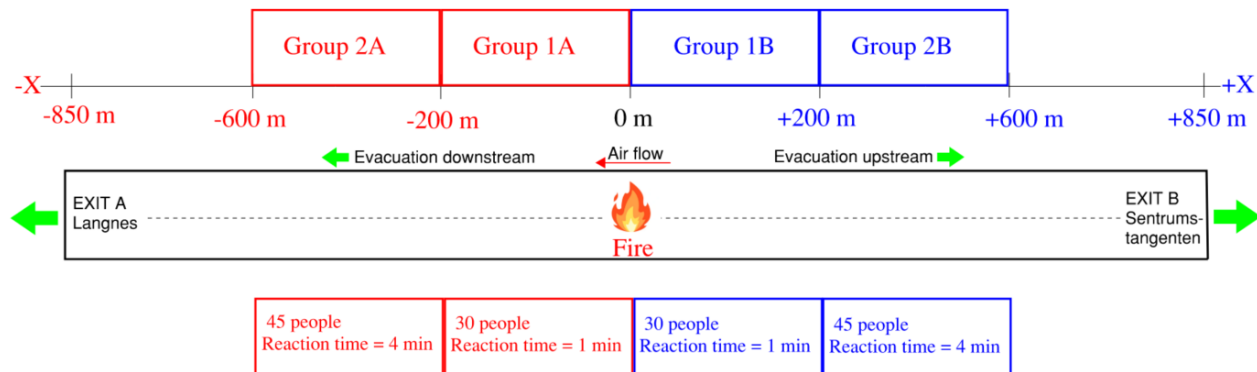
Figure 19 - Illustration of the egress groups and reaction times for the (A) 1-minute delay simulations.

5.8   Challenges with FDS

In general, FDS simulations will provide more accurate results compared with hand calculations or two-zone models. This is mainly because FDS can account for parameters which more simpler models are not able to. However, the results should be treated critically. The simplifications in the FDS model should be considered, as that could influence the results, without being apparent to the user. Uncertainties related to FDS will discussed in Chapter (7.6). Following, some of the challenges related to numerical instabilities with the FDS tunnel model will be presented.

5.8.1   Numerical instabilities

The fire scenario with 50 MW were completed without issues, however, the 100 MW and 200 MW fire scenarios stopped. After t = 1100 s, high fluctuations in pressure fields caused numerical instabilities for both of the, 100 MW and 200 MW simulations. The FDS User Guide [36] recommends creating as cubic shaped cells as possible to avoid instabilities, which were considered to fix the issues with the 100 MW and 200 MW fire. Originally, the fire mesh had a width, length and height of respectively, 20-, 20- and 19 cm. As a result, the length, width and height of the grids were changed to 20 cm. However, the issue was not resolved. Furthermore, the user guide recommends creating small air vents to avoid high fluctuations in pressure. Five small air vents were added on each side of the fire. For this case, the small air vents fixed the issues for the 100 MW fire and managed to prolong the simulation time for 200 MW fire. The 200 MW fire

35

stopped after ca. 29 minutes of the 45 minutes of simulation, which were considered enough time for the study.

5.9 Measurements

This section gives an explanation on how visibility and fractional effective dose are measured in the thesis.

5.9.1 Visibility

The visibility in tunnel fires is important to consider. Generally, the more optical dense the smoke- and gas particles are, the less visible objects become through the smoke. Low visibility might reduce the effectiveness of both evacuation and emergency efforts. To quantify the visibility, devices to measure the visibility are placed at different lengths in the model. The visibility through smoke is determined by using the following equation [36]

$$S = \frac{C}{K} \, , \tag{5.1}$$

where C is the non-dimensional constant characteristic of the object being view through smoke and K is the extinction coefficient. For structures with light-emitting signs, the recommended value of C = 5 – 10. The Langnes tunnel has illuminated signs. Hence, C = 8 are using in the simulations which might be a reasonable value for C. K is calculated using the following light extinction equation [41]

$$K = K_m \rho_s \, , \tag{5.1a}$$

where K_m is mass specific extinction coefficient which is $8700\,\frac{m^2}{kg}$ with an uncertainty $\pm$ $1100\,\frac{m^2}{kg}$. The value for K_m are recommended for flaming fires and is the default value in FDS [41]. Furthermore, ρ_s is the smoke density $(\frac{kg}{m^2})$. The smoke density depends on the soot yield, which is defined as mass fraction of fuel that is converted into soot in the "simple chemistry" approach is used.

5.9.2 Fraction Effective Dose (FED)

The FED index is a common measure of human incapacitation due to toxic gases from a fire. There are placed devices at 2 m heights at different lengths to measure FED values at several locations in the tunnel. The following equation are used to calculate FED values in FDS.

$$FED_{tot} = (FED_{CO} + FED_{CN} + FED_{NOx} + FLD_{irr}) \cdot HV_{CO2} + FED_{O2} \qquad (5.2)$$

Equation 5.2 are explained in further detail in the FDS User's Guide [36]. The FED values are dependent on factors such as fire characteristics, ventilation effects, tunnel geometry etc. Hence, the FED values might represent uncertainty related to the actual tenable conditions in the tunnel. This is because of the small geometrical variations in the existing road tunnel, which can be a challenge to model in FDS. However, the FED values might be valuable in terms of comparing the values with different configurations in the tunnel model. Furthermore, FED values are calculated for each occupant during the evacuation scenarios in Pathfinder. The calculated FED values for each occupant can be used to compare differences related to where occupants are in the tunnel.

The Pathfinder User Manual [42] describes how output data from FDS can be used. Pathfinder uses the PLOT3D data output from FDS for; *CO -, CO_2 - and O_2 Volume Fractions*. Pathfinder limits the results to the concentrations of the narcotic gases CO, CO_2 and O_2 . These outputs will be used to calculate the FED values each evacuee that are exposed over time [42]. According to the Technical Reference Manual [43], the following equation can be used to calculate FED.

$$FED_{tot} = FED_{CO} \cdot V_{CO_2} + FED_{O_2} , \qquad (5.3)$$

Equation 5.3 only considers the effect of increased breathing rate by CO_2 which are related to increased uptake of CO. FED_{CO} is the fraction of an incapacitating dose of CO,

$$FED_{CO} = \frac{(3.317 \cdot 10^{-5})[CO]^{1.036}(V)(t)}{D} \qquad (5.3a)$$

where [CO] is the carbon monoxide concentration (ppm v/v $20°C$), V is the volume of air breathed each minute (L/min) which is assumed to be 25 L/min for activity level of light work and walking to escape, t is time (min) and D is exposure dose (% COHb) which is assumed to be 30% for the activity level described above. The effects of CO_2 related to increased uptake of air is given by the multiplication factor given by e

$$V_{CO_2} = \frac{\exp(0.1903 \cdot \%CO_2 + 2.0004)}{7.1}, \qquad (5.3b)$$

where $\%CO_2$ is the volume fraction of CO_2 (v/v). For the fraction of an incapacitation dose of low O_2 hypoxia is calculated with the following equation

$$FED_{O_2} = \frac{t}{\exp\big(8.13 - 0.54(20.9 - \%O_2)\big)}, \qquad (5.3c)$$

where t is time (min) and $\%O_2$ is the volume fraction of O_2 (v/v).

6 Results

This chapter presents the results for the fire- and evacuation simulations. All the fire scenarios lasted for a minimum of 25 minutes (1500s). The sections 6.1 - 6.4 present the fire results from FDS, while section 6.5 show the evacuation results related to evacuation time and FED exposure from Pathfinder. Finally, a summary of the FDS is presented in section 6.6.

6.1 Heat Release Rate

The HRR for the following fire scenarios are presented: (1) 50 MW HGV-fire, (2) 100 MW HGV-fire, (3) 200 MW HGV-fire, (4) Fans evenly distributed in the tunnel (5) 4,5 m/s air velocity, and (6) Middle fans stop. HRR of 100 MW were used for the last three fire scenarios.
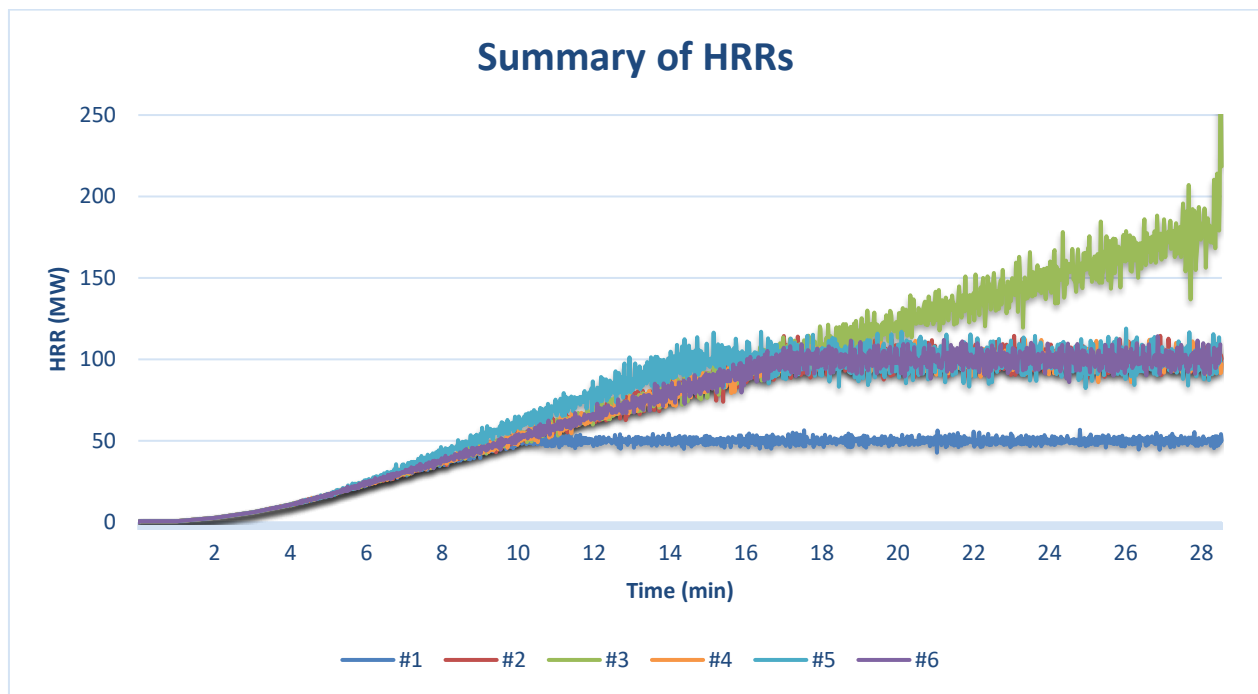
Figure 20 - Heat Release Rate for 1 - 50 MW HGV-Fire, 2 - 100 MW HGV-fire, 3 - 200 MW HGV-fire, 4 – Fans evenly distributed (100MW), 5 – 30 m³/s air flow (100MW) & 6 - Middle fans stop (100MW).

All the fire scenarios reached HRR of 50 MW between 9 min and 32 s (572 s) and 9 min and 39 s (579 s), except for fire scenario 5 which reached 50MW after (525s). Fire scenario 3 were expected to reach 200 MW at approx. 31 minutes. However, the simulations stopped after 28 min 32 s (1712 s) due to numerical instabilities. High fluctuations in graph 3 (green lines, Figure 20) provides proof of that statement. Furthermore, the results in Figure 17 show that the simulations correspond with the input data.

39

6.2 Backlayering and Air Velocity

This section presents the results related to backlayering. The data on backlayering are based on visual observations in the fire simulations and quantified using distance measurements. Furthermore, the recorded air velocities downstream and upstream are presented in this section.

6.2.1 t < 570 s

The main fire scenarios 1-,2- and 3 has the same fire and smoke development until t = 570 s, while fire scenario 2 and 6 are similar until middle fans stops between from t = [360,480]. Figure 19 shows the smoke locations at t = 120 s, t = 360 s (fire development at 25 MW) and t = 570 (50 fire development at 50 MW) for the main fire scenarios. At t = 120 (2 min) when fire ventilation was activated, the backlayering length (L_b) was 86 m.
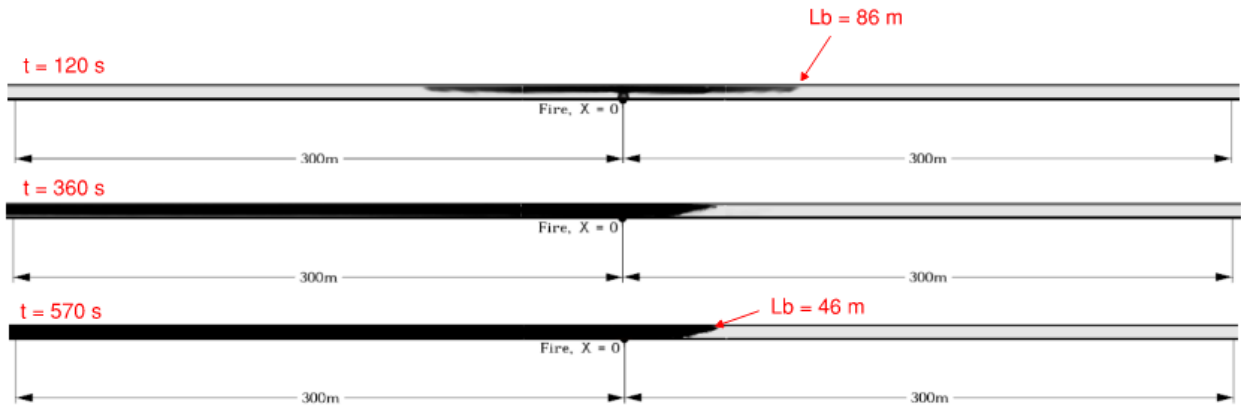
Figure 21 - Illustration of initial backlayering between t = [120 s, 570 s] for fire scenario 1, 2 and 3 with backlayering length, Lb

6.2.2 t > 570 s

Fire Scenario 1 – 50 MW: The backlayering length (Lb) is stable at 46 m for the HRR 50 MW scenario.
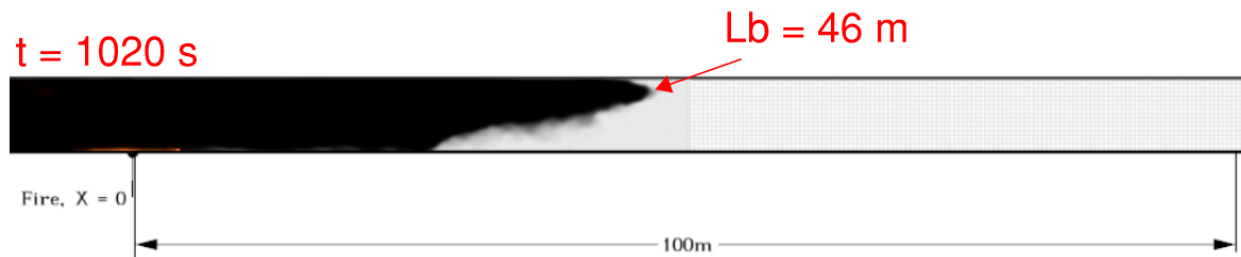
Figure 22 - The Lb stabilizes at 46 meters in fire scenario 1.

Fire scenario 2- & 3 – 100 & 200 MW:

40

#2: t = 1020 s

Lb = 50 m

Fire, X = 0

100m

#2: t = 1500 s

Lb = 55.4 m

Fire, X = 0
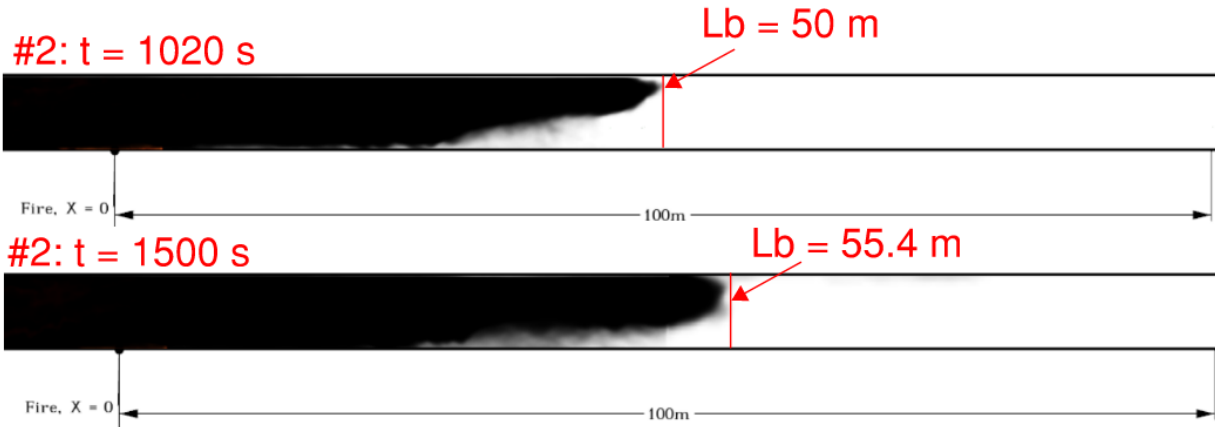
100m

Figure 23 - Illustration of the the smoke upstream of the fire in fire scenario 2 (100 MW).

The forces produced by the fire exceeds the forces produced by the jet fans, which results in increased L_b. Upstream, the smoke moves ca. 0.7 m/min in Figure 23.

#3: t = 1020 s

Lb = 51,4 m

Fire, X = 0

99.9999m

#3: t = 1500 s

Lb = 67,3 m

Fire, X = 0

99.9999m
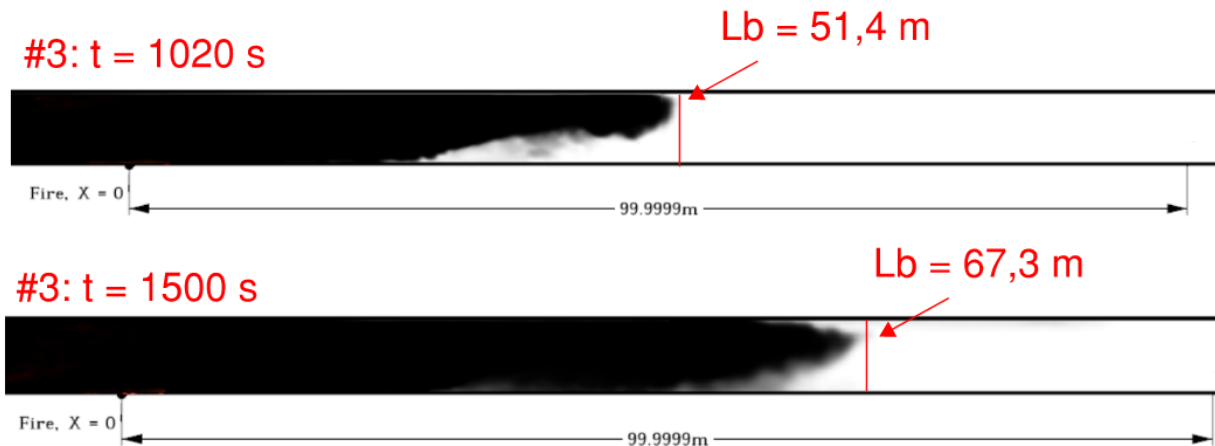
Figure 24- Illustration of the smoke upstream of the fire in fire scenario 3 (200 MW).

Average smoke velocity upstream were 0.7 m/min between t = [570 – 1020] in the fire growth phase and ca. 1.9 m/min between t = [1020,1500] when the fire was fully developed.

6.2.3 Other Backlayering Results

Fire Scenario 4 - Jet fans evenly distributed
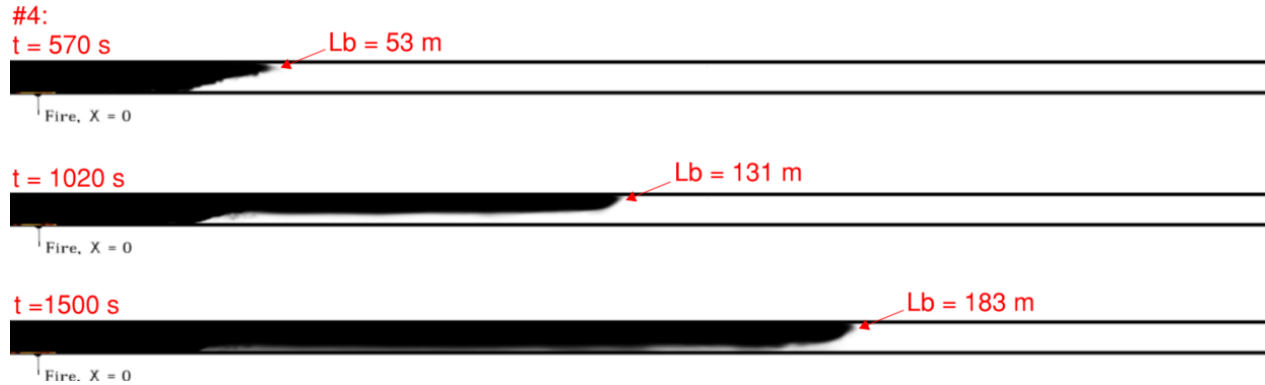
Figure 25 - Illustration of smoke upstream of the fire in fire senario 4 (100 MW, even dist. fans).

The evenly distributed jet fans were not able to prevent smoke backstream. The movement of smoke backstream occurred rapid in fire scenario 4 compared to the main fire scenarios. Average smoke velocity upstream were 10,4 m/min between t = [570 – 1020] in the fire growth phase and 6,5 m/min between t = [1020,1500] when the fire was fully developed.

Fire Scenario 5 - 30 m3/s jet fan capacity

No backlayering was observed during fire scenario 5.

Fire Scenario 6 - Middle fans stop
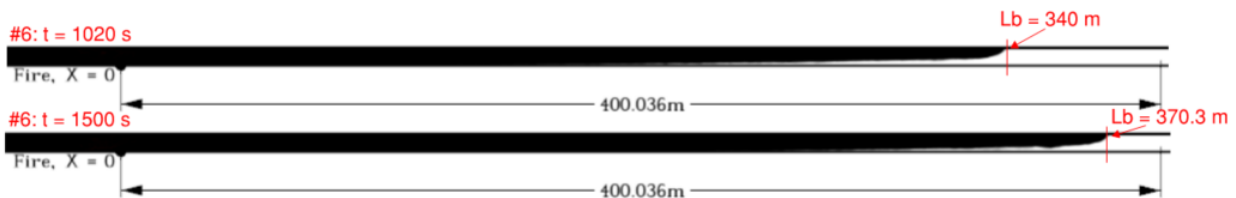
Figure 26 - Illustration of smoke upstream of the fire in fire senario 6 (100 MW, middle fans stop).

The smoke moves upstream significantly faster in fire scenario 6 than other fire scenarios. Between t = [360,1020], Bl = 294 m, which gives an average smoke velocity of 26,7 m/min. For t = [1020, 1500], ΔBl = 30.3 m with an average smoke velocity of 3,8 m/min upstream.

6.2.4 Air Flow

The air velocities vary slightly for the different scenarios. Upstream of the fire, the air velocity decreases as the HRR increases. Figure 25 illustrates the air velocity results for all the fire scenarios at t = 1500 s at X = [0, 200]m upstream.
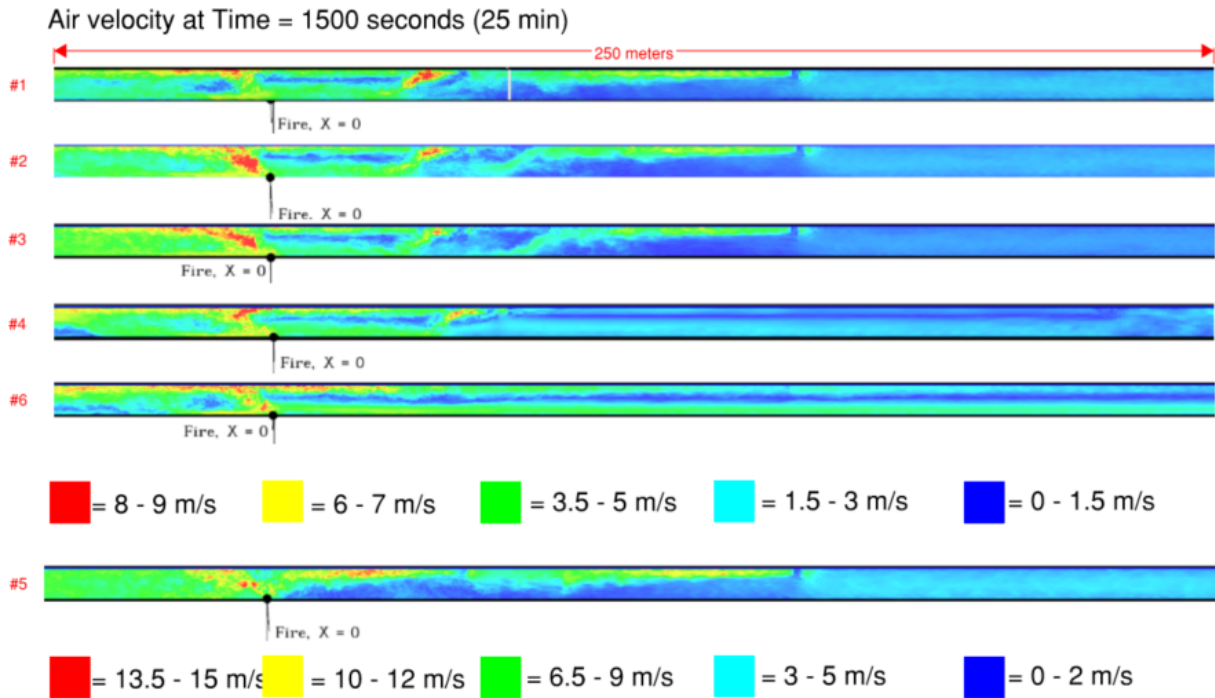
Figure 27 - Illustration of the air velocity at t = 1500 s for fire scenario 1(50 MW), 2: (100 MW), 3: (200 MW), 4: (100 MW, Even dist. fans), 5: (100 MW, 30 m3/s), 6: (100 MW, Middle fans stop).

In fire scenario 1, 2, 3, 4 and 6 an area with low air velocity, between 0 m/s < 1.5 m/s, which are present upstream. This area represents the boundary between two airflows moving in different directions. The airflow above the boundary moves upstream, while the airflow below move towards the fire. The arrows in Figure 26 indicates the direction of the airflow.
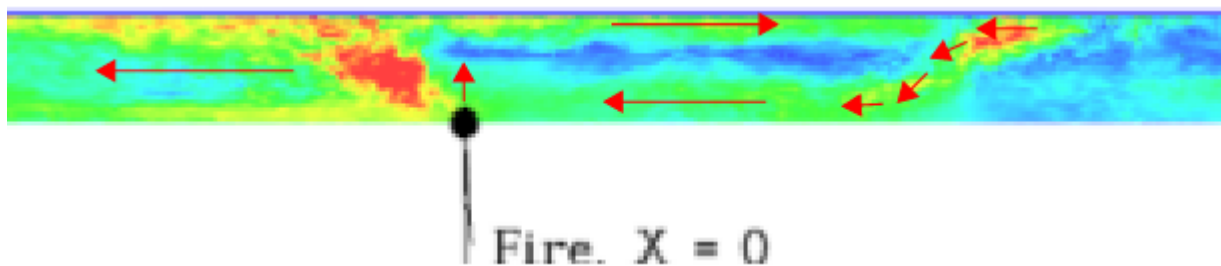
Figure 28 - Illustration of a boundary (middle blue area) between different airflow directions. The illustration is from fire scenario 2 (100 MW).

Furthermore, the air velocity results at X = [-300, -100] m downstream of the fire are presented. The similarities with air velocities downstream in fire scenario 1-, 2- & 3 were expected because of the identical jet fan configuration. Fire scenario 2 & 4 are presented to compare the existing jet fan configuration with an uniform jet fan configuration.
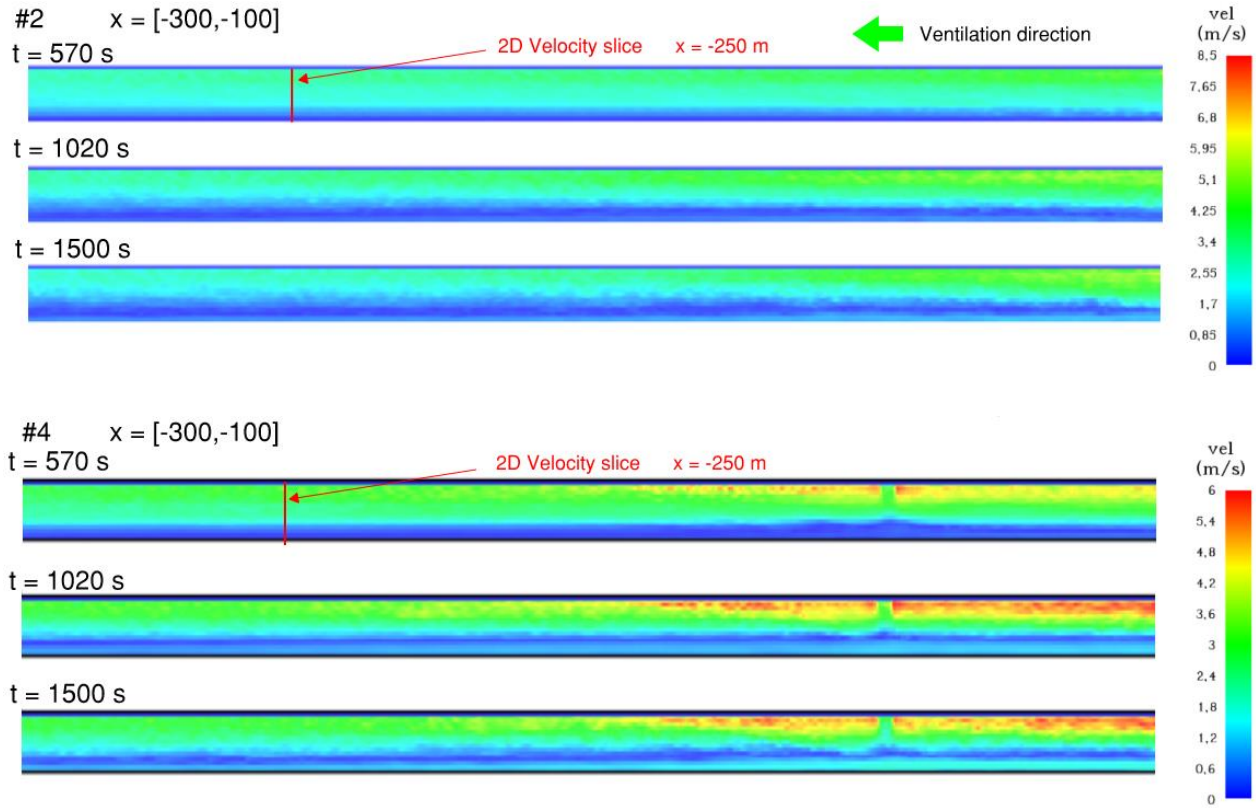
Figure 29 - Air velocity results at 300 to 100 meters downstream for fire scenario 2 and 4.
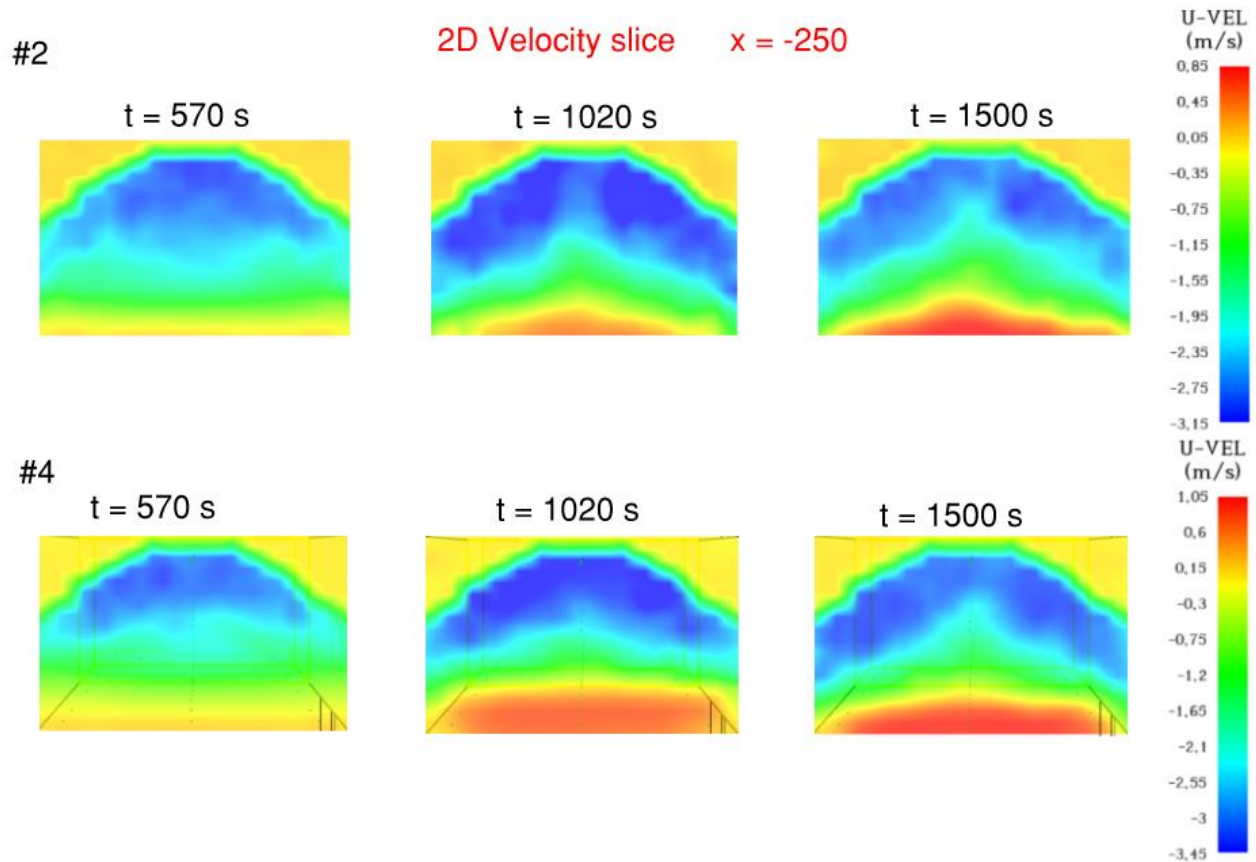
Figure 30 - Air velocity results of the tunnel cross-section 250 meters downstream of the fire for fire scenario 2 and 4.

The air velocity of the tunnel cross-section at 250 m downstream show some differences. The U-VEL graph indicates the specific air – velocity and – direction. Negative values are air moving downstream while positive values indicate upstream movement of air. The results show that the air near the ground moves in the opposite direction of the jet induced air flow and towards the fire source upstream. In addition, the air velocity seems to increase when the HRR increase, as the demand of air to the fire becomes higher. Furthermore, the air flow towards the fire in fire scenario 4 is greater compared with Fire scenario 2. As shown in Figure 30, there are a larger red area, which indicates a larger amount of air flow upstream towards the fire in fire scenario 4 when t = 1500s.

6.3 Visibility results

This section will present the visibility results for all the fire simulations. The visibility charts show different locations in the road tunnel (X = - 800, - 700, -500, -300, -100, +100, +300), as well as the visibility change over time. More explanation on visibility measurement is given in chapter 5.7.

The following figure illustrate the visibility results.
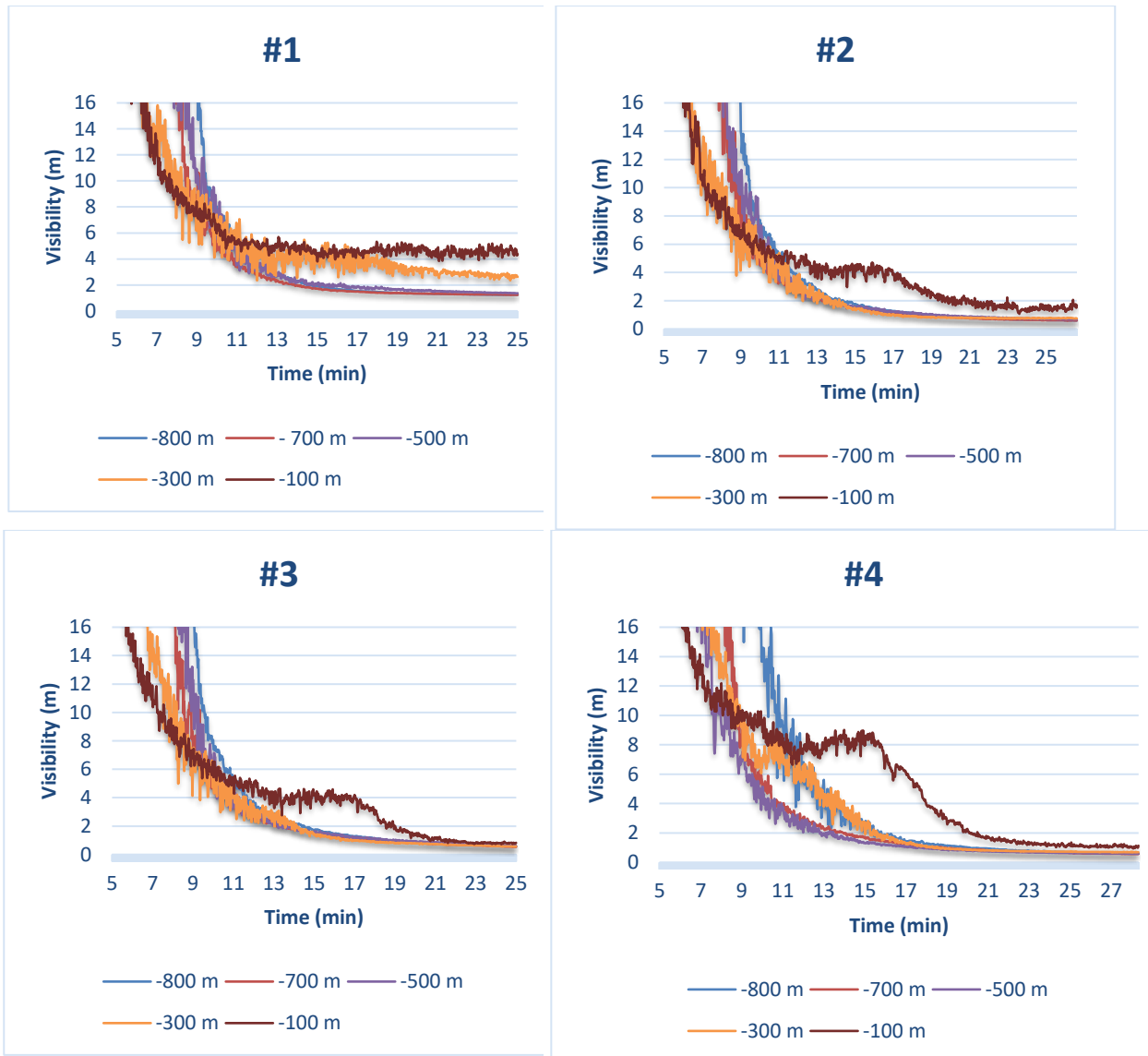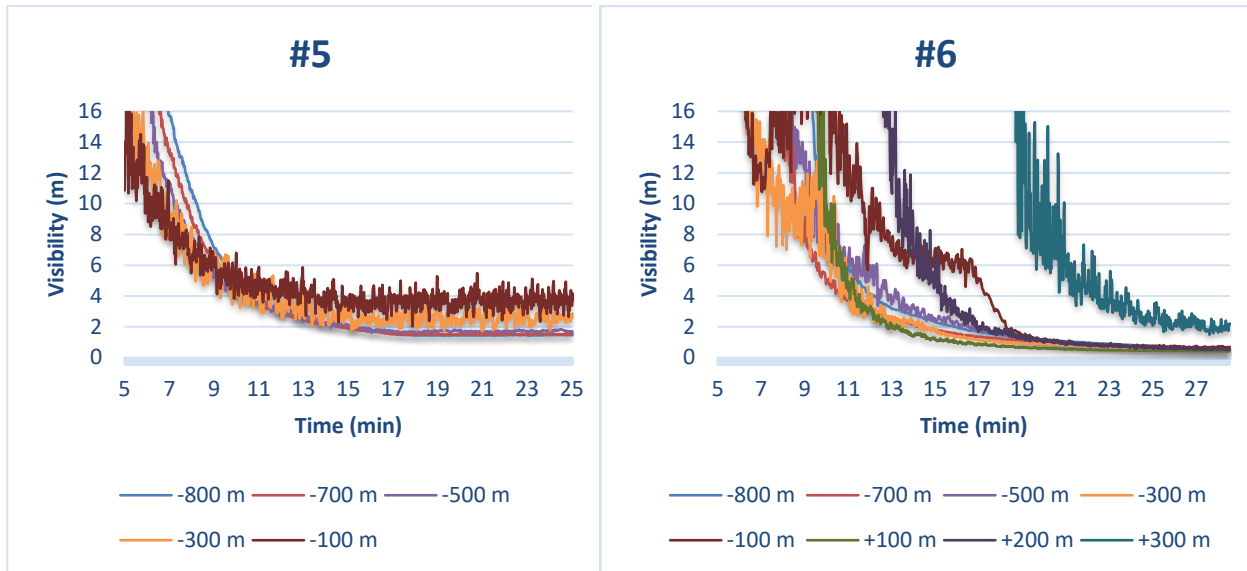
Figure 31 - Chart showing the visibiliy results for the fire simulations. #1 - 50 MW HGV-fire, #2 - 100 MW HGV-fire, #3 - 100 200 HGV-fire, #4 - Evenly distributed jet fans, #5 - 30 m3/s scenario, #6 - Middle fans stop.

Fire scenario 1

300 m and 100 m downstream visibility less than 10 m are reached after ca. 450 s. 800 m, 700 m and 500 m downstream the time to reach visibility > 10 m are between 500 s and 560 s. The time to reach visibility < 5 m are between 590 s and 640 s in the tunnel

Fire scenario 2

 300 m and 100 m downstream visibility less than 10 m are reached after ca. 440 s. 800 m, 700 m and 500 m downstream the time to reach visibility > 10 m are between 520 s and 570 s. The time to reach visibility < 5 m are between 590 s and 660 s in the tunnel.

Fire scenario 3

300 m and 100 m downstream visibility less than 10 m are reached after ca. 450 s. 800 m, 700 m and 500 m downstream the time to reach visibility < 10 m are between 510 s and 570 s. The time to reach visibility < 5 m are between 580 s and 660 s in the tunnel.

Fire scenario 4

300 m and 100 m downstream visibility less than 10 m are reached after ca. 510 s. 800 m, 700 m and 500 m downstream the time to reach visibility < 10 m are between 480 s and 640 s. The time to reach visibility < 5 m are between 570 s and 1060 s in the tunnel.

Fire scenario 5

300 m and 100 m downstream visibility less than 10 m are reached after ca. 370 s. 800 m, 700 m and 500 m downstream the time to reach visibility < 10 m are between 435 s and 490 s. The time to reach visibility < 5 m are between 540 s and 600 s in the tunnel.

Fire scenario 6

300 m and 100 m downstream visibility less than 10 m are reached after respectively 480 s and 700 s. 800 m, 700 m and 500 m downstream the time to reach visibility < 10 m are between 510 s and 590 s. The time to reach visibility < 5 m are between 600 s and 1010 s in the tunnel.

6.4 FED results

This section shows the measured FED values at different locations in the road tunnel at heights of 2 m. Typically, FED values begin to increase 5 minutes after ignition in most of the fire scenarios.

6.4.1 1 – 50 MW

Between 7 min – 13 min, FED values have an exponential growth. Ca. 3 minutes after the maximum HRR is reached, which is 13 minutes into simulation, the FED values tend to increase linearly. The highest FED values are recorded 300 m downstream of the fire.
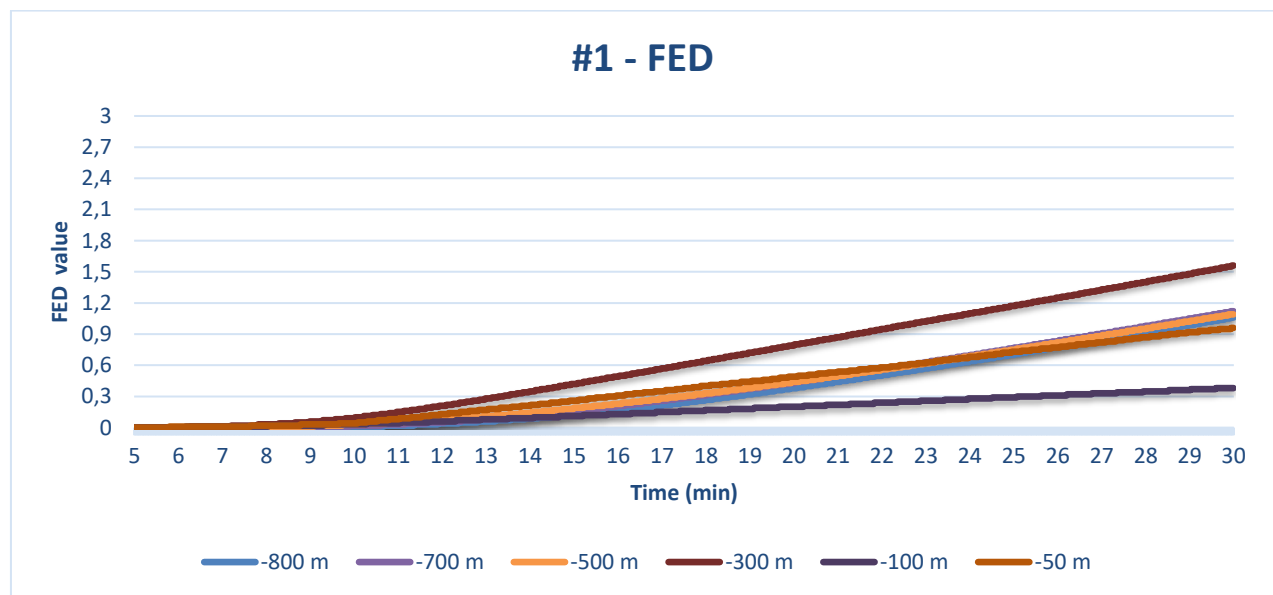
Figure 32 – Chart with FED values for fire scenario 1

48

After 13 min 20 sec the FED values reach 0.3 at 300 m downstream. For other locations, the FED values have a lower increase. 50 m downstream the FED value reach 0.3 after 15 min and 44 sec. 800-, 700- and 500 m downstream and reaches FED values of 0.3 between 17 min 20 sec and 18 min 30 sec. At 100 m downstream, FED value of 0.3 is reached after 25 minutes.

6.4.2   2 – 100 MW

The FED values grow exponentially with time in fire scenario 2. The highest FED values are recorded 300 m downstream of the fire. Between 5 and 20 minutes, the highest growth is 300 m donwstream. However, 20 minutes into the simulation, the highest growth rate is located 100 m downstream.

Figure 33 - Chart with FED values for fire scenario 2.

After 12 min 44 sec the FED values reach 0.3 at 300 m downstream. For other locations, the FED values have a slower growth. 800-, 700-, 500-, 100- and 50 m downstream, the FED value of 0.3 is reached between 15 min and 50 sec - 17 min 30 sec. The FED values 100 m downstream are expected to exceed the FED values 300 m downstream after 30 minutes.

6.4.3   3 – 200 MW Fire

The FED values grow exponentially with time. The highest FED values are recorded 300 m downstream of the fire. Between 5 and 15 minutes, the highest increase is 300 m downstream. However, 15 minutes into the simulation, the highest growth rate is located 100 m downstream. After 22 minutes, the highest FED values are 100 m downstream.
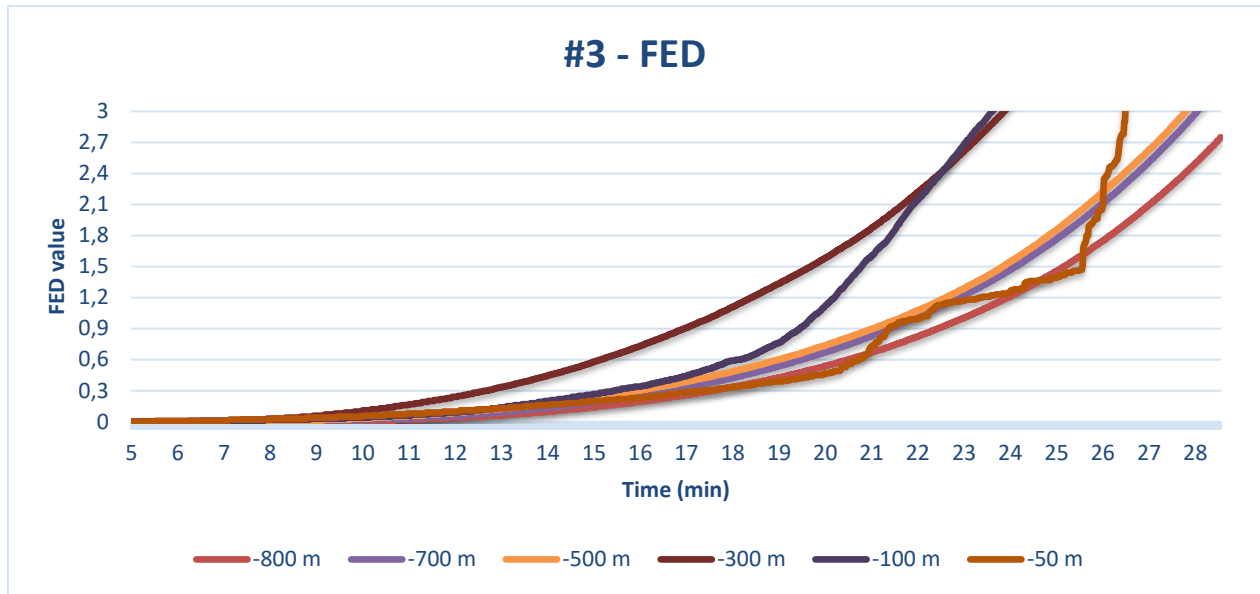
Figure 34 – Chart with FED values for fire scenario 3.

After 12 min 40 sec the FED values reach 0.3 at 300 m downstream, which is similar to scenario 2. 800-, 700-, 500-, 100- and 50 m downstream, the FED value of 0.3 is reached between 15 min and 25 sec - 17 min 30 sec.

6.4.4   4 – Even distribution

The FED values increased exponentially. The highest FED values are recorded 300 m downstream. At 300 m downstream, the FED values reach 0.3 after 13 min 54 sec.
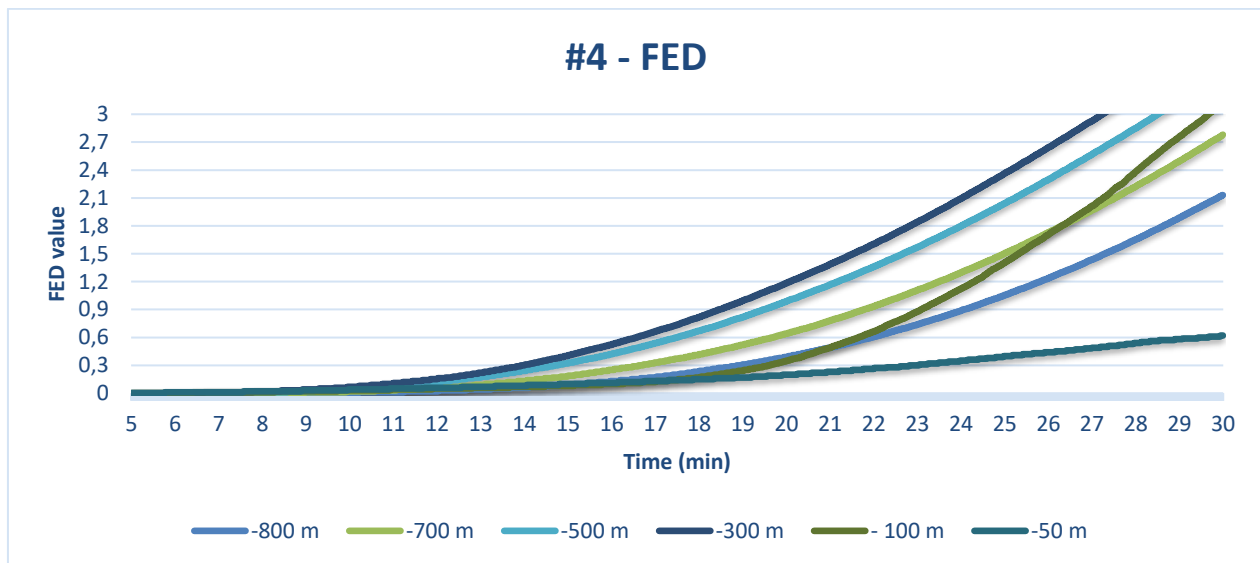
Figure 35 - Chart with FED values for fire scenario 4.

Furthermore, the FED value of 0.3 is reached between 14 min 40 sec and 19 min 37 sec at 800-, 700-, 500- and 100 m downstream. At 50 m downstream the FED increase is slow compared to the other locations. It takes ca. 23 min to reach tenability criteria of 0.3 for FED.

6.4.5 5 – 30 m³/s fan capacity
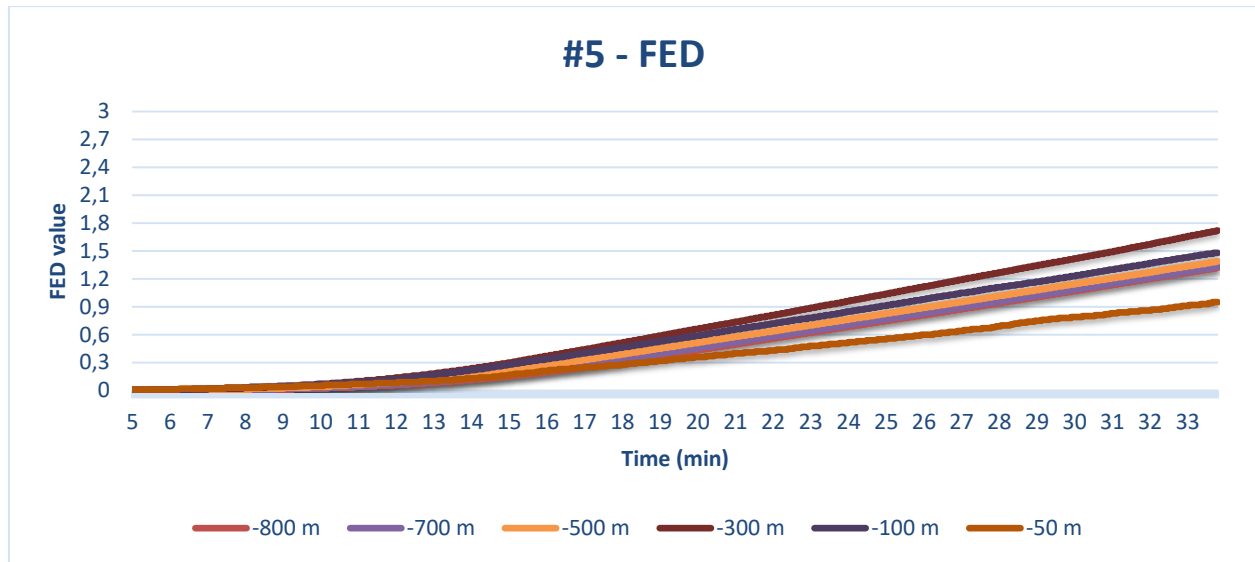
Figure 36 - Chart with FED values for fire scenario 5.

In fire scenario 5, the FED values reach 0.3 at 300 m downstream after 14 min 57 sec. The FED values have a linear increase for all locations in the tunnel. The results in fire scenario 5 show a slightly lower increase in the measured FED values, compared to fire scenario 2.

6.4.6 6 – Stop middle fans (Robustness test)

The FED values grow exponentially with time in fire scenario 6. The highest FED values are recorded 300 m downstream of the fire. Between 5 and 20 minutes, the highest growth is 300 m donwstream. However, 20 minutes into the simulation, the highest growth rate is located 100 m downstream.

Figure 37 - Chart with FED values for fire scenario 6.

After 13 min 52 sec the FED values reach 0.3 at 300 m downstream. Furthermore, the FED value of 0.3 is reached between 17 min 50 sec and 19 min 13 sec at 800-, 700-, 500- and 100 m downstream. Fire scenario 6 were the only scenario which reach FED values above 0.3 upstream of the fire. The time to reach tenability criteria at 50 m and 100 m, were respectively 15 min 45 sec and 15 min 52 sec.

6.5   Evacuation results

This section presents the results for the evacuation simulations. The goal of the evacuation simulations was to identify how reaction times affect FED exposure for the different fire scenarios. In all the fire scenarios, the evacuees upstream of the fire were not affected by heat and smoke. Therefore, the evacuation results upstream of the fire is not included in section 6.5. The focus in Chapter 6 is on the 75 evacuees downstream of the fire.
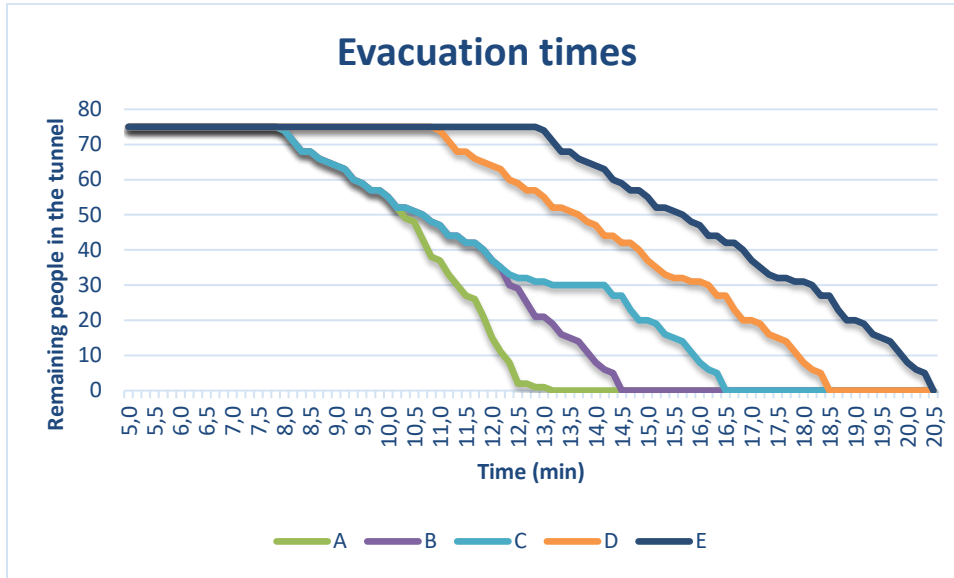
Figure 38 - Evacuation time for all the scenarios involving different reaction times. A = 1 min delay, B = 3 min delay, C = 5 min delay, D = 7 min delay & E = 9 min delay.

The evacuation times varies between 13 min 2 sec to 20 min 29 sec for all the simulations depending on the initial delay. Evacuation time is the time from fire start to all evacuees are out of the tunnel. The data emphasises the importance of reaction times for fast-developing vehicle fires. Based on the results, the evacuees with 1 min-, 3 min- and 5 min reaction time were not exposed to FED values above the tenability limit of 0.3. This was the case for all the fire simulations. Furthermore, the some of the evacuees with 7 min- and 9 min reaction time were exposed to FED values above 0.3. Table 12 summarizes the evacuation results related to FED exposure.

Scenario	Category [letter:number]	Time to evacuate [mm:ss]	FED < 0.3 [Exposed]	FED > 0.3 [Exposed]	Average FED exposure t = [5 last min of simulation]	Max FED exposure	Average exposure time to FED > 0.3
1: 50 MW	A01	13:02	75 (100%)	-	0.01	0.06	0
	B01	14:30	75 (100%)	-	0.03	0.13	0
	C01	16:30	75 (100%)	-	0.09	0.25	0
	D01	18:28	64 (85%)	11 (15%)	0.18	0.38	53 s/person
	E01	20:29	56 (61%)	29 (39%)	0.29	0.51	112 s/person
2: 100 MW	A02	13:02	75 (100%)	-	0.01	0.05	0

	B02	14:30	75 (100%)	-	0.03	0.14	0
	C02	16:30	75 (100%)	-	0.10	0.28	0
	D02	18:28	56 (75%)	19 (25%)	0.22	0.51	79 s/person
	E02	20:30	39 (52%)	36 (48%)	0.36	0.82	169 s/person
3: 200 MW	A03	13:02	75 (100%)	-	0.01	0.05	0
	B03	14:30	75 (100%)	-	0.03	0.14	0
	C03	16:30	75 (100%)	-	0.10	0.29	0
	D03	18:28	57 (76%)	18 (24%)	0.22	0.51	85 s/person
	E03	20:29	39 (52%)	36 (48%)	0.37	0.84	173 s/person
4: Even fan distribution	A04	13:02	75 (100%)	-	0.01	0.04	0
	B04	14:29	75 (100%)	-	0.03	0.11	0
	C04	16:29	75 (100%)	-	0.07	0.22	0
	D04	18:29	68 (91%)	7 (9%)	0.15	0.39	49 s/person
	E04	20:29	46 (61%)	29 (39%)	0.20	0.60	107 s/person
5: 4,5 m/s air velocity	A05	13:02	75 (100%)	-	0.03	0.1	0
	B05	14:29	75 (100%)	-	0.06	0.17	0
	C05	16:29	75 (100%)	-	0.12	0.29	0
	D05	18:29	56 (75%)	19 (25%)	0.22	0.44	79 s/person
	E05	20:29	39 (52%)	36 (48%)	0.33	0.61	151 s/person
6 – Stop middle fans	A06	13:02	75	-	0.01	0.05	0
	B06	14:30	75	-	0.03	0.11	0
	C06	16:30	75	-	0.08	0.21	0
	D06	18:30	72 (96%)	3 (4%)	0.15	0.33	43 s/person
	E06	20:29	49 (65%)	26 (35%)	0.24	0.53	92 s/person

Table 13 - A summary of the evacuation results. In the category column, the letters A-E represents reaction times 1-9 minutes, while the numbers 01-06 represents the specific fire scenario.

Average FED exposure shows the average FED value the evacuees were exposed to the last 5 minutes of the evacuation time. The data indicates the conditions in which the evacuees experience before they exit the tunnel. The Max exposure is the highest recorded FED value an evacuee was exposed to. In addition, the average exposure time to FED > 0.3 were measured. This value indicates the average time each of the exposed evacuee was exposed to untenable conditions above FED > 0.3.

6.6 Summary of the fire simulations

Location	Fire scenario	Time to reach $Visibility < 10\,m$ (min:sec)	Time to reach $Visibility < 5\,m$ (min:sec)	Time to reach $Visibility < 2\,m$ (min:sec)	Time to reach FED > 0.3 (min:sec)	Time to reach T > 80 ℃ (min:sec)
X = -100 (+100) *: X=-150	#1	07:30	12:10	-	25:05	10:00*
	#2	07:10	11:17	19:42	16:05	09:10*
	#3	07:14	11:15	18:36	15:25	09:10*
	#4	08:32	17:40	20:05	19:37	13:26*
	#5	06:10	09:54	-	15:20	08:02*
	#6	11:40 (09:55)	16:54 (10:54)	18:15 (16:05)	17:56 (15:52)	11:45*
X = -300 *: X=-350	#1	07:45	10:30	-	13:20	36:07*
	#2	07:20	10:40	13:40	12:40	16:30*
	#3	07:54	10:00	14:00	12:37	16:20*
	#4	08:39	12:37	15:17	13:54	26:26*
	#5	06:40	09:15	15:09	14:57	10:19*
	#6	08:00	10:35	14:16	13:52	26:25*
X = -500 *: X=-550	#1	09:00	11:00	14:54	17:20	-
	#2	09:00	10:45	13:40	16:00	-
	#3	09:03	10:25	13:18	15:53	-
	#4	08:00	09:41	12:55	14:40	-
	#5	07:20	09:27	15:15	16:25	19:45*
	#6	09:20	12:20	16:45	18:26	-
X= -700	#1	08:30	09:50	13:54	16:40	-
	#2	08:45	10:04	13:40	16:47	-
	#3	08:33	10:20	13:12	16:34	-
	#4	08:50	10:15	14:00	16:40	-
	#5	07:45	09:37	14:35	17:26	-
	#6	08:35	10:08	14:30	17:50	-
X= -800	#1	09:30	11:00	14:36	18:32	-
	#2	09:30	11:02	14:10	17:30	-
	#3	09:34	11:05	14:24	17:32	-
	#4	10:40	12:25	15:25	18:55	-

#5	08:15	10:04	14:50	17:46	-
#6	10:00	11:27	15:55	19:13	-

Table 14 - Summary of FDS results related to tenability criteria

Table 14 summarizes the FDS results presented in section 6.3 and 6.4 related to acceptance criteria. Furthermore, the table show the time to reach temperatures < 80 ℃ 150 m, 350 m and 550 m downstream. The temperature results indicates that the evacuees were able to avoid temperatures above tenability criteria. However, fire scenario 5 reach 80 ℃ slightly fast which means that a few evacuees were exposed to temperatures above the limit. Furthermore, time to reach visibility < 2 m were also included in table 14 for the purpose of comparing the fire scenarios.

7   Discussion

The discussion of the results is presented in this chapter. The following sections are included in Chapter 7: Heat release rate, backlayering, visibility, FED values, evacuation, uncertainties, and lastly, recommendations are presented.

7.1   Heat Release Rate

The results show the assigned HRRs were achieved for all fire scenarios except the scenario 3. This indicates that most of the fires were fuel controlled. Furthermore, the fluctuations in scenario 3 might indicate that turbulence created by the fire increases with the HRR. As the HRR exceeded ca. 160 MW, the fluctuations caused by the fire became too extensive for FDS. This might be because the degree of turbulence requires a finer mesh to resolve the fire Furthermore, the baroclinic torque term may have leaded to numerical instability because of the high HRR. However, as explained in Chapter 5, the high-pressure differences caused the fire simulation to become numerically unstable and stop after ca. 28 minutes.

7.2   Backlayering / emergency efforts

Backlayering can make it challenging for firefighters to approach and extinguish the fire. The potential for early fire extinction is high in urban road tunnels compared to remote road tunnels as fire departments tend to be located closer to the tunnels. In Tromso, the fire services are located relatively close (< 2 km) to the Langnes tunnel. The time to approach the fire and begin extinguishing efforts is likely between $5 - 10$ minutes. If the firefighters can approach the fire, the ASET might be improved. This is because extinguishing efforts can reduce the HRR and potentially extinguish the fire. Therefore, the prevention of backlayering is an important safety strategy for the ventilation system.

Our computations indicate that the existing ventilation configuration did not prevent backlayering for the 50 MW, 100 MW and, the 200 MW fire scenario. According to the results, the smoke reached 86 m upstream of the ventilation before the fire ventilation started after 2 minutes. As the fire ventilation started, the recorded backlayering length was 46 m. This indicates that the air flow of 14.4 m³/s was insufficient to prevent smoke from moving upstream along the tunnel length. Similar results were identified for fire scenarios 4 and 6. The 100 MW fire scenario 5 with

air flow of 30 m³/s was able to prevent backlayering, which indicates sufficient air flow velocity to prevent backlayering for a 100 MW fire.

7.2.1 Scenario 2 vs. Scenario 4

The goal of fire scenario 4 (evenly distributed jet fans) was to identify if the ventilation configuration could provide different results than the existing configuration. As mentioned in Chapter 3, air flow velocity is not depended on the configuration of the jet fans. Therefore, the results for the 100 MW fire scenario 2 and 4 were expected to be similar. However, the results indicated significant differences in upstream smoke velocity. At t = 540 s, the backlayering length was similar in fire scenarios 2 and 4, at respectively, 46 m and 53 m. At t = 1500 s, the recorded backlayering length reached, respectively 55.4 and 183 m for fire scenarios. The average smoke velocity upstream was 0.7 m/min for scenario 2 and 8.4 m/min for scenario 4. The results indicate that the existing jet fan configuration were able to reduce the smoke velocity upstream. The jet fans were able to create a smoke barrier, causing the smoke to move slower upstream in fire scenario 2. This might be because the jet fans are closer together in scenario 2 compared to scenario 4, causing higher air flows over a shorter area. Also, the longer distances there are between jet fans, the air flow might be more affected by wall friction. This will likely reduce air flow upstream in scenario 4 and a larger backlayering length. Furthermore, the results suggest that placing jet fans in groups might be beneficial to reduce the backlayering length. However, the backlayering length in all the fire scenarios, except fire scenario 5, could make extinguishing efforts challenging for a rapid-developing fire.

7.3 Visibility

Visibility has proven to be a challenge for fires in enclosures, such as tunnels, as the path of smoke is the same as the evacuation path downstream. The results confirmed this as the visibility criteria of < 5 m were met in all the fire scenarios. Visibility might be the most important parameter for evacuation. The evacuees are dependent on sufficient visibility to be able walk towards the exit. Walking speeds might significantly be reduced by low visibility, hence, increasing the evacuation time.

Most of the results are similar regarding visibility. The 50MW, 100MW, and 200 MW fire scenarios with the existing configuration reached visibility < 10 m between ca. 8 min 20 s and 9 min 30 s at 800 m, 700 m, and 500 m downstream. Between 9 min 40 s and 11 min the visibility < 5 m. As the results show, the visibility is reduced relatively fast for all the scenarios. This is due to the smoke production from the 50 MW, 100 MW, and 200 MW HGV-fires and the longitudinal ventilation with no extraction points for smoke other than the tunnel portal.

7.3.1 Groups of fans vs. Evenly distributed fans

Significant differences between the 100 MW fires in scenarios 2 and 4 was observed. According to the results in scenario 4, the locations at X = -100, -300, -700, -800, managed to maintain visibility for the longest duration. It is well established that different jet fans configurations do not influence the airflow velocity [13]. Hence, the results from fire scenario 2 and 4 were expected to be similar.

Location from fire	-100 m	-300 m	-500 m	-700 m	-800 m	Total
Fire scenario 2: Time Visibility < 5 m (min:s)	11:15	10:00	10:25	10:20	11:05	53:05
Fire scenario 4: Time Visibility < 5 m (min:s)	17:40	12:37	09:41	10:15	12:25	62:38

Table 15 – The difference in time to reach visibility less than 5 meters for fire scenario 2 and 4.

As seen in Table 15, the visibility results for fire scenario 2 is slightly worse. There might be several reasons for longer times to reach visibility < 5 m when the fans were evenly distributed along the tunnel, compared to when the fans were placed in zones. Jet fans in concentrated zones may increase turbulence. This could have caused the ceiling smoke layer to become more

unstable, hence reducing visibility faster. Secondly, the air movement might be more stable in a road tunnel for evenly distributed jet fans. On the other hand, one could expect the evenly distributed jet fans to disrupt the smoke layerto a higher extent. It would be reasonable to assume that the more jet fans the ceiling smoke passes through downstream, the more unstable the smoke layer would become. In scenario 4, the ceiling smoke layer travels downstream through 4 jet fan pairs (8 jet fans in total), while the ceiling smoke layer travels through 1 zone with three pairs of jet fans (6 jet fans in total) in scenario 3. Therefore, the results could indicate that having evenly distributed jet fans along the tunnel might improve visibility. This suggests that jet fans concentrated in zones could destroy smoke stratification, while even distribution of jet fans may improve tenable conditions.

7.3.2   Scenario 1 (50 MW) and scenario 5 (30 m^3/s)

All the fire scenarios reached the visibility criteria of < 5 m. However, fire scenarios 1 and 5, showed beneficial results regarding visibility compared to the other fire scenarios. The visibility is reduced rapidly in most fire scenarios from 20 m to 1 meter between 5 minutes and 15 minutes in scenarios 2, -3,-4 and -6. However, in scenarios 1 and 5, the visibility decrease begins to slow down when visibility is at approximately 2 m. For scenario 5, the visibility becomes stable at 1.7 m, while scenario 1 experience a decrease in visibility from 1.8 m to 1.4 m from between 15 to 25 minutes. The significantly improved visibility for the two scenarios is likely a result of two different reasons. Fire scenario 1 has a lower HRR, which might result in less smoke production. Fire scenario 5 has a higher airflow velocity, which might provide a higher extraction rate of smoke/air out of the tunnel. Hence, the results could be expected. However, there might be a large difference between the visibility of 1.7 m and 1 m during an evacuation in the road tunnel.

7.4   FED results

The FED results exceeded the tenability criteria for all the fire scenarios. In general, there were low differences in the time to reach FED values > 0.3. The results show that tenability criteria are first met 300 m downstream of the fire. For most of the scenarios, the time to reach FED = 0.3 is ca. 13 minutes at here. This might suggest that the tenable conditions will worsen at a certain distance away from the fire source (in this case, 200-300 m downstream), as the hot, toxic gases cool down and descends. Therefore, the results might not come as a surprise. However, fire

scenario 2 reaches tenability criteria faster than the other fire scenarios with HRR of 100 MW.

Figure 39 show the increase in FED values 300 m downstream for the 100 MW scenarios.
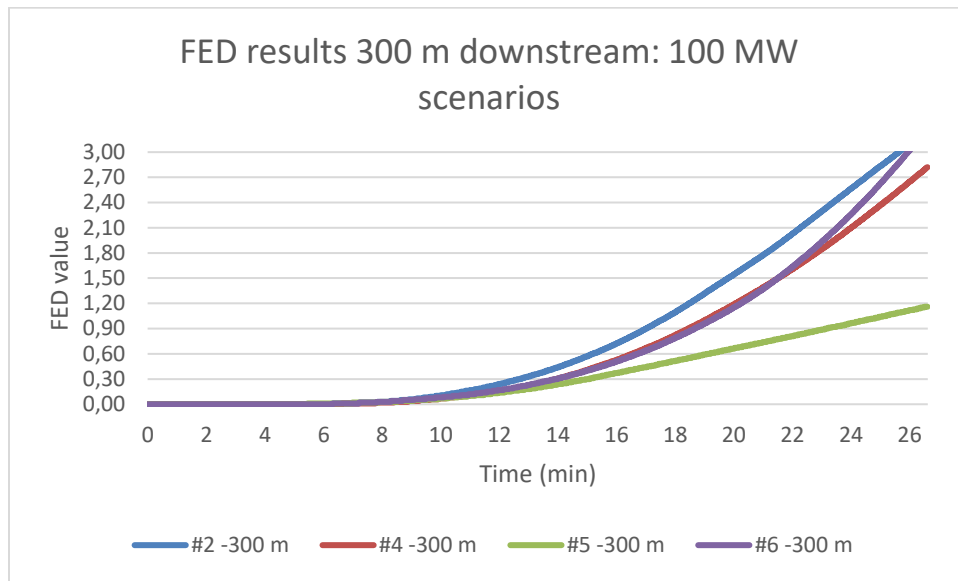
Figure 39 - FED results 300 m downstream of the fire for fire scenarios 2,-4,-5 and 6 (HRR 100 MW) at a height of 2 m.

Fire scenario 2 (blue function) with the existing fan configurations reach FED = 0.3 after 12 min 40 sec. The results are 1 min 14 sec faster than scenario 4, 2 min 17 sec faster than scenario 5 and, 1 min 12 sec faster than scenario 6. As mentioned, the smoke front in fire scenarios -2 and 4 reaches the end portal at the same time, which indicate similar average air velocities. However, Figure 27 suggests that evenly distributed jet fans can create two distinct areas with different air velocities. The air flow seems to decrease gradually with height in fire scenario 2. In fire scenario 4, the air flow changes more rapidly from high velocity to low velocity. Figure 40 attempt to illustrate the effect shown at t = 570 at X = [-250, -200].

61
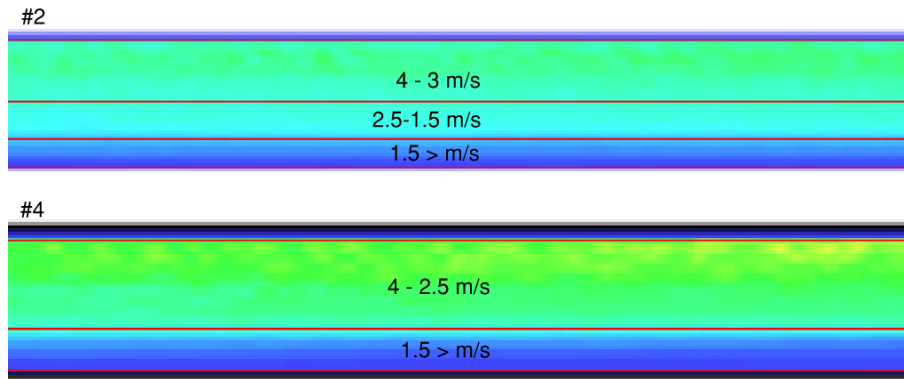
Figure 40 – A sketch 150 to 200 m downstream of the fire that show air velocities at t = 570 s in fire scenario 2 and 4.

Figure 40 shows that the air velocity decreases more rapidly with the height in fire scenario 4 at t = 570 s. Hence, one could assume the local pressure differences to be higher in the tunnel's upper- and lower region in fire scenario 4 compared to fire scenario 2. If this is the case, smoke particles could stay at a higher height for a longer duration before descending. Furthermore, this might explain why FED values reach 0.3 significantly faster in fire scenario 2. However, the parameters and inputs used in the fire model can influence the results. There might be uncertainties related to the results, which can question the validity of the results. This effect related to how the configuration of jet fans might affect air flow should be investigated further.

7.5   Evacuation

The evacuation scenarios show promising results related to FED exposures. None of the evacuees were exposed to FED values above 0.3 when reaction times were between 1 – 5 minutes. This means that evacuees with reaction times below 5 minutes might manage to evacuate the road tunnel downstream without being exposed to untenable conditions. If ASET were limited the toxicity parameter, FED, the ASET would be in the range of 16 min 30 sec. However, one must consider other parameters which affect tenable conditions downstream, such as temperature and visibility.

As expected, temperature exposure of T > 80 ℃ posed a relatively low threat for evacuees for all the evacuation scenarios. The temperature criteria were breached after 9 min 10 sec 100 m downstream in fire scenarios 2 and 3 and after 8 minutes in Fire scenario 5. This indicates that ca. 10 of the evacuees with reaction times of 9 minutes would potentially be exposed to temperatures above 80 ℃ for a short period. However, the visibility criteria were breached relatively fast.

As mentioned, 700 m downstream, the visibility < 5 was reached between 9 min 37 sec and 10 min 20 sec in all the fire scenarios. These results indicate that evacuees will be exposed to visibility < 5 m, independent of reaction times. Based on the quantitative results, the ASET is determined to be in the range of 9 min 40 and 10 min and 20 sec. The RSET could be more difficult to determine precisely, based on uncertainties in reaction times for the evacuees. However, the RSET would be in the range of 13 minutes and 20 min and 30 sec considering the fire scenarios in the thesis. The quantitative comparison of the safety concepts, ASET and RSET give the following result for the scenario-based risk analysis; $ASET < RSET$. The study indicates that the available safe evacuation time (ASET) is less than the required safe evacuation time (RSET) for the fire scenarios involving fast-developing 50 MW, 100 MW, and 200 MW. Therefore, the results suggest that additional measures should be implemented to increase ASET and decrease RSET.

7.6   Uncertainties

When using simulation tools, such as FDS, the users should acknowledge the possibilities for error. FDS is widely used and accepted in the fire safety community for its ability to resolve fire scenarios. The development of FDS is a continuous process and will continue to improve over time. Meanwhile, many experiments have been conducted to verify and improve FDS, and more experiments will be conducted in the future. However, given ability FDS has to provide accurate results in fire modelling, the users are still responsible for the input in the fire model and the interpretation of the results. This section discuss some of the input parameters used in the FDS model.

The accuracy of the design fire?

The research regarding tunnel fire dynamics is relatively new, and the need for more knowledge will continue to increase in the future. The full-scale fire experiments described in Chapter 2 have been influential in the development of tunnel fire dynamics and the inputs used in the thesis. However, more full-scale tunnel fire experiments might be needed for further development on the subject. The costs associated full-scale fire tests in tunnels limits the quantity of these tests.

The actual fuel material and -geometry, and ignition source might provide uncertainties regarding fire design. The design fire is based on data from the Singapore 2012 full-scale tests [12], which

involved very fast developing HGV-fires consisting of wood- and plastic pallets. There could be uncertainties related to how a real HGV-fire might develop. The set-up promotes a fast-developing fire in full-scale tunnel fire experiments and actual fuel material and geometry. Furthermore, Table 2 in Chapter 2 shows that the height in multiple of the full-scale tunnel fire tests are below 6 meters. The height of the Langnes tunnel is significantly higher than the test tunnels, which again can facilitate a slower fire growth rate than the fire growth rate used in the design fire. As a result, the fire growth calculations might not be suitable for the design fire.

An initiating event leading up to the fire is not considered in the FDS model. At t = 60 s, the design fire was already close to reaching HRR of 1 MW and extensive smoke production. Therefore, adding a certain amount of time "before" the fire simulation starts, e.g., by defining an incipient period between t = [-120, 0] seconds might be reasonable. However, the argument is from a practical-perspective, and not necessarily from a safety perspective. Nonetheless, more research on tunnel fire safety and tunnel fire experiments will be necessary, and hopefully, be able to reduce uncertainties related to tunnel fire modelling and tunnel fires in the future.

The Existing Geometry vs. The Model Geometry

The FDS tunnel model contains a specific width of 10.4 m, the height of 6.4 m and a cross-section of 57.6 m². These measures are a result of the average width and height distances along the tunnel length using data from a point-cloud system, explained in Chapter 4. As expected, this work revealed some variations in width and height depending on location in the road tunnel. The distances were measured at several points, ca every 100 m along the tunnel, which might not be optimal for measuring average width and length. As a result, there might be minor deviations in the geometry when comparing the actual tunnel geometry and the FDS model geometry.

The uncertainties in width and height through the tunnel might have affected the fire simulations regarding backlayering. If the average and actual cross-section of the existing road tunnel were smaller than the tunnel model, one could expect the longitudinal ventilation to provide slightly higher air flows. On the other hand, the air flow could be somewhat lower if the average cross-section of the existing tunnel were larger than the tunnel model. The larger the cross-section is, the more air need to be moved by the longitudinal ventilation system. Furthermore, the jet fans would be required to produce a higher air flow to achieve critical velocity. However, the geometrical uncertainties might be reduced due to the accuracy of the point-cloud system.

Furthermore, the assigned properties to the tunnel wall surfaces in the tunnel could provide uncertainties. The tunnel walls thermal properties, such as mass density, specific heat and thermal conductivity, might influence heat transfer from the smoke layer. In addition, the roughness parameter might influence air flow near the surface boundaries along the tunnel model. As a consequence, the dynamics of the hot layer ,including the smoke stratification, could be affected.

7.7   Recommendations

The findings of this study were interesting from a fire safety perspective. Safety measures to prevent backlayering and facilitate firefighting efforts might be the most cost-effective and beneficial given the short distance for the fire department to the existing road tunnel. Based on the results and findings, the thesis will present a selection of recommendations. The following fire safety recommendations might improve the effect of the longitudinal ventilation and general fire safety in case of a fire scenario with fast developing fire growth.

1. *Jet fan capacity and longitudinal ventilation strategy*

The topic regarding longitudinal ventilation strategy might be challenging. Longitudinal ventilation will reduce tenable conditions downstream of a fire at a faster rate, compared with no ventilation. On the other hand, longitudinal ventilation which provides critical air velocity can prevent backlayering and promote early fire extinction.

According to the results, the existing capacity of 14.4 m³/s for the 16 jet fans did not prevent backlayering in the 50 MW, 100 MW and 200 MW fire scenarios. As mentioned, there could be uncertainties with the fire models and the results in the thesis. However, it is recommended to perform further investigations to determine if the existing capacity of the 16 jet fans are sufficient to prevent backlayering for 50 MW and 100 MW fires in the road tunnel. This would help to assure the success of the existing ventilation strategy, which is to facilitate early firefighting efforts.

2. *Water supply*

The case study in Chapter 4 states the road tunnel does not have sufficient water supply. According to the N500 standard and EU directive, presented in Chapter 3.4.3, water supply is

mandatory for all tunnels at least every 250 m. The amount of water needed to extinguish a fire will depend on the vehicle and fire. Experience shows that many vehicle fires, especially electrical vehicle fires, require extensive amounts of water. Hence, without additional water supply in the tunnel, the time to extinguish the fire might increase. In addition, the increase of electrical vehicles in Norway emphasises the importance of water supply.

3. Technical safety measures

The case study did not involve technical safety measures due to the limited scope of the thesis. However, the author would like to emphasize the importance of technical safety measures in road tunnels. A few recommendations will be briefly explained regarding technical installations which can facilitate effective reaction times and improve required safe evacuation time (RSET).

Guidance system / Evacuation lights and loudspeakers

As mentioned in Chapter 4.1, the electrical guidance system consists of evacuation lights every 62.5 m. According to Table 6 in 3.4.3, evacuation lights should be placed every 25 m for tunnels < 5 000 m. Therefore, the author recommends the implementation of evacuation lights every 25 m. Given the low visibility results in the fire scenarios, this safety measure might significantly improve a potential evacuation scenario. Furthermore, the author recommends loudspeaker system to effectively provide evacuees with information. The latter is not mandatory for tunnels < 3 000 m in Norway. However, given the complexity of the whole tunnel system and possible benefits regarding reaction time, a loudspeaker system might be beneficial to improve RSET.

8 Conclusion

Longitudinal ventilation systems in road tunnels are used to control smoke- and heat movement. The longitudinal ventilation creates a one-directional air flow through the tunnel by ceiling-mounted jet fans. In case of a tunnel fire, the ventilation system should prevent smoke movement upstream of the fire. Prevention of backlayering is a widely used ventilation strategy to facilitate firefighting efforts from one side of the fire.

The thesis conducted a scenario-based fire risk analysis of the existing road tunnel to examine the effect of the longitudinal ventilation. The work aimed to investigating the ventilation system's ability to control fires to facilitate safe evacuation and emergency efforts, as formulated in Chapter 1.3. Based on the research questions and the results, the following conclusion of the work will be presented.

Firstly, the thesis examined the ventilation system's ability to prevent backlayering. The fire scenarios with 50-, 100- and 200 MW HGV-fires with a jet fan capacity of 14.4 m³/s revealed that the longitudinal ventilation did reduce backlayering length. Furthermore, the fire scenario with increased jet fan capacity, 30 m³/s, was sufficient to prevent backlayering. However, the fire simulation results indicate that the ventilation system's ability to prevent backlayering is insufficient as backlayering lengths reached lengths between 46 to 67.3 m.

The second question the thesis attempts to answer is related to the tenability conditions for evacuees. The fire simulations were conducted to determine ASET for the 50 MW, 100 MW and 200 MW fire scenarios. The determining factor for ASET was visibility, which exceeded the performance criteria after between 9 min and 50 sec to 11 minutes. Furthermore, performance criteria related to toxicity, FED, were reached 500 m downstream of the fire after 15 min 53 sec to 17 min 20 sec. The evacuation model determined the evacuation time to be between 13 min and 20 min and 30 sec.

The results from the thesis indicate that the thesis statement failed. The longitudinal ventilation was not able to control fires to facilitate safe evacuation and emergency efforts. However, as mentioned in Chapter 7, the uncertainties with the design fire and tunnel model challenge the work's outcome. Therefore, the findings of the work will only be considered valid for the tunnel

model and not for the existing road tunnel. The author believes further research, preferably on a full-scale, is necessary to determine if the thesis is valid for the existing road tunnel.

9   Further work

This study has been motivated to gain more knowledge of a longitudinal ventilation system in an existing road tunnel, and to evaluate if the ventilation system is able to maintain an acceptable level of fire safety in the tunnel. The author suggests the following four topics, which could be of interest for further research.

➢ **Low ambient temperature and its effect on tenable conditions in road tunnels.**
In recent years there have been performed research on the effect of ambient pressure related to high-altitude tunnels. Likewise, the author believes there is a need for increased knowledge regarding cold temperature tunnels and how this can affect the fire safety. The effect of low ambient temperatures on tenable conditions in tunnels might be relevant for many countries in colder temperature regions. Therefore, this could be an interesting research topic for further work.

➢ **The effect of the jet fans configuration regarding tenable conditions in road tunnels with longitudinal ventilation.**
As mentioned in Chapter 3, the airflow velocity is dependent on the number of active fans and the thrust, and not on the configuration of the fans. However, the thesis results indicate that the configuration of the jet fans in a longitudinal ventilation system can affect tenable conditions in road tunnels. The topic needs further research to verify the results. Therefore, the author believes this topic might be interesting to look further into.

➢ **Conduct work to improve the fire model and investigate the performance with different jet fan capacities**
The thesis is a result of decisions made by the author. The decisions regarding the input data for the fire- and model design might benefit further verification and possible improvements. In addition, the optimal jet fan capacity to prevent backlayering in the road tunnel could be an interesting topic to investigate further.

➢ **Conduct fire safety research on road tunnel systems with multiple connected tubes.**
The road tunnel system in Tromso, Norway, are bi-directional system of connected tubes. For similar complex tunnel systems, there might be of great research value to investigate longitudinal ventilation from multiple directions and how this might affect heat- and smoke transfer. Other aspects, such as evacuation and human behaviour might also be interesting for future research.

10 References

[1] Statens vegvesen, "Vegkart," Statens vegvesen, 2020. [Online]. Available: https://vegkart.atlas.vegvesen.no/. [Accessed 26 October 2020].

[2] Directive 2004/54/EC on the European Parliament and of the Council, "on minimum safety requirements for tunnels in the Trans-European Road Network," *L167/39,* 2004.

[3] EFTA Surveillance Authority, "Letter of formal notice to Norway concerning Minimum safety requirements for tunnels in the Trans-European Road Network," EFTA Surveillance Authority, Brussels, 2020.

[4] "Brannstatistikk: Tunnelbrann - Brann i kjøretøy," Direktoratet for samfunnssikkerhet og beredskap, [Online]. Available: https://www.brannstatistikk.no/brus-ui/search?searchId=66A86F08-BFA2-43DB-ADF4-859BD81A04BB&type=SEARCH_DEFINITION. [Accessed 10 3 2021].

[5] P. Ntzeremes and K. Kirytopoulos, "Evaluating the role of risk assessment for road tunnel fire safety: A comparative review within the EU," vol. 6, no. 3, 2019.

[6] "Scopus," [Online]. Available: https://www.scopus.com/home.uri. [Accessed 17 March 2021].

[7] H. Ingason, Y. Zhen Li and A. Lönnermark, Tunnel Fire Dynamics, New York: Springer, 2015.

[8] Australasian Fire Authorities Council (AFAC), "Fire Safety Guidelines for Road Tunnels," 2001.

[9] A. Haack, "Fire Protection in Traffic Tunnels: General Aspects and Results of the EUREKA project," *Tunnelling and Underground Space Technology,* vol. 13, no. 4, pp. 377-381, 1998.

[10] A. Beard and R. Carvel, Handbook Of Tunnel Fire Safety, London: Institution of Civil Engineers, 2011.

[11] H. Ingason, Y. Zhen Li and A. Lönnermark, "Runehamar tunnel fire tests," *Fire Safety Journal,* vol. 71, pp. 134-149, 2015.

[12] M. Cheong, W. Cheong, K. Leong, A. Lemaire and L. Noordijk, "Heat Release Rate of Heavy Goods Vehicle Fire in Tunnels with Fixed Water Based Fire-Fighting System," *Fire Technology,* vol. 50, pp. 249-266, 2014.

[13] Massachusetts Highway Department and Federal Highway Administration, "Memorial Tunnel Fire Ventilation Test Program - Test Report," 1995.

[14] A. Kelly and Giblin, P.E., "The Memorial Tunnel Fire Ventilation Test Program," *ASHRAE,* pp. 26-30, 1997.

[15] T. Lemaire and Y. Kenyon, "Large Scale Fire Tests in the Second Benelux Tunnel," *Fire Technology,* vol. 42, pp. 329-350, 2006.

[16] J. Brekelmans and R. van den Bosch, "Summary of Large Scale Fire Tests in the Runehamar Tunnel in Norway," Uptun, TNO, Promat, 2003.

[17] Statens vegvesen, "Vegtunneler: Håndbok N500," 2020.

[18] D. Rosberg, A. Purchase and K. Fridolf, "Acceptance Criteria in Fire Safety Engineering: A Review and Case Study," in *Fire and Evacuation Modeling Technical Conference (FEMTC)*, Gaithersburg, Maryland, 2018.

[19] B. Schröder, "Multivariate Methods for Life Safety Analysis in Case of Fire," Julich Forschungszentrum, 2017.

[20] D. Drysdale, "An Introduction to Fire Dynamics, 3rd Edition," Wiley, 2011.

[21] L. He, Z. Xu, F. Markert, J. Zhao, E. Xie, Q. Liu and C. Fan, "Ceiling jet velocity during the whole process of fire development in a tunnel," *Journal of Wind Engineering and Industrial Aerodynamics,* vol. Volume 212, 2021.

[22] C. Shi, J. Li and X. Xu, "Full-scale tests on smoke temperature distribution in long-large subway tunnels with longitudinal mechanical ventilation," *Tunnelling and Underground Space Technology,* vol. Volume 109, 2021.

[23] A. Król and M. Król, "Numerical investigation on fire accident and evacuation in a urban tunnel for different traffic conditions," *Tunnelling and Underground Space Technology,* no. 109, 2021.

[24] A. Lönnermark, "On the Characteristics of Fires in Tunnels," Department of Fire Safety Engineering and Systems Safety, Lund University, 2005.

[25] S. F. Martin, I. del Rey Llorente and A. Fraile de Lerma, "Tunnel ventilation Analysis Using a PRobabilistic Approach: Case Study, Fire in Road Tunnels with Longitudinal Ventilation," *Fire Technology,* vol. 57, pp. 1115-1134, 2021.

[26] NFPA, "NFPA 502: Standard for Road Tunnels, Bridges, and Other Limited Access Highways," 2014.

[27] H. K. Kim, A. Lönnermark and H. Ingason, "Effective Firefighting Operations in Road Tunnels," SP Technical Research Institute of Sweden, Borås, Sweden, 2010.

[28] E. D. Kuligowski, "Human Behavior in Fire," in *SFPE Handbook of Fire Protection Engineering*, New York, NY, Springer, 2016.

[29] N. P. Høj, R. Brandt, K. Appel and M. Martens, "NordFoU: Evakuering i vegtunneler," 2014.

[30] Byggforskserien, "520.385 Nødvendig rømningstid ved brann," 2016.

[31] Y. Zhang, H. Zhu, Q. Guo, R. Carvel and Z. Yan, "The Effect of Technical Installations on Evacuation Performance in Urban Road Tunnel Fires," *Tunneling and Underground Space Technology,* vol. 107, no. 103608, 2021.

[32] Statens vegvesen, "Sikker atferd ved hendelser i vegtunneler," 2018.

[33] Samferdselsdepartementet, "Forskrift om mimimum sikkerhetskrav til visse vegtunneler (Tunnelsikkerhetsforskriften)," https://lovdata.no/dokument/SF/forskrift/2007-05-15-517, 15.05.2007.

[34] ViaTech, "ViaPPS: Bruk av høyteknologiske lasere sikrer nøyaktige data," ViaTech, [Online]. Available: https://www.viatech.no/products.aspx?lang=no&id=6. [Accessed 3 12 2020].

[35] Autodesk, "ReCap - Overview," Autodesk, [Online]. Available: https://www.autodesk.com/products/recap/overview?term=1-YEAR. [Accessed 5 4 2021].

[36] K. McGrattan, S. Hostikka, J. Floyd, R. McDermott and M. Vanella, "Fire Dynamics Simulator User's Guide," NIST Special Publication 1019, 2021.

[37] X. Wang, C. Fleischmann and M. Spearpoint, "Assessing the influence of fuel geometrical shape on fire dynamics simulator (FDS) predictions for a large-scale heavy goods vehicle tunnel fire experiment," *Case Studies in Fire Safety,* no. 5, pp. 34-41, 2016.

[38] SFPE, "Appendix," in *SFPE Handbook of Fire Protection Engineering, Fifth Edition*, New York, Springer, 2016, pp. 3466-3471.

[39] B. Persson, M. Simonson and M. Månsson, "Utsläpp från bränder till atmosfären," SP Sveriges Provnings- och Forskningsinstitut, Borås, Sweden, 1995.

[40] L. K. Chern, "Tunnel fire Suppression Systems & Ventilation Design - Master thesis," The University of Edinburgh, 2018.

[41] Thunderhead Engineering, "Smoke Visibility and Obscuration," Thunderhead Engineering, 2020. [Online]. Available: https://support.thunderheadeng.com/tutorials/pyrosim/smoke-visibility-obscuration/. [Accessed 16 6 2021].

[42] Thunderhead Engineering, "Pathfinder - User Manual," Thunderhead Engineering, 2021.

[43] Thunderhead Engineering, "Pathfinder Technical Reference Manual," Thunderhead Engineering, 2021.

Appendix

A.1 Hand calculations

This appendix describes the hand calculations in preparation of the FDS simulations

Area of the burner

$$A_{burner} = length \cdot width$$

$$A_{burner} = 7,6 \, m \cdot 2,2 \, m$$

$$A_{burner} = \mathbf{16,7 \, m^2}$$

Fire Growth calculations

$$\frac{dQ}{dt} = 1,2 \times 10^{-3} u_o \sum_{i=1}^{N} C_{f,i} w_{p,i}$$

$$\frac{dQ}{dt} = 1,2 \times 10^{-3} \cdot (3,4 \; or \; 4,4)(1447 \cdot 9,7 + 2441 \cdot 5,9)$$

1) 16 jet fans w. capacity of 14,4 m³/s

$$\frac{dQ}{dt} = 116 \frac{kW}{s} = 6960 \frac{kW}{min} \approx \mathbf{7000 \frac{kW}{min}}$$

2) 16 Jet fans w. capacity of 30 m³/s

$$\frac{dQ}{dt} = 150 \frac{kW}{s} = \mathbf{9000 \frac{kW}{min}}$$

Characteristic Fire Diameter, D*

The following equation are used to determine the characteristic fire diameter:

$$D^* = \left(\frac{Q}{\rho_\infty c_p T_\infty \sqrt{g}}\right)^{\frac{2}{5}}$$

Density, $\rho_\infty = 1.2$ kg/m³

Specific Heat, $c_p = 1$ kJ/kgK

Ambient temperature, $T_\infty = 278$ K (5 °C)

Q is the heat release rate [kW].

Fire scenario 1, Q = 50 000 kW. Fire scenario 2, Q = 100 000 kW. Fire scenario 3, Q = 200 000 kW.

The input of different Q gives the following value for D*:

	100 MW	50 MW	200 MW
D*	6.2	4.7	8.2

Relationship, D*/dx

$$\frac{\left(\frac{Q}{\rho_\infty c_p T_\infty \sqrt{g}}\right)^{\frac{2}{5}}}{dx} = \frac{D^*}{dx}$$

	100 MW	50 MW	200 MW
Grid size (m)	D* = 6.2	D* = 4.7	D* = 8.2
0,2	31	23,5	40,6

B.1 FDS input file for fire scenario 2 (100 MW)

100MW_v02.fds

Generated by PyroSim - Version 2020.3.0729

22.apr.2021 15:06:40

&HEAD CHID='100MW_v02', TITLE='HGV Fire in Road Tunnel'/

&TIME T_END=2700.0/

&DUMP COLUMN_DUMP_LIMIT=.TRUE., DT_DEVC=1.0, DT_HRR=1.0, DT_ISOF=1.0,
DT_PL3D=10.0, DT_RESTART=300.0, WRITE_XYZ=.TRUE.,
PLOT3D_QUANTITY='VOLUME FRACTION','VOLUME FRACTION','VOLUME
FRACTION','HRRPUV','VELOCITY', PLOT3D_SPEC_ID(1:3)='CARBON
DIOXIDE','CARBON MONOXIDE','OXYGEN'/

&MISC TMPA=5.0, VISIBILITY_FACTOR=8.0,
CONSTANT_SPECIFIC_HEAT_RATIO=.TRUE./

&MESH ID='Mesh01', IJK=1000,27,17, XB=0.0,400.0,-10.6,0.2,0.0,6.8/

&MESH ID='Mesh02', IJK=1000,27,17, XB=400.0,800.0,-10.6,0.2,0.0,6.8/

&MESH ID='Mesh03', IJK=500,54,34, XB=800.0,900.0,-10.6,0.2,0.0,6.8/

&MESH ID='Mesh04', IJK=1000,27,17, XB=900.0,1300.0,-10.6,0.2,0.0,6.8/

&MESH ID='Mesh05', IJK=1000,27,17, XB=1300.0,1700.0,-10.6,0.2,0.0,6.8/

&REAC ID='HVG Fire',

    FUEL='REAC_FUEL',

    C=1.0,

    H=2.0,

    O=0.62,

    AUTO_IGNITION_TEMPERATURE=0.0,

CO_YIELD=0.059,

SOOT_YIELD=0.032,

HEAT_OF_COMBUSTION=2.55E4/

&DEVC ID='FED -800m', QUANTITY='FED', XYZ=50.0,-2.0,2.0/

&DEVC ID='FED01 -800m', QUANTITY='FED', XYZ=50.0,-8.4,2.0/

&DEVC ID='FED02 -700m', QUANTITY='FED', XYZ=150.0,-8.4,2.0/

&DEVC ID='FED03 -700m', QUANTITY='FED', XYZ=150.0,-2.0,2.0/

&DEVC ID='FED04 -500m', QUANTITY='FED', XYZ=350.0,-8.4,2.0/

&DEVC ID='FED05 -500m', QUANTITY='FED', XYZ=350.0,-2.0,2.0/

&DEVC ID='FED06 -300m', QUANTITY='FED', XYZ=550.0,-8.4,2.0/

&DEVC ID='FED07 -300m', QUANTITY='FED', XYZ=550.0,-2.0,2.0/

&DEVC ID='FED08 -100m', QUANTITY='FED', XYZ=750.0,-8.4,2.0/

&DEVC ID='FED09 -100m', QUANTITY='FED', XYZ=750.0,-2.0,2.0/

&DEVC ID='FED10 -50m', QUANTITY='FED', XYZ=802.0,-8.4,2.0/

&DEVC ID='FED11 -50m', QUANTITY='FED', XYZ=802.0,-2.0,2.0/

&DEVC ID='FED12 +50m', QUANTITY='FED', XYZ=898.0,-8.4,2.0/

&DEVC ID='FED13 +50m', QUANTITY='FED', XYZ=898.0,-2.0,2.0/

&DEVC ID='FED14 +100m', QUANTITY='FED', XYZ=950.0,-2.0,2.0/

&DEVC ID='FED15 +100m', QUANTITY='FED', XYZ=950.0,-8.4,2.0/

&DEVC ID='FED16 +300m', QUANTITY='FED', XYZ=1150.0,-2.0,2.0/

&DEVC ID='FED17 +300', QUANTITY='FED', XYZ=1150.0,-8.4,2.0/

&DEVC ID='FED18 +500m', QUANTITY='FED', XYZ=1350.0,-2.0,2.0/

&DEVC ID='FED19 +500m', QUANTITY='FED', XYZ=1350.0,-8.4,2.0/

&DEVC ID='FED20 +700m', QUANTITY='FED', XYZ=1550.0,-2.0,2.0/

&DEVC ID='FED21 +700m', QUANTITY='FED', XYZ=1550.0,-8.4,2.0/

&DEVC ID='THCP -550m', QUANTITY='THERMOCOUPLE', XYZ=300.0,-5.2,6.0/

&DEVC ID='THCP01 -550m', QUANTITY='THERMOCOUPLE', XYZ=300.0,-5.2,4.0/

&DEVC ID='THCP02 -550m', QUANTITY='THERMOCOUPLE', XYZ=300.0,-5.2,2.0/

&DEVC ID='THCP03 -350m', QUANTITY='THERMOCOUPLE', XYZ=500.0,-5.2,6.0/

&DEVC ID='THCP04 -350m', QUANTITY='THERMOCOUPLE', XYZ=500.0,-5.2,4.0/

&DEVC ID='THCP05 -350m', QUANTITY='THERMOCOUPLE', XYZ=500.0,-5.2,2.0/

&DEVC ID='THCP06 -150m', QUANTITY='THERMOCOUPLE', XYZ=700.0,-5.2,6.0/

&DEVC ID='THCP07 -150m', QUANTITY='THERMOCOUPLE', XYZ=700.0,-5.2,4.0/

&DEVC ID='THCP08 -150m', QUANTITY='THERMOCOUPLE', XYZ=700.0,-5.2,2.0/

&DEVC ID='THCP09 -50m', QUANTITY='THERMOCOUPLE', XYZ=805.0,-5.2,6.0/

&DEVC ID='THCP10 -50m', QUANTITY='THERMOCOUPLE', XYZ=805.0,-5.2,4.0/

&DEVC ID='THCP11 -50m', QUANTITY='THERMOCOUPLE', XYZ=805.0,-5.2,2.0/

&DEVC ID='THCP12 -5m', QUANTITY='THERMOCOUPLE', XYZ=845.0,-3.1,5.8/

&DEVC ID='THCP13 -5m', QUANTITY='THERMOCOUPLE', XYZ=845.0,-3.1,4.0/

&DEVC ID='THCP14 -5m', QUANTITY='THERMOCOUPLE', XYZ=845.0,-3.1,2.0/

&DEVC ID='THCP15 +5m', QUANTITY='THERMOCOUPLE', XYZ=855.0,-3.1,5.8/

&DEVC ID='THCP16 +5m', QUANTITY='THERMOCOUPLE', XYZ=855.0,-3.1,4.0/

&DEVC ID='THCP17 +5m', QUANTITY='THERMOCOUPLE', XYZ=855.0,-3.1,2.0/

&DEVC ID='THCP18 +50m', QUANTITY='THERMOCOUPLE', XYZ=895.0,-5.2,6.0/

&DEVC ID='THCP19 +50m', QUANTITY='THERMOCOUPLE', XYZ=895.0,-5.2,4.0/

&DEVC ID='THCP20 +50m', QUANTITY='THERMOCOUPLE', XYZ=895.0,-5.2,2.0/

&DEVC ID='THCP21 +150m', QUANTITY='THERMOCOUPLE', XYZ=1000.0,-5.2,6.0/

&DEVC ID='THCP22 +150m', QUANTITY='THERMOCOUPLE', XYZ=1000.0,-5.2,4.0/

&DEVC ID='THCP23 +150m', QUANTITY='THERMOCOUPLE', XYZ=1000.0,-5.2,2.0/

&DEVC ID='THCP24 +350m', QUANTITY='THERMOCOUPLE', XYZ=1200.0,-5.2,6.0/

&DEVC ID='THCP25 +350m', QUANTITY='THERMOCOUPLE', XYZ=1200.0,-5.2,4.0/

&DEVC ID='THCP26 +350m', QUANTITY='THERMOCOUPLE', XYZ=1200.0,-5.2,2.0/

&DEVC ID='THCP27 +550m', QUANTITY='THERMOCOUPLE', XYZ=1400.0,-5.2,6.0/

&DEVC ID='THCP28 +550m', QUANTITY='THERMOCOUPLE', XYZ=1400.0,-5.2,4.0/

&DEVC ID='THCP29 +550m', QUANTITY='THERMOCOUPLE', XYZ=1400.0,-5.2,2.0/

&DEVC ID='Velocity000 -800m', QUANTITY='VELOCITY', XYZ=40.0,-5.2,6.0/

&DEVC ID='Velocity001 -600m', QUANTITY='VELOCITY', XYZ=240.0,-5.2,6.0/

&DEVC ID='Velocity002 -400m', QUANTITY='VELOCITY', XYZ=440.0,-5.2,6.0/

&DEVC ID='Velocity003 -200m', QUANTITY='VELOCITY', XYZ=640.0,-5.2,6.0/

&DEVC ID='Velocity01 -10m', QUANTITY='VELOCITY', XYZ=840.0,-5.2,6.0/

&DEVC ID='Velocity +10m', QUANTITY='VELOCITY', XYZ=860.0,-5.2,6.0/

&DEVC ID='Velocity02 +200m', QUANTITY='VELOCITY', XYZ=1060.0,-5.2,6.0/

&DEVC ID='Velocity03 +400m', QUANTITY='VELOCITY', XYZ=1260.0,-5.2,6.0/

&DEVC ID='Visibility -800m', QUANTITY='VISIBILITY', XYZ=50.0,-5.2,2.0/

&DEVC ID='Visibility01 -700m', QUANTITY='VISIBILITY', XYZ=150.0,-5.2,2.0/

&DEVC ID='Visibility02 -600m', QUANTITY='VISIBILITY', XYZ=250.0,-5.2,2.0/

&DEVC ID='Visibility03 -500m', QUANTITY='VISIBILITY', XYZ=350.0,-5.2,2.0/

&DEVC ID='Visibility04 -400m', QUANTITY='VISIBILITY', XYZ=450.0,-5.2,2.0/

&DEVC ID='Visibility05 -300m', QUANTITY='VISIBILITY', XYZ=550.0,-5.2,2.0/

&DEVC ID='Visibility06 -200m', QUANTITY='VISIBILITY', XYZ=650.0,-5.2,2.0/

&DEVC ID='Visibility07 -100m', QUANTITY='VISIBILITY', XYZ=750.0,-5.2,2.0/

&DEVC ID='Visibility08+100m', QUANTITY='VISIBILITY', XYZ=950.0,-5.2,2.0/

&DEVC ID='Visibility09 +200m', QUANTITY='VISIBILITY', XYZ=1050.0,-5.2,2.0/

&DEVC ID='Visibility10 +300m', QUANTITY='VISIBILITY', XYZ=1150.0,-5.2,2.0/

&DEVC ID='Visibility11 +400m', QUANTITY='VISIBILITY', XYZ=1250.0,-5.2,2.0/

&DEVC ID='Visibility12 +500m', QUANTITY='VISIBILITY', XYZ=1350.0,-5.2,2.0/

&DEVC ID='Visibility13 +600m', QUANTITY='VISIBILITY', XYZ=1450.0,-5.2,2.0/

&DEVC ID='Visibility14 +700m', QUANTITY='VISIBILITY', XYZ=1550.0,-5.2,2.0/

&DEVC ID='Visibility15 +800m', QUANTITY='VISIBILITY', XYZ=1650.0,-5.2,2.0/

&MATL ID='CONCRETE',

    FYI='NBSIR 88-3752 - ATF NIST Multi-Floor Validation',

    SPECIFIC_HEAT=1.04,

    CONDUCTIVITY=1.8,

    DENSITY=2280.0/

&SURF ID='TUNNELWALL',

    RGB=146,202,166,

    DEFAULT=.TRUE.,

    BACKING='VOID',

    MATL_ID(1,1)='CONCRETE',

    MATL_MASS_FRACTION(1,1)=1.0,

    THICKNESS(1)=1.0,

    ROUGHNESS=0.05/

&SURF ID='Fire',

    COLOR='RED',

    HRRPUA=5980.0,

    RAMP_Q='Fire_RAMP_Q',

    TMP_FRONT=300.0/

&RAMP ID='Fire_RAMP_Q', T=60.0, F=6.75E-3/

&RAMP ID='Fire_RAMP_Q', T=120.0, F=0.027/

&RAMP ID='Fire_RAMP_Q', T=180.0, F=0.0608/

&RAMP ID='Fire_RAMP_Q', T=240.0, F=0.10805/

&RAMP ID='Fire_RAMP_Q', T=300.0, F=0.16884/

&RAMP ID='Fire_RAMP_Q', T=360.0, F=0.2393/

&RAMP ID='Fire_RAMP_Q', T=390.0, F=0.2743/

&RAMP ID='Fire_RAMP_Q', T=600.0, F=0.5193/

&RAMP ID='Fire_RAMP_Q', T=1020.0, F=1.0/

&OBST ID='Obstruction', XB=0.0,1700.0,-10.4,-10.2,3.8,4.0, SURF_ID='TUNNELWALL'/

&OBST ID='Obstruction', XB=0.0,1700.0,-10.2,-10.0,4.0,4.2, SURF_ID='TUNNELWALL'/

&OBST ID='Obstruction', XB=0.0,1700.0,-10.0,-9.8,4.2,4.4, SURF_ID='TUNNELWALL'/

&OBST ID='Obstruction', XB=0.0,1700.0,-9.8,-9.6,4.4,4.6, SURF_ID='TUNNELWALL'/

&OBST ID='Obstruction', XB=0.0,1700.0,-9.6,-9.4,4.6,4.8, SURF_ID='TUNNELWALL'/

&OBST ID='Obstruction', XB=0.0,1700.0,-9.4,-9.2,4.8,5.0, SURF_ID='TUNNELWALL'/

&OBST ID='Obstruction', XB=0.0,1700.0,-9.2,-9.0,5.0,5.2, SURF_ID='TUNNELWALL'/

&OBST ID='Obstruction', XB=0.0,1700.0,-9.0,-8.6,5.2,5.4, SURF_ID='TUNNELWALL'/

&OBST ID='Obstruction', XB=0.0,1700.0,-8.6,-8.2,5.4,5.6, SURF_ID='TUNNELWALL'/

&OBST ID='Obstruction', XB=0.0,1700.0,-7.8,-7.4,5.8,6.0, SURF_ID='TUNNELWALL'/

&OBST ID='Obstruction', XB=0.0,1700.0,-7.4,-7.0,6.0,6.2, SURF_ID='TUNNELWALL'/

&OBST ID='Obstruction', XB=0.0,1700.0,-7.0,-6.6,6.2,6.4, SURF_ID='TUNNELWALL'/

&OBST ID='Obstruction', XB=0.0,1700.0,-0.2,0.0,3.8,4.0, SURF_ID='TUNNELWALL'/

&OBST ID='Obstruction', XB=0.0,1700.0,-0.4,-0.2,4.0,4.2, SURF_ID='TUNNELWALL'/

&OBST ID='Obstruction', XB=0.0,1700.0,-0.6,-0.4,4.2,4.4, SURF_ID='TUNNELWALL'/

&OBST ID='Obstruction', XB=0.0,1700.0,-0.8,-0.6,4.4,4.6, SURF_ID='TUNNELWALL'/

&OBST ID='Obstruction', XB=0.0,1700.0,-1.0,-0.8,4.6,4.8, SURF_ID='TUNNELWALL'/

&OBST ID='Obstruction', XB=0.0,1700.0,-1.2,-1.0,4.8,5.0, SURF_ID='TUNNELWALL'/

&OBST ID='Obstruction', XB=0.0,1700.0,-1.4,-1.2,5.0,5.2, SURF_ID='TUNNELWALL'/

&OBST ID='Obstruction', XB=0.0,1700.0,-1.8,-1.4,5.2,5.4, SURF_ID='TUNNELWALL'/

&OBST ID='Obstruction', XB=0.0,1700.0,-2.2,-1.8,5.4,5.6, SURF_ID='TUNNELWALL'/

&OBST ID='Obstruction', XB=0.0,1700.0,-2.6,-2.2,5.6,5.8, SURF_ID='TUNNELWALL'/

&OBST ID='Obstruction', XB=0.0,1700.0,-3.0,-2.6,5.8,6.0, SURF_ID='TUNNELWALL'/

&OBST ID='Obstruction', XB=0.0,1700.0,-3.4,-3.0,6.0,6.2, SURF_ID='TUNNELWALL'/

&OBST ID='Obstruction', XB=0.0,1700.0,-3.8,-3.4,6.2,6.4, SURF_ID='TUNNELWALL'/

&OBST ID='Obstruction', XB=0.0,1700.0,-8.2,-7.8,5.6,5.8, SURF_ID='TUNNELWALL'/

&OBST ID='Top', XB=0.0,1700.0,-6.6,-3.8,6.4,6.6, SURF_ID='TUNNELWALL'/

&OBST ID='Fan structure2x3(1)', XB=250.0,252.0,-6.6,-5.6,5.2,6.2, SURF_ID='INERT'/

&OBST ID='Fan structure2x3(1)', XB=250.0,252.0,-4.8,-3.8,5.2,6.2, SURF_ID='INERT'/

&OBST ID='Fan structure2x3(1)', XB=890.0,892.0,-6.6,-5.6,5.2,6.2, SURF_ID='INERT'/

&OBST ID='Fan structure2x3(1)', XB=890.0,892.0,-4.8,-3.8,5.2,6.2, SURF_ID='INERT'/

&OBST ID='Fan structure2x3(1)', XB=1350.0,1352.0,-6.6,-5.6,5.2,6.2, SURF_ID='INERT'/

&OBST ID='Fan structure2x3(1)', XB=1350.0,1352.0,-4.8,-3.8,5.2,6.2, SURF_ID='INERT'/

&OBST ID='Fan structure2x3(2)', XB=320.0,322.0,-6.6,-5.6,5.2,6.2, SURF_ID='INERT'/

&OBST ID='Fan structure2x3(2)', XB=320.0,322.0,-4.8,-3.8,5.2,6.2, SURF_ID='INERT'/

&OBST ID='Fan structure2x3(2)', XB=960.0,962.0,-6.6,-5.6,5.2,6.2, SURF_ID='INERT'/

&OBST ID='Fan structure2x3(2)', XB=960.0,962.0,-4.8,-3.8,5.2,6.2, SURF_ID='INERT'/

&OBST ID='Fan structure2x3(2)', XB=1420.0,1422.0,-6.6,-5.6,5.2,6.2, SURF_ID='INERT'/

&OBST ID='Fan structure2x3(2)', XB=1420.0,1422.0,-4.8,-3.8,5.2,6.2, SURF_ID='INERT'/

&OBST ID='Fan structure2x3(3)', XB=390.0,392.0,-6.6,-5.6,5.2,6.2, SURF_ID='INERT'/

&OBST ID='Fan structure2x3(3)', XB=390.0,392.0,-4.8,-3.8,5.2,6.2, SURF_ID='INERT'/

&OBST ID='Fan structure2x3(3)', XB=1490.0,1492.0,-6.6,-5.6,5.2,6.2, SURF_ID='INERT'/

&OBST ID='Fan structure2x3(3)', XB=1490.0,1492.0,-4.8,-3.8,5.2,6.2, SURF_ID='INERT'/

&OBST ID='Wall ground', XB=0.0,400.0,-10.6,-10.6,0.0,3.6, SURF_ID='TUNNELWALL'/

&OBST ID='Wall ground', XB=400.0,800.0,-10.6,-10.6,0.0,3.6, SURF_ID='TUNNELWALL'/

&OBST ID='Wall ground', XB=800.0,830.0,-10.6,-10.4,0.0,3.8, SURF_ID='TUNNELWALL'/

&OBST ID='Wall ground', XB=830.0,830.2,-10.6,-10.4,0.0,0.2, SURF_ID='TUNNELWALL'/

&OBST ID='Wall ground', XB=830.0,830.2,-10.6,-10.4,0.4,3.8, SURF_ID='TUNNELWALL'/

&OBST ID='Wall ground', XB=830.2,840.0,-10.6,-10.4,0.0,3.8, SURF_ID='TUNNELWALL'/

&OBST ID='Wall ground', XB=840.0,840.2,-10.6,-10.4,0.0,0.2, SURF_ID='TUNNELWALL'/

&OBST ID='Wall ground', XB=840.0,840.2,-10.6,-10.4,0.4,3.8, SURF_ID='TUNNELWALL'/

&OBST ID='Wall ground', XB=840.2,850.0,-10.6,-10.4,0.0,3.8, SURF_ID='TUNNELWALL'/

&OBST ID='Wall ground', XB=850.0,850.2,-10.6,-10.4,0.0,0.2, SURF_ID='TUNNELWALL'/

&OBST ID='Wall ground', XB=850.0,850.2,-10.6,-10.4,0.4,3.8, SURF_ID='TUNNELWALL'/

&OBST ID='Wall ground', XB=850.2,860.0,-10.6,-10.4,0.0,3.8, SURF_ID='TUNNELWALL'/

&OBST ID='Wall ground', XB=860.0,860.2,-10.6,-10.4,0.0,0.2, SURF_ID='TUNNELWALL'/

&OBST ID='Wall ground', XB=860.0,860.2,-10.6,-10.4,0.4,3.8, SURF_ID='TUNNELWALL'/

&OBST ID='Wall ground', XB=860.2,870.0,-10.6,-10.4,0.0,3.8, SURF_ID='TUNNELWALL'/

&OBST ID='Wall ground', XB=870.0,870.2,-10.6,-10.4,0.0,0.2, SURF_ID='TUNNELWALL'/

&OBST ID='Wall ground', XB=870.0,870.2,-10.6,-10.4,0.4,3.8, SURF_ID='TUNNELWALL'/

&OBST ID='Wall ground', XB=870.2,900.0,-10.6,-10.4,0.0,3.8, SURF_ID='TUNNELWALL'/

&OBST ID='Wall ground', XB=900.0,1300.0,-10.6,-10.6,0.0,3.6, SURF_ID='TUNNELWALL'/

&OBST ID='Wall ground', XB=1300.0,1700.0,-10.6,-10.6,0.0,3.6, SURF_ID='TUNNELWALL'/

&OBST ID='Wall ground 2', XB=0.0,400.0,-0.2,0.2,0.0,3.6, SURF_ID='TUNNELWALL'/

&OBST ID='Wall ground 2', XB=400.0,800.0,-0.2,0.2,0.0,3.6, SURF_ID='TUNNELWALL'/

&OBST ID='Wall ground 2', XB=800.0,830.0,-3.941292E-15,0.2,0.0,3.8, SURF_ID='TUNNELWALL'/

&OBST ID='Wall ground 2', XB=830.0,830.2,-3.941292E-15,0.2,0.0,0.2, SURF_ID='TUNNELWALL'/

&OBST ID='Wall ground 2', XB=830.0,830.2,-3.941292E-15,0.2,0.4,3.8, SURF_ID='TUNNELWALL'/

&OBST ID='Wall ground 2', XB=830.2,840.0,-3.941292E-15,0.2,0.0,3.8, SURF_ID='TUNNELWALL'/

&OBST ID='Wall ground 2', XB=840.0,840.2,-3.941292E-15,0.2,0.0,0.2, SURF_ID='TUNNELWALL'/

&OBST ID='Wall ground 2', XB=840.0,840.2,-3.941292E-15,0.2,0.4,3.8, SURF_ID='TUNNELWALL'/

&OBST ID='Wall ground 2', XB=840.2,850.0,-3.941292E-15,0.2,0.0,3.8, SURF_ID='TUNNELWALL'/

&OBST ID='Wall ground 2', XB=850.0,850.2,-3.941292E-15,0.2,0.0,0.2, SURF_ID='TUNNELWALL'/

&OBST ID='Wall ground 2', XB=850.0,850.2,-3.941292E-15,0.2,0.4,3.8, SURF_ID='TUNNELWALL'/

&OBST ID='Wall ground 2', XB=850.2,860.0,-3.941292E-15,0.2,0.0,3.8, SURF_ID='TUNNELWALL'/

&OBST ID='Wall ground 2', XB=860.0,860.2,-3.941292E-15,0.2,0.0,0.2, SURF_ID='TUNNELWALL'/

&OBST ID='Wall ground 2', XB=860.0,860.2,-3.941292E-15,0.2,0.4,3.8, SURF_ID='TUNNELWALL'/

&OBST ID='Wall ground 2', XB=860.2,870.0,-3.941292E-15,0.2,0.0,3.8, SURF_ID='TUNNELWALL'/

&OBST ID='Wall ground 2', XB=870.0,870.2,-3.941292E-15,0.2,0.0,0.2, SURF_ID='TUNNELWALL'/

&OBST ID='Wall ground 2', XB=870.0,870.2,-3.941292E-15,0.2,0.4,3.8, SURF_ID='TUNNELWALL'/

&OBST ID='Wall ground 2', XB=870.2,900.0,-3.941292E-15,0.2,0.0,3.8, SURF_ID='TUNNELWALL'/

&OBST ID='Wall ground 2', XB=900.0,1300.0,-0.2,0.2,0.0,3.6, SURF_ID='TUNNELWALL'/

&OBST ID='Wall ground 2', XB=1300.0,1700.0,-0.2,0.2,0.0,3.6, SURF_ID='TUNNELWALL'/

&VENT ID='Vent05', SURF_ID='HVAC', XB=250.0,250.0,-6.6,-5.6,5.2,6.2/

&VENT ID='Vent06', SURF_ID='HVAC', XB=252.0,252.0,-6.6,-5.6,5.2,6.2/

&VENT ID='Vent07', SURF_ID='HVAC', XB=250.0,250.0,-4.8,-3.8,5.2,6.2/

&VENT ID='Vent08', SURF_ID='HVAC', XB=252.0,252.0,-4.8,-3.8,5.2,6.2/

&VENT ID='Vent01', SURF_ID='HVAC', XB=320.0,320.0,-6.6,-5.6,5.2,6.2/

&VENT ID='Vent02', SURF_ID='HVAC', XB=322.0,322.0,-6.6,-5.6,5.2,6.2/

&VENT ID='Vent03', SURF_ID='HVAC', XB=320.0,320.0,-4.8,-3.8,5.2,6.2/

&VENT ID='Vent04', SURF_ID='HVAC', XB=322.0,322.0,-4.8,-3.8,5.2,6.2/

&VENT ID='Vent10', SURF_ID='HVAC', XB=390.0,390.0,-6.6,-5.6,5.2,6.2/

&VENT ID='Vent11', SURF_ID='HVAC', XB=392.0,392.0,-6.6,-5.6,5.2,6.2/

&VENT ID='Vent12', SURF_ID='HVAC', XB=390.0,390.0,-4.8,-3.8,5.2,6.2/

&VENT ID='Vent13', SURF_ID='HVAC', XB=392.0,392.0,-4.8,-3.8,5.2,6.2/

&VENT ID='Langnes', SURF_ID='OPEN', XB=0.0,0.0,-10.4,0.0,0.0,6.4/

&VENT ID='Sentrumstangent', SURF_ID='OPEN', XB=1700.0,1700.0,-10.4,0.0,0.0,6.4/

&VENT ID='Vent14', SURF_ID='HVAC', XB=890.0,890.0,-6.6,-5.6,5.2,6.2/

&VENT ID='Vent15', SURF_ID='HVAC', XB=892.0,892.0,-6.6,-5.6,5.2,6.2/

&VENT ID='Vent16', SURF_ID='HVAC', XB=890.0,890.0,-4.8,-3.8,5.2,6.2/

&VENT ID='Vent17', SURF_ID='HVAC', XB=892.0,892.0,-4.8,-3.8,5.2,6.2/

&VENT ID='Vent18', SURF_ID='HVAC', XB=960.0,960.0,-6.6,-5.6,5.2,6.2/

&VENT ID='Vent19', SURF_ID='HVAC', XB=962.0,962.0,-6.6,-5.6,5.2,6.2/

&VENT ID='Vent20', SURF_ID='HVAC', XB=960.0,960.0,-4.8,-3.8,5.2,6.2/

&VENT ID='Vent21', SURF_ID='HVAC', XB=962.0,962.0,-4.8,-3.8,5.2,6.2/

&VENT ID='Vent22', SURF_ID='HVAC', XB=1350.0,1350.0,-6.6,-5.6,5.2,6.2/

&VENT ID='Vent23', SURF_ID='HVAC', XB=1352.0,1352.0,-6.6,-5.6,5.2,6.2/

&VENT ID='Vent24', SURF_ID='HVAC', XB=1350.0,1350.0,-4.8,-3.8,5.2,6.2/

&VENT ID='Vent25', SURF_ID='HVAC', XB=1352.0,1352.0,-4.8,-3.8,5.2,6.2/

&VENT ID='Vent26', SURF_ID='HVAC', XB=1420.0,1420.0,-6.6,-5.6,5.2,6.2/

&VENT ID='Vent27', SURF_ID='HVAC', XB=1422.0,1422.0,-6.6,-5.6,5.2,6.2/

&VENT ID='Vent28', SURF_ID='HVAC', XB=1420.0,1420.0,-4.8,-3.8,5.2,6.2/

&VENT ID='Vent29', SURF_ID='HVAC', XB=1422.0,1422.0,-4.8,-3.8,5.2,6.2/

&VENT ID='Vent30', SURF_ID='HVAC', XB=1490.0,1490.0,-6.6,-5.6,5.2,6.2/

&VENT ID='Vent31', SURF_ID='HVAC', XB=1492.0,1492.0,-6.6,-5.6,5.2,6.2/

&VENT ID='Vent32', SURF_ID='HVAC', XB=1490.0,1490.0,-4.8,-3.8,5.2,6.2/

&VENT ID='Vent33', SURF_ID='HVAC', XB=1492.0,1492.0,-4.8,-3.8,5.2,6.2/

&VENT ID='HGV fire', SURF_ID='Fire', XB=846.2,853.8,-4.2,-2.0,0.0,0.0/

&VENT ID='YMAX', SURF_ID='OPEN', XB=0.0,1700.0,0.2,0.2,0.0,6.4/

&VENT ID='YMIN', SURF_ID='OPEN', XB=0.0,1700.0,-10.6,-10.6,0.0,6.4/

&HVAC ID='Node01', TYPE_ID='NODE', DUCT_ID='Duct01', VENT_ID='Vent05'/

&HVAC ID='Node02', TYPE_ID='NODE', DUCT_ID='Duct01', VENT_ID='Vent06'/

&HVAC ID='Node03', TYPE_ID='NODE', DUCT_ID='Duct02', VENT_ID='Vent07'/

&HVAC ID='Node04', TYPE_ID='NODE', DUCT_ID='Duct02', VENT_ID='Vent08'/

&HVAC ID='Duct01', TYPE_ID='DUCT', AREA=1.0, PERIMETER=4.0, VOLUME_FLOW=-14.4, RAMP_ID='Duct01_RAMP_ID', NODE_ID='Node01','Node02', ROUGHNESS=1.0E-3, LENGTH=2.0/

&HVAC ID='Duct02', TYPE_ID='DUCT', AREA=1.0, PERIMETER=4.0, VOLUME_FLOW=-14.4, RAMP_ID='Duct02_RAMP_ID', NODE_ID='Node03','Node04', ROUGHNESS=1.0E-3, LENGTH=2.0/

&HVAC ID='Duct03', TYPE_ID='DUCT', AREA=1.0, PERIMETER=4.0, VOLUME_FLOW=-14.4, RAMP_ID='Duct03_RAMP_ID', NODE_ID='Node13','Node06', ROUGHNESS=1.0E-3, LENGTH=2.0/

&HVAC ID='Duct04', TYPE_ID='DUCT', AREA=1.0, PERIMETER=4.0, VOLUME_FLOW=-14.4, RAMP_ID='Duct04_RAMP_ID', NODE_ID='Node07','Node08', ROUGHNESS=1.0E-3, LENGTH=2.0/

&HVAC ID='Node06', TYPE_ID='NODE', DUCT_ID='Duct03', VENT_ID='Vent02'/

&HVAC ID='Node07', TYPE_ID='NODE', DUCT_ID='Duct04', VENT_ID='Vent03'/

&HVAC ID='Node08', TYPE_ID='NODE', DUCT_ID='Duct04', VENT_ID='Vent04'/

&HVAC ID='Node13', TYPE_ID='NODE', DUCT_ID='Duct03', VENT_ID='Vent01'/

&HVAC ID='Node14', TYPE_ID='NODE', DUCT_ID='Duct07', VENT_ID='Vent14'/

&HVAC ID='Node15', TYPE_ID='NODE', DUCT_ID='Duct07', VENT_ID='Vent15'/

&HVAC ID='Node16', TYPE_ID='NODE', DUCT_ID='Duct08', VENT_ID='Vent16'/

&HVAC ID='Node17', TYPE_ID='NODE', DUCT_ID='Duct08', VENT_ID='Vent17'/

&HVAC ID='Duct07', TYPE_ID='DUCT', AREA=1.0, PERIMETER=4.0, VOLUME_FLOW=-14.4, RAMP_ID='Duct07_RAMP_ID', NODE_ID='Node14','Node15', ROUGHNESS=1.0E-3, LENGTH=2.0/

&HVAC ID='Duct08', TYPE_ID='DUCT', AREA=1.0, PERIMETER=4.0, VOLUME_FLOW=-14.4, RAMP_ID='Duct08_RAMP_ID', NODE_ID='Node16','Node17', ROUGHNESS=1.0E-3, LENGTH=2.0/

&HVAC ID='Duct09', TYPE_ID='DUCT', AREA=1.0, PERIMETER=4.0, VOLUME_FLOW=-14.4, RAMP_ID='Duct09_RAMP_ID', NODE_ID='Node21','Node18', ROUGHNESS=1.0E-3, LENGTH=2.0/

&HVAC ID='Duct10', TYPE_ID='DUCT', AREA=1.0, PERIMETER=4.0, VOLUME_FLOW=-14.4, RAMP_ID='Duct10_RAMP_ID', NODE_ID='Node19','Node20', ROUGHNESS=1.0E-3, LENGTH=2.0/

&HVAC ID='Node18', TYPE_ID='NODE', DUCT_ID='Duct09', VENT_ID='Vent19'/

&HVAC ID='Node19', TYPE_ID='NODE', DUCT_ID='Duct10', VENT_ID='Vent20'/

&HVAC ID='Node20', TYPE_ID='NODE', DUCT_ID='Duct10', VENT_ID='Vent21'/

&HVAC ID='Node21', TYPE_ID='NODE', DUCT_ID='Duct09', VENT_ID='Vent18'/

&HVAC ID='Node22', TYPE_ID='NODE', DUCT_ID='Duct11', VENT_ID='Vent22'/

&HVAC ID='Node23', TYPE_ID='NODE', DUCT_ID='Duct11', VENT_ID='Vent23'/

&HVAC ID='Node24', TYPE_ID='NODE', DUCT_ID='Duct12', VENT_ID='Vent24'/

&HVAC ID='Node25', TYPE_ID='NODE', DUCT_ID='Duct12', VENT_ID='Vent25'/

&HVAC ID='Duct11', TYPE_ID='DUCT', AREA=1.0, PERIMETER=4.0, VOLUME_FLOW=-14.4, RAMP_ID='Duct11_RAMP_ID', NODE_ID='Node22','Node23', ROUGHNESS=1.0E-3, LENGTH=2.0/

&HVAC ID='Duct12', TYPE_ID='DUCT', AREA=1.0, PERIMETER=4.0, VOLUME_FLOW=-14.4, RAMP_ID='Duct12_RAMP_ID', NODE_ID='Node24','Node25', ROUGHNESS=1.0E-3, LENGTH=2.0/

&HVAC ID='Duct13', TYPE_ID='DUCT', AREA=1.0, PERIMETER=4.0, VOLUME_FLOW=-14.4, RAMP_ID='Duct13_RAMP_ID', NODE_ID='Node29','Node26', ROUGHNESS=1.0E-3, LENGTH=2.0/

&HVAC ID='Duct14', TYPE_ID='DUCT', AREA=1.0, PERIMETER=4.0, VOLUME_FLOW=-14.4, RAMP_ID='Duct14_RAMP_ID', NODE_ID='Node27','Node28', ROUGHNESS=1.0E-3, LENGTH=2.0/

&HVAC ID='Node26', TYPE_ID='NODE', DUCT_ID='Duct13', VENT_ID='Vent27'/

&HVAC ID='Node27', TYPE_ID='NODE', DUCT_ID='Duct14', VENT_ID='Vent28'/

&HVAC ID='Node28', TYPE_ID='NODE', DUCT_ID='Duct14', VENT_ID='Vent29'/

&HVAC ID='Node29', TYPE_ID='NODE', DUCT_ID='Duct13', VENT_ID='Vent26'/

&HVAC ID='Node09', TYPE_ID='NODE', DUCT_ID='Duct05', VENT_ID='Vent10'/

&HVAC ID='Node10', TYPE_ID='NODE', DUCT_ID='Duct05', VENT_ID='Vent11'/

&HVAC ID='Node11', TYPE_ID='NODE', DUCT_ID='Duct06', VENT_ID='Vent12'/

&HVAC ID='Node12', TYPE_ID='NODE', DUCT_ID='Duct06', VENT_ID='Vent13'/

&HVAC ID='Duct05', TYPE_ID='DUCT', AREA=1.0, PERIMETER=4.0, VOLUME_FLOW=-14.4, RAMP_ID='Duct05_RAMP_ID', NODE_ID='Node09','Node10', ROUGHNESS=1.0E-3, LENGTH=2.0/

&HVAC ID='Duct06', TYPE_ID='DUCT', AREA=1.0, PERIMETER=4.0, VOLUME_FLOW=-14.4, RAMP_ID='Duct06_RAMP_ID', NODE_ID='Node11','Node12', ROUGHNESS=1.0E-3, LENGTH=2.0/

&HVAC ID='Node30', TYPE_ID='NODE', DUCT_ID='Duct15', VENT_ID='Vent30'/

&HVAC ID='Node31', TYPE_ID='NODE', DUCT_ID='Duct15', VENT_ID='Vent31'/

&HVAC ID='Node32', TYPE_ID='NODE', DUCT_ID='Duct16', VENT_ID='Vent32'/

&HVAC ID='Node33', TYPE_ID='NODE', DUCT_ID='Duct16', VENT_ID='Vent33'/

&HVAC ID='Duct15', TYPE_ID='DUCT', AREA=1.0, PERIMETER=4.0, VOLUME_FLOW=-14.4, RAMP_ID='Duct15_RAMP_ID', NODE_ID='Node30','Node31', ROUGHNESS=1.0E-3, LENGTH=2.0/

&HVAC ID='Duct16', TYPE_ID='DUCT', AREA=1.0, PERIMETER=4.0, VOLUME_FLOW=-14.4, RAMP_ID='Duct16_RAMP_ID', NODE_ID='Node32','Node33', ROUGHNESS=1.0E-3, LENGTH=2.0/

&RAMP ID='Duct13_RAMP_ID', T=0.0, F=0.1/

&RAMP ID='Duct13_RAMP_ID', T=120.0, F=0.1/

&RAMP ID='Duct13_RAMP_ID', T=180.0, F=1.0/

&RAMP ID='Duct13_RAMP_ID', T=360.0, F=1.0/

&RAMP ID='Duct06_RAMP_ID', T=0.0, F=0.1/

&RAMP ID='Duct06_RAMP_ID', T=120.0, F=0.1/

&RAMP ID='Duct06_RAMP_ID', T=180.0, F=1.0/

&RAMP ID='Duct06_RAMP_ID', T=360.0, F=1.0/

&RAMP ID='Duct12_RAMP_ID', T=0.0, F=0.1/

&RAMP ID='Duct12_RAMP_ID', T=120.0, F=0.1/

&RAMP ID='Duct12_RAMP_ID', T=180.0, F=1.0/

&RAMP ID='Duct12_RAMP_ID', T=360.0, F=1.0/

&RAMP ID='Duct07_RAMP_ID', T=0.0, F=0.1/

&RAMP ID='Duct07_RAMP_ID', T=120.0, F=0.1/

&RAMP ID='Duct07_RAMP_ID', T=180.0, F=1.0/

&RAMP ID='Duct07_RAMP_ID', T=360.0, F=1.0/

&RAMP ID='Duct04_RAMP_ID', T=0.0, F=0.1/

&RAMP ID='Duct04_RAMP_ID', T=120.0, F=0.1/

&RAMP ID='Duct04_RAMP_ID', T=180.0, F=1.0/

&RAMP ID='Duct04_RAMP_ID', T=360.0, F=1.0/

&RAMP ID='Duct11_RAMP_ID', T=0.0, F=0.1/

&RAMP ID='Duct11_RAMP_ID', T=120.0, F=0.1/

&RAMP ID='Duct11_RAMP_ID', T=180.0, F=1.0/

&RAMP ID='Duct11_RAMP_ID', T=360.0, F=1.0/

&RAMP ID='Duct09_RAMP_ID', T=0.0, F=0.1/

&RAMP ID='Duct09_RAMP_ID', T=120.0, F=0.1/

&RAMP ID='Duct09_RAMP_ID', T=180.0, F=1.0/

&RAMP ID='Duct09_RAMP_ID', T=360.0, F=1.0/

&RAMP ID='Duct08_RAMP_ID', T=0.0, F=0.1/

&RAMP ID='Duct08_RAMP_ID', T=120.0, F=0.1/

&RAMP ID='Duct08_RAMP_ID', T=180.0, F=1.0/

&RAMP ID='Duct08_RAMP_ID', T=360.0, F=1.0/

&RAMP ID='Duct16_RAMP_ID', T=0.0, F=0.1/

&RAMP ID='Duct16_RAMP_ID', T=120.0, F=0.1/

&RAMP ID='Duct16_RAMP_ID', T=180.0, F=1.0/

&RAMP ID='Duct16_RAMP_ID', T=360.0, F=1.0/

&RAMP ID='Duct03_RAMP_ID', T=0.0, F=0.1/

&RAMP ID='Duct03_RAMP_ID', T=120.0, F=0.1/

&RAMP ID='Duct03_RAMP_ID', T=180.0, F=1.0/

&RAMP ID='Duct03_RAMP_ID', T=360.0, F=1.0/

&RAMP ID='Duct02_RAMP_ID', T=0.0, F=0.1/

&RAMP ID='Duct02_RAMP_ID', T=120.0, F=0.1/

&RAMP ID='Duct02_RAMP_ID', T=180.0, F=1.0/

&RAMP ID='Duct02_RAMP_ID', T=360.0, F=1.0/

&RAMP ID='Duct10_RAMP_ID', T=0.0, F=0.1/

&RAMP ID='Duct10_RAMP_ID', T=120.0, F=0.1/

&RAMP ID='Duct10_RAMP_ID', T=180.0, F=1.0/

&RAMP ID='Duct10_RAMP_ID', T=360.0, F=1.0/

&RAMP ID='Duct01_RAMP_ID', T=0.0, F=0.1/

&RAMP ID='Duct01_RAMP_ID', T=120.0, F=0.1/

&RAMP ID='Duct01_RAMP_ID', T=180.0, F=1.0/

&RAMP ID='Duct01_RAMP_ID', T=360.0, F=1.0/

&RAMP ID='Duct15_RAMP_ID', T=0.0, F=0.1/

&RAMP ID='Duct15_RAMP_ID', T=120.0, F=0.1/

&RAMP ID='Duct15_RAMP_ID', T=180.0, F=1.0/

&RAMP ID='Duct15_RAMP_ID', T=360.0, F=1.0/

&RAMP ID='Duct05_RAMP_ID', T=0.0, F=0.1/

&RAMP ID='Duct05_RAMP_ID', T=120.0, F=0.1/

&RAMP ID='Duct05_RAMP_ID', T=180.0, F=1.0/

&RAMP ID='Duct05_RAMP_ID', T=360.0, F=1.0/

&RAMP ID='Duct14_RAMP_ID', T=0.0, F=0.1/

&RAMP ID='Duct14_RAMP_ID', T=120.0, F=0.1/

&RAMP ID='Duct14_RAMP_ID', T=180.0, F=1.0/

&RAMP ID='Duct14_RAMP_ID', T=360.0, F=1.0/

&SLCF QUANTITY='VELOCITY', CELL_CENTERED=.TRUE., PBY=-5.2/

&SLCF QUANTITY='PRESSURE', CELL_CENTERED=.TRUE., PBX=200.0/

&SLCF QUANTITY='PRESSURE', VECTOR=.TRUE., PBX=300.0/

&SLCF QUANTITY='PRESSURE', VECTOR=.TRUE., PBX=100.0/

&SLCF QUANTITY='PRESSURE', VECTOR=.TRUE., PBX=600.0/

&SLCF QUANTITY='PRESSURE', VECTOR=.TRUE., PBX=900.0/

&SLCF QUANTITY='PRESSURE', VECTOR=.TRUE., PBX=1200.0/

&SLCF QUANTITY='PRESSURE', VECTOR=.TRUE., PBX=1500.0/

&SLCF QUANTITY='PRESSURE', VECTOR=.TRUE., PBX=1650.0/

&SLCF QUANTITY='VISIBILITY', PBY=-1.8/

&SLCF QUANTITY='VISIBILITY', PBY=-5.2/

&SLCF QUANTITY='TEMPERATURE', PBY=-5.2/

&SLCF QUANTITY='VISIBILITY', PBY=8.8/

&SLCF QUANTITY='VELOCITY', VECTOR=.TRUE., PBY=-1.8/

&SLCF QUANTITY='VELOCITY', VECTOR=.TRUE., PBY=8.8/

&SLCF QUANTITY='VISIBILITY', PBZ=2.0/

&SLCF QUANTITY='VISIBILITY', PBZ=3.0/

&SLCF QUANTITY='VISIBILITY', PBZ=4.0/

&SLCF QUANTITY='TEMPERATURE', PBZ=2.0/

&SLCF QUANTITY='TEMPERATURE', PBZ=3.0/

&SLCF QUANTITY='TEMPERATURE', PBZ=4.0/

&SLCF QUANTITY='TEMPERATURE', PBZ=6.0/

&SLCF QUANTITY='VELOCITY', VECTOR=.TRUE., PBZ=6.0/

&SLCF QUANTITY='VOLUME FRACTION', SPEC_ID='CARBON MONOXIDE', PBZ=2.0/

&SLCF QUANTITY='VOLUME FRACTION', SPEC_ID='CARBON DIOXIDE', PBZ=2.0/

&SLCF QUANTITY='VOLUME FRACTION', SPEC_ID='OXYGEN', PBZ=2.0/

&SLCF QUANTITY='VOLUME FRACTION', SPEC_ID='SOOT', PBZ=2.0/

&TAIL /